SEDIMENTOLOGY AND SEQUENCE STRATIGRAPHY OF THE PALEOPROTEROZOIC ROVE AND VIRGINIA FORMATIONS, SOUTHWEST SUPERIOR PROVINCE

by

Mike Maric

A thesis submitted in partial

fulfillment of the requirements for

the degree of Master of Science

Lakehead University, Thunder Bay, Ont.

May 2006

Your file Votre référence
ISBN: 978-0-494-15630-8
Our file Notre référence
ISBN: 978-0-494-15630-8

ACKNOWLEDGEMENTS

I would like to thank Mark Smyk and Gerry White, of the Ministry of Northern Development and Mines, who assisted me in the Thunder Bay drill core repository. Steven A. Hauck helped me extensively and provided access to drill cores in the Hibbing, Minnesota drill core storage site. Mark J. Serverson told me about the existence of core LWD-99-1 stored at the Hibbing site.

The assistance of Sam Spivak who drafted most of the diagrams is greatly appreciated, as well as Robert Scott who worked as my assistant in the Conmee core storage site. Kristine Carey provided aid for printing drafts of my thesis and Anne Hammond made the thin sections and provided encouragement after my dad passed away.

Special thanks of course goes to Dr. Phil Fralick, for his guidance, encouragement, enthusiasm and time. His help was truly indispensable in the completion of this thesis. Also, many thanks to the Geology department professors at Lakehead University.

Lastly my Mom and Dad. Thanks for everything.

TABLE OF CONTENTS

LIST OF FIGURES

Abstract

The Paleoproterozoic Rove and Virginia Formations are lithostratigraphically and chronostratigraphically correlative units which comprise the upper sedimentary strata in the Animikie basin. They sharply overlie an intensely altered zone within the upper Gunflint and Biwabik iron formations which was subaerially exposed by compressional forces during the Penokean Orogeny. Dating of volcaniclastic zircons from the upper Gunflint yielded a pre-Penokean age of 1878 Ma. Tuffaceous layers very near the base of the Rove and Virginia Formations provided U-Pb zircon ages of approximately 1835 Ma placing commencement of sedimentation into the newly resubmerged basin during the final stages of Penokean igneous activity.

This study involved examination of 3200 m of drill core from eleven continuously drilled holes and one twiced drilled hole extending over 424 km from south of Duluth to south of Thunder Bay. Observation of the lithofacies present and their stratigraphic relationships provided insight into the depositional environment as well as the tectonic regime operating at the time.

The basal Rove and Virginia Formations were deposited as transgression progressed across the depressed basinal area. They consist of black, carbonaceous shale with thin interbeds of siltstone, very-fine grained sandstone and friable green tuffaceous layers, possibly contributed by volcanic activity within the Penokean terrain. From approximately 5 m above the base, siltstone and sandstone layers gradually diminish in frequency upward, until the succession is almost completely dominated by approximately 100 to 150 m of fissile black shale. Microscopic examination of thin sections of this unit revealed the presence of very thin shale laminae and other laminae composed of angular silt grains or microlayers consisting of carbon. This sediment-starved, condensed sequence developed with increasing water depth, and with anoxic conditions probably caused by high organic loading in the bottom sediments. A siltstone and very-fine grained sandstone-rich unit traceable across the basin occurs midway through the shale-dominated succession. This coarser unit thickens near both the northern and southern margins of the basin. Above it another coarser-grained interval within the shale-dominated succession is observed in the southern third of the basin, probably representing sediment contributed by Penokean sources to the south. A gradational transition between the shale and an overlying sandstone-shale unit occurs over 80 m in the north, thinning to the south. The upper sandstone-shale unit varies in thickness, with a maximum of 350 m, and consists of over one hundred individual coarsening upwards parasequences. The individual packages are composed of graded, commonly massive, fine-grained sandstones separated by shale layers millimetres to centimetres thick. Shale units separating the parasequences are decimeters to one or two meters in thickness. The sandstone-shale assemblage fines to the south. Approximately 500 m above the base of the section the uppermost unit is dominated by lenticular bedding of fine-grained sandstones in the black shale, with both current and wave ripples present. The entire succession represents the transition from a sediment-starved basin, with exceedingly slow deposition rates, to active deltaic progradation with sediment probably derived from the Trans-Hudson orogenic zone to the north.

CHAPTER 1: INTRODUCTION

1.1 Introduction

The Paleoproterozoic Rove and Virginia Formations comprise the upper units of a series of chemical and clastic sediments which were deposited approximately 1.8 billion years ago in a shelf-slope setting within the Animikie basin. The elongate Animikie basin covers the southern margin of Superior Province in east-central and northern Minnesota, adjacent parts of Ontario, northern Wisconsin and the northern peninsula of Michigan (Morey, 1983)(Fig.1). Exposures occur within an east-trending oval-shaped area of approximately 700 km by 400 km. The original size of the basin is indeterminate due to partial removal by erosion, with other portions covered by younger Proterozoic and Phanerozoic strata.

Subsidence, due to extensional forces along the southern margin of the Superior Province allowed the Animikie Sea to spread slowly across the low-lying land mass, initiating sedimentation in a back-arc basin environment (Hemming, 1994; Kissin and Fralick, 1994; Hemming et al., 1995; Pufahl and Fralick, 1995; Pufahl, 1996). Deposition of a basal sequence of shallow-water clastic sediments comprising the Kakabeka Formation on the Gunflint range, Pokegama Quartzite on the Mesabi range and Mahnoman Formation on the Cuyuna range followed. The argillite, quartzite and conglomerate developed as a southward thickening wedge of shallow marine, fine-grained clastics fringed by a thin strand-

line deposit of sandstone and conglomerate. Evidence of tidal activity is ubiquitous in the nearshore deposits (Ojakangas, 1983).

A fairly abrupt change to a chemical depositional regime produced the Gunflint, Biwabik, and Trommald iron formations on the Gunflint, Mesabi, and Cuyuna ranges respectively (Fig. 2). Several horizons of volcanic material within the iron formation indicate the region was volcanically active at the time (Goodwin, 1956, Hassler and Simonson, 1989; Kissin and Fralick, 1994). Uplift of the basin with subaerial exposure (Addison et al., 2005) was followed by resubmergence and a transition to a clastic depositional regime in a foreland basin (Hemming et al.,1995).

The Rove Formation on the Gunflint range, Virginia Formation on the Mesabi range, Rabbit Lake Formation on the Cuyuna range, and Thomson Formation in east-central Minnesota comprise a succession of intercalated black to dark gray mudstone, siltstone and graywacke, with lesser amounts of quartzite, limestone, and several types of iron formation that record deposition during the foreland stage of the basin (Fig. 2). The units form a gently dipping homocline striking east-northeast and dipping 5° to 15° to the south. The homoclinal structure is locally interrupted by faults and southwest plunging folds (Lucente and Morey, 1983). Penokean deformation caused intense folding in the south. The Virginia Formation forms the majority of the upper Mesabi range and is inferred to extend southward beneath a thick mantle of drift to east-central Minnesota where it reappears as the Thomson Formation. Rocks of the Thomson Formation extend westward to the Cuyuna range where they are called

the Rabbit Lake Formation. The Rove Formation, as exposed along the international boundary in Minnesota, is separated from the other middle Precambrian rocks by approximately 75 km of Middle Keweenawan gabbroic intrusives. The Rove is calculated to be at least 975 m thick in Minnesota (Morey, 1967). Actual thickness cannot be determined accurately as the top of the Rove-Virginia-Thompson-Rabbit Lake assemblage has been erosively removed.

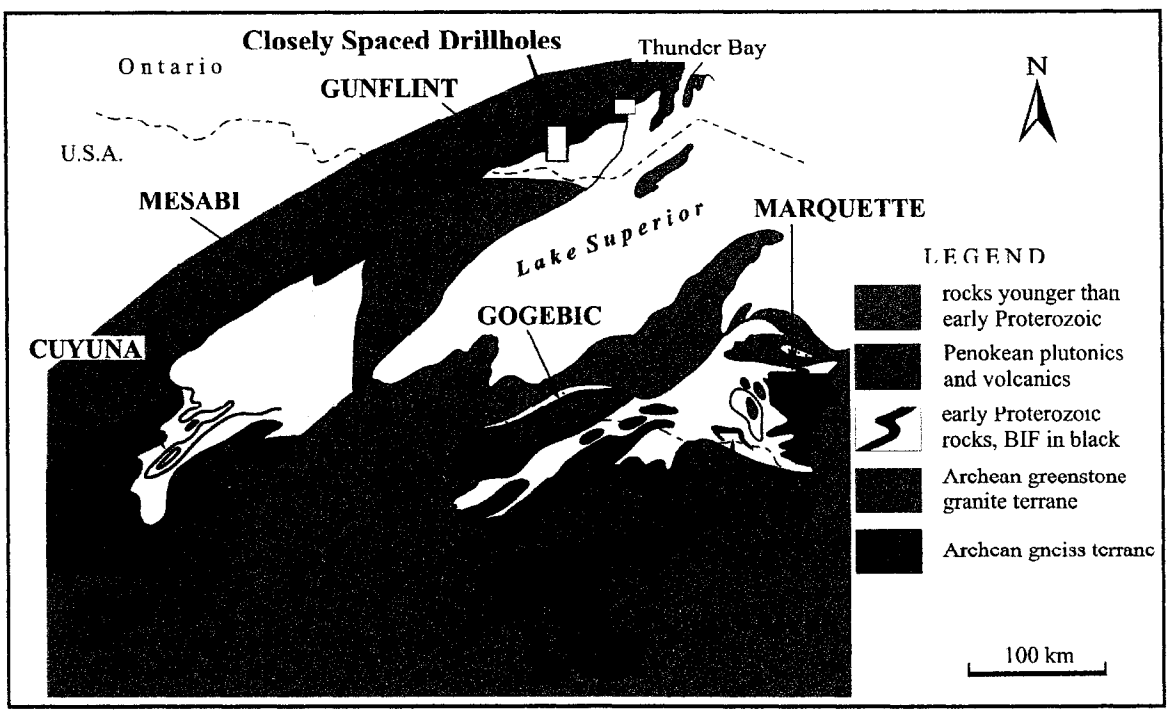

Fig. 1. Regional Geology of the study area (Gunflint and Mesabi ranges) and related rocks to the south-east. Sedimentary Rocks deposited in the Animikie basin are represented by the early Proterozoic rocks, BIF (Banded Iron Formation) in black (Pufahl and Fralick, 2004).

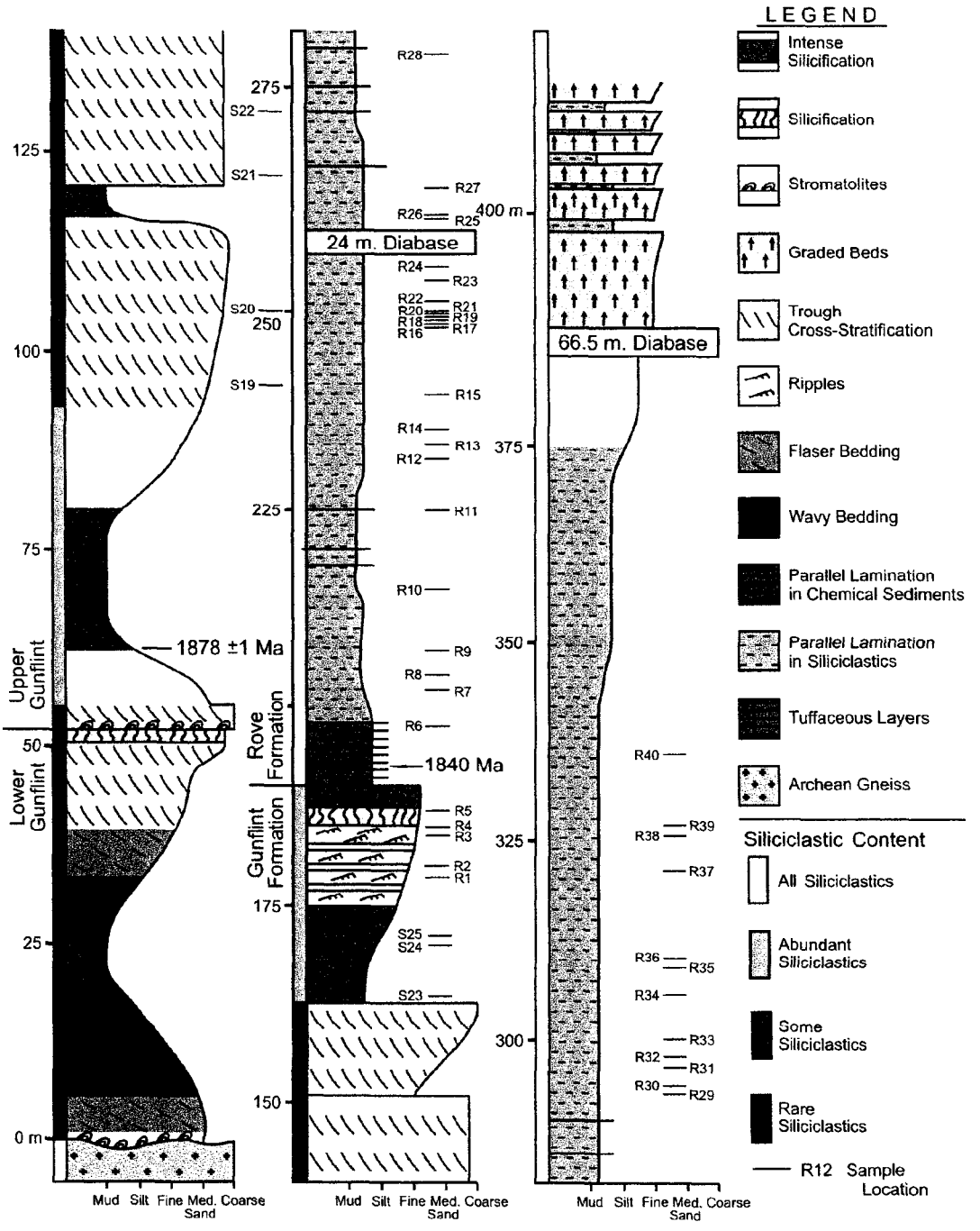

Fig. 2. Cross section from the Archean Gneiss through the Gunflint Formation and up to and including the lower argillaceous and transitional zone of the Rove Formation (Poulton et al., 2004)

1.2 Regional Geologic Setting

The Animikie basin was one of several basins that formed over and approximately parallel to the Great Lakes tectonic zone (Morey, 1983) which extends eastward more than 1200 km from central south Dakota to the Grenville Front in eastern Ontario. The northern part of the basin is underlain by Archean greenstone-granite terrane (2.75 –2.6 Ga) while the southern part is underlain by migmatitic gneiss and amphibolite (3.6 Ga). These two terranes were juxtaposed along the Great Lakes tectonic zone during the Neoarchean (Sims et al., 1989). The southern boundary of the basin consists of a mostly coeval assemblage of dominantly mafic to felsic volcanics and intrusives which form an east-trending belt across much of north-central Wisconsin (Sims et al., 1989).

During the Paleoproterozoic (2.5-1.8 Ga) as the Superior Province moved toward the hinge of a northward-dipping subduction zone (Van Wyck and Johnson, 1997), extensional forces thinned the crust along its southern margin producing a shallow back-arc basin (Hemming et al., 1995; Pufahl and Fralick, 1995). A thin discontinuous basal conglomerate facies 0-15 m thick is thought to have formed prior to transgression of the Animikie Sea (Ojakangas, 1983). The clasts consist of subrounded to rounded cobbles of underlying Archean bedrock and vein quartz, and were produced by residual in-situ weathering coupled with minor fluvial activity (Ojakangas, 1983). They occur in small low-relief depressions on a peneplaned surface. Thicker accumulations may have been deposited by fluvial action. Some reworking of the conglomerate occurred as

transgression progressed. Deposition of finer grained sediment of the Pokegama and Palms Formations succeeded the basal conglomerate. Tidal influence is evidenced by bimodal-bipolar paleocurrent directions, sedimentary structures, facies relationships, and mineralogical maturity of the sediment (Ojakangas, 1983). Ojakangas (1983) also showed that coastal, tidal and shallow marine facies were deposited side by side on the broad, shallow, slowly subsiding shelf rimming the basin, and stacked vertically with progressive transgression. Muds deposited from suspension form shales of the upper tidal flat, the most proximal marine facies. These were succeeded by associated interbeds of mud, silt, and sand, products of deposition from alternating bed load and suspension processes. Wavy, lenticular, flaser, and parallel laminated beds are common in these intertidal flats. The lower tidal flat and subtidal facies are composed primarily of parallel laminated or planar cross-stratified sandstone beds. The sands probably accumulated as lower tidal sand flats or as subtidal sand shoals in water above wave base, for symmetrical ripple marks are abundant (Ojakangas, 1983). While the Pokegama and Palms quartzites accumulated in tidally influenced nearshore settings, the Mahnomen Formation developed simultaneously in more distal shelf settings by pelagic settling and waning turbidity currents. A general coarsening upwards trend is displayed in most of the clastic shallow marine assemblage, with a few fining upwards successions indicating minor transgressions. The thin (0-150 m) basal clastics grade fairly sharply into the overlying iron formations which exceed 200 m in thickness. Deposition of iron formation occurred seaward of the subtidal sandstone facies

accumulating in the nearshore. Two major facies formed: a shallow-water, coarser grained, clastic, reworked and cross-bedded oxide-silicate "cherty" facies and in adjacent but somewhat deeper water, a finer-grained silicate-carbonate "slaty" facies (Ojakangas, 1983). The cherty facies includes successions of strand-proximal stromatolites, flaser and wavy bedded chert-carbonate grainstones and parallel bedded and hummocky cross-stratified hematite-rich cherty grainstones deposited on a non-barred microtidal, storm enhanced shoreline with little clastic influx (Fralick, 1988; Pufahl, 1996; Pufahl and Fralick, 2000). The inner shelf accumulated coarse-grained shoaling upwards, chert-carbonate grainstone successions, possible associated with offshore bar development (Pufahl and Fralick, 2000). The tidal aspect is consistent with a geochemical model of iron formation deposition on continental margins near upwelling silica and iron-rich bottom water (Cloud, 1973; Drever, 1974). Current activity is evidenced by redistributed rip-up grains of the chemical precipitates. Paleocurrent data suggests the deposition occurred on a southward facing paleoslope (Pufahl and Fralick, 2000). Storm generated turbidity currents originating on the inner shelf where grain production occurred may have been instrumental for transferring sediment to the distal shelf (Pufahl and Fralick, 2004). With erosion of the source terrain to near base level and reduced clastic supply, iron formation was able to accumulate in the nearshore and directly onlap the Superior Province (Pufahl and Fralick, 2000). Volcanic activity is evidenced by the presence of tuffaceous and volcaniclastic horizons within the iron formation (Hassler and Simonson, 1989).

Dating of zircons from tuffaceous layers near the top of the Gunflint has yielded a pre-Penokean age of 1878 ±1 Ma (Fralick et al., 2002). Euhedral zircons were extracted from rainout and storm-reworked volcanoclastic beds in the upper Gunflint Formation near Kakabeka Falls, Ontario (Fralick et al., 2002). The average $^{207}Pb/^{206}Pb$ age determination of 1878.3 ± 1.3 Ma places the Gunflint Formation sedimentation prior to the Penokean orogeny, supporting a back-arc extensional setting for deposition (Fralick et al., 2002). During the Penokean Orogeny, collision of ~ 1860 to 1889 Ma volcanics of the Wisconsin magmatic terrane with the southern edge of the Superior craton at ~ 1860 Ma (Sims et al., 1989) exposed the basin subaerially (Addison et al., 2005). This age is based on U-Pb geochronology of zircons from tuffaceous layers in the basal Rove and Virginia Formation (Fig. 3). Continued orogenic loading caused resubmergence due to subsequent isostatic depression of the basinal area. A transition to a clastic depositional regime with sediment influx from both northerly and southerly directions (Sims and Peterman, 1983) ensued at 1835 Ma (Addison et al., 2005). Thrusting and development of basement gneiss domes during the Penokean caused deformation and metamorphism of the sedimentary rocks in the southern portion of the basin (Southwick et al., 1988). Syn and post-orogenic calc-alkaline plutonic intrusions into the sedimentary and volcanic rocks were accompanied by a collision of a southern assemblage of arc-related volcanics (Marshfield terrane, Sims et al., 1989). Penokean deformation is intense in the iron formations located in the southern-most portion of the basin

and minor thrusting has recently been recognized in even the northern-most Gunflint iron formation (Hill and Smyk, 2005).

As noted above, at approximately 1835 Ma (Addison et al., 2005), during the final phase of Penokean felsic volcanism to the south, the basin was again flooded by the ocean. The clastic sediments which were deposited during this phase form the research focus of this thesis and are described in more detail in the next section.

At 1.1 Ga a north-northeast trending branch of the mid-continent rift system separated the Animikie basin into two segments. A second, generally north-northwest trending branch of this rift system also truncated what is now the eastern end of the basin (Morey, 1983). Much of the region was then covered by an extremely thick succession of volcanic and sedimentary, rift related rocks.

The Animikie rocks are locally folded where intruded by Keweenawan gabbros of the Logan dikes and sills, and the Duluth complex (Morey, 1983). The sedimentary rocks and intrusives were both affected by later folding and faulting that appear to have been the result of movement along older structures (Morey, 1983). Steeply dipping gravity faults probably of Keweenawan age are common, some with vertical displacements of as much as 100 m (Morey, 1972). The clastic rocks were transformed by contact metamorphic effects to pyroxene-hornfels facies adjacent to thick sills and the Duluth complex and to hornblende-hornfels facies adjacent to thinner sills (Morey, 1972). Some southward tilting appears to have occurred prior to Keweenawan time as evidenced by a

northward overstep of lower Keweenawan strata (the Sibley Group) over the older Precambrian rocks in the Thunder Bay area.

Age of Tuffaceous Zone Horizons

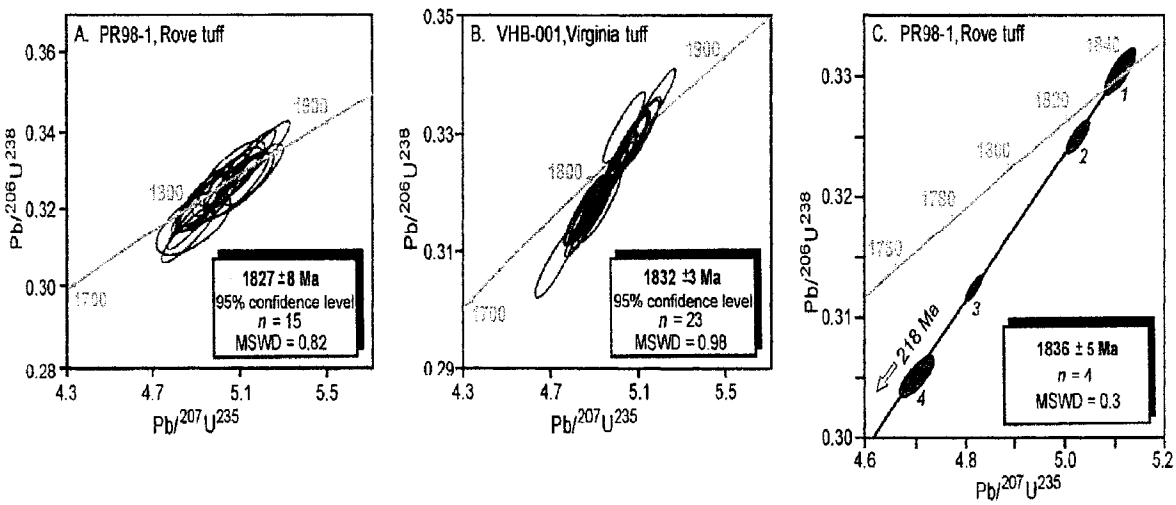

Fig.3. Age of Tuffaceous Zone at the base of the Rove and Virginia Formation (Addison et al., 2005).

1.3 Previous Work:

1.3.1 Rove Formation

Morey (1965, 1967) described the stratigraphy and sedimentology of the Rove Formation, identifying three lithologic units from the study of 120 incomplete sections. They are:

1. a lower argillite unit 120 to 150 m thick.
2. a transition zone of interbedded graywacke and silty argillite, 20 to 30 m thick.
3. an upper unit of graywacke and argillaceous siltstone 823 m thick with thin quartzitic beds within the upper 214 m.

Morey (1965, 1967) described the base of the lower argillite unit as gradational with the underlying iron formation, though more recent work (Addison et al., 2005) reports a disconformity here. Three principal rock types occur within the lower argillitic unit. Thin to thick bedded light gray argillaceous siltstone with sporadic grading and cross-lamination commonly forms the coarsest grained lithofacies. Thinly-bedded dark gray silty argillite and black fissile carbonaceous argillite with laminae generally less than 1.5 mm also occur. These three rock types generally exhibit a stacking from a basal siltstone bed grading to a silty argillite and finally to a carbonaceous argillite (Morey, 1967). The lower portion of the unit is composed mostly of alternating beds of dark gray silty argillite and black carbonaceous argillite. Silt-size material is more abundant in stratigraphically higher beds of the unit (Morey, 1967). Several coarse-grained sandstone beds and many lenses and irregular beds of limestone and dolomite

occur near the base of the unit. Calcite and dolomite concretions are also common within the lower 100 m.

The transitional succession consists of a series of interbedded argillites and sandstones, the sandstone beds increasing in abundance and grain size upward (Morey, 1967). The sandstone beds range in thickness from less than 15 cm to 30 cm. Generally much coarser grained than associated argillites, they are mostly medium dark to dark gray, poorly sorted, and composed of angular grains of quartz and feldspar in a matrix of muscovite and chlorite (Morey, 1967). The felsic grains fine upward within the beds. Thin lag deposits of feldspathic quartzite of varying thicknesses overlie many of the graywacke beds. Contacts between the two are gradational. The upper surfaces of the quartzite beds are irregular and may be rippled, with sharp contacts with overlying argillite beds. Argillite layers varying from less than 25 cm to 3 m thick are interbedded with the sandstones and have a higher silt content than in the lower unit (Morey, 1967).

The uppermost unit composed of interbedded light to dark gray graywacke and argillaceous siltstone constitutes the major part of the Rove Formation (Morey, 1967). It varies in thickness from about 30 m in western Cook County (immediately south of the U.S. border) to about 820 m eastward, though this is a result of the level of erosion. Sandstone beds of less than 30 cm to greater than 1 m in thickness are interbedded with 15 cm to 1 m thick beds of silty argillite and argillaceous siltstone. Gray, white or pinkish-gray feldspathic quartzite beds of varying thicknesses occur within the upper 210 m. Most are graded with sharp upper and lower contacts. These are coarser grained, better sorted and lighter in

colour than those in the transition sequence. They also occur in thicker, more regular beds (Morey, 1967).

A variety of sedimentary structures and bedding types occur within the Rove Formation. The most distinctive feature of the middle and upper units is the remarkably uniform thickness of the individual argillite and sandstone beds (Morey, 1967). Uniform thicknesses were present in the majority of beds observed for extents of at least 900 m along outcrops, although some pinchouts are present. Structures within sandstone beds can include a variety of bedding types including massive, cross-bedding, parallel lamination and convolute bedding. The occurrence of all types within an individual bed is rare, however most beds show several types, which always occur in the same order. The general sequence of structures from the bottom upwards in graded beds is: massive, with or without intraformational clasts; parallel lamination; cross bedding; and parallel lamination which may or may not be convoluted. The consistency of the sequences implies that each of the sandstone beds is most likely the product of a single depositional event (Morey, 1967). Intraformational conglomerates occur at or near the base of some of the sandstone beds. Graded bedding with a fining upward trend is common, as are horizontal laminae with average thicknesses of less than 1 mm. Planar cross-bedding is rare while festoon (trough) cross-bedding occurs commonly (Morey, 1967). Convoluted laminae are rare, occurring near the top of approximately 2% of siltstone beds. Current ripple marks are preserved on the tops of several beds, particularly in the upper unit.

Soft sediment deformation structures are common and include contorted bedding, bed pull-aparts, overfolds and micro-faults. Load casts, clastic dikes and flame structures also occur commonly. Some groove casts of varying size are present and flutes and flute casts are relatively rare (Morey, 1967).

Paleocurrent data indicate that sediments were introduced primarily by currents flowing in a southeasterly direction perpendicular to the basin axis. (Morey, 1967). Morey (1965, 1967) used the orientation of directional sedimentary structures (sole marks, cross bedding, ripples) to determine paleocurrent directions. Each recognized directional structure was measured at each exposure for general orientation by taking at least three readings on three different individuals in each bed (Morey, 1967). Greatest consistency was obtained from flutes and grooves (60 measurements) which indicated a predominantly south-south-easterly flow direction (170°) with a spread of only 70°. Greater scatter of 135° was obtained from cross bedding (50 measurements) with variability from south-west to south-east (180°-170°). A limited number of ripple marks (40 measurements) indicated southwesterly-flowing (260°) bottom currents approximately parallel to the axis of the basin (Morey, 1967). Flow directions of ripple marks found on tops of beds containing sole marks conflicted nearly perpendicularly with flow directions of the sole marks indicating reworking of some of the previously deposited sediments (Morey, 1967).

The nature of the sediments indicates a primary source area to the north consisting of early Precambrian granite, gneiss, and metamorphosed

sedimentary and volcanic rocks (Morey, 1967). The beginning of Rove deposition was initiated by uplift of the source area, resulting in an influx of fine-grained clastic material which accumulated in a shallow, though quiet anoxic environment. Basin subsidence exceeding fill rate produced a bottom slope allowing the progression of coarser silt and sand size material to greater depths (Morey 1967).

A 25 to 70 cm thick laterally correlative layer within a recrystallized silicified carbonate unit immediately below the base of the Rove and Virginia Formations contains evidence of meteorite impact ejecta (Addison et al., 2005). Zircon geochronologic data from tuffaceous horizons bracketing the layer reveal it formed between 1878 Ma and 1835 Ma, indicating the Sudbury impact event as the probable source (Addison et al., 2005). Zircons extracted from tuffaceous layers near the base of the Rove and Virginia Formations were dated by sensitive high-resolution ion microprobe (SHRIMP) (Addison et al., 2005). U-Pb ages of 1827 ± 8 Ma and 1832 ± 3 Ma were derived from the Rove and Virginia Formations respectively (Fig.3). Rove zircons were also analyzed by isotope-dilution thermal ionization mass spectrometer (ID-TIMS), yielding an age of 1836 ± 5 Ma (Addison et al, 2005) (Fig. 3). This evidence strongly supports the correlation of the Rove and Virginia Formations, and the underlying Gunflint and Biwabik Formations. It also indicates a major hiatal surface between the 1878 Ma upper iron formation and 1835 Ma lower clastic succession. Detrital zircons in sandstone from the upper Rove Formation approximately 400 m above the base yielded a U-Pb minimum detrital zircon age of 1780 Ma (L. Heaman, personal

communication, University of Alberta) (Fig. 4). Subaerial exposure of the iron formation concurrent with the Penokean Orogenic activity to the south was followed by resubmergence of the basin probably caused by isostatic readjustment following continued orogenic loading. Transgression initiated deposition of siliciclastic sediments. The age determinations (above) place sedimentation commencing during the final stages of Penokean igneous activity and continuing over an extended period of at least 60 Ma.

Poulton et al. (2004) have postulated that a change from oxic to sulphidic conditions in the oceans influenced the end of deposition of banded iron formation. They suggest that increasing atmospheric oxygen levels enhanced sulphide weathering on land resulting in an influx of sulphate to the oceans. Rove Formation sediment geochemistry indicates increasingly sulphidic conditions upward through the successions (Poulton et al., 2004).

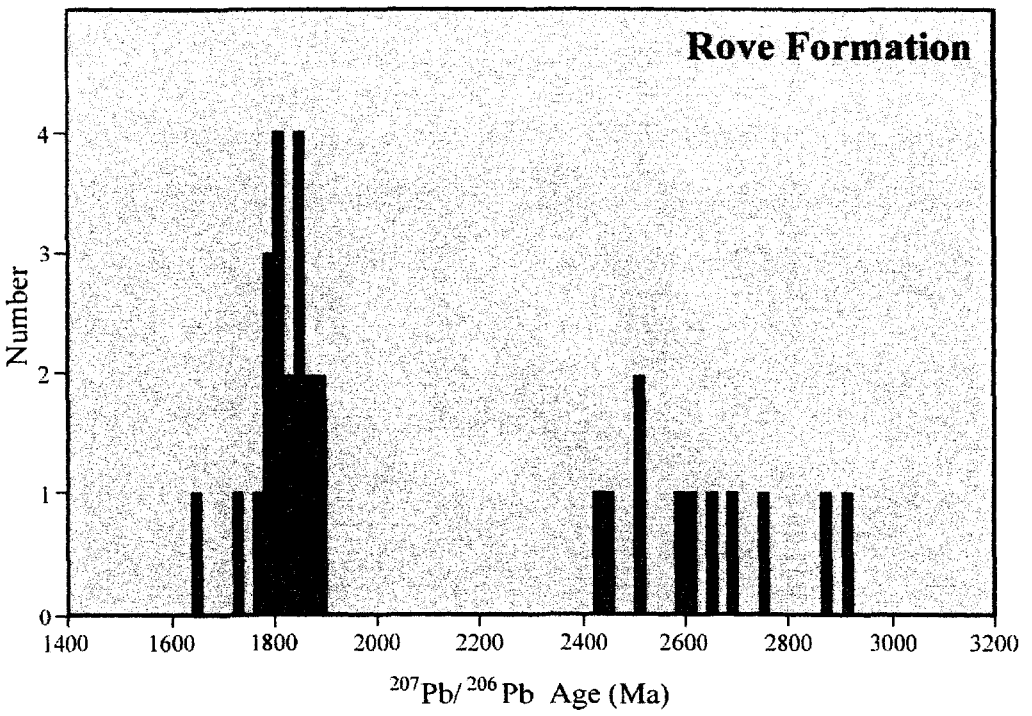

Fig.4. U-Pb, ICP-MS age determinations of detrital zircons in a sample from the upper Rove Formation. The sample was collected by M. Easton (Ontario Geological Survey) and analyzed by L. Heaman personal communication (University of Alberta). The 1630 Ma age has a 100 m.y. error bar and the 1660Ma is negatively discordant . Thus, the analyses indicate an age of 1780 Ma or younger for the upper Rove.

1.3.2 Virginia Formation

Through examination of approximately 1060 m of drill core (Fig. 5) of unmetamorphosed Virginia Formation from 4 sites, Lucente and Morey (1983) identified two distinct members, a lower argillaceous lithosome and an upper silty and sandy lithosome (Fig. 6).

The lower argillaceous unit thickens westward varying from approximately 125 m at the eastern end of the Mesabi range to approximately 300 m south of Calumet, both upper and lower contacts being gradational (Lucente and Morey, 1983). Lucente and Morey (1983) further believed that interbedded limestone, argillite, chert, slaty silicate-carbonate facies iron formation and ash-fall tuff forming the lower transition zone from Biwabik iron formation, indicate that clastic and chemical sedimentation and volcanism operated contemporaneously during this interval. The unit is dominated by an abundance of dark-coloured, fissile carbonaceous argillite. Very thin beds and laminae of dark argillaceous siltstone, lighter silty argillite and bluish-gray to white chert occur locally toward the eastern drill hole. South of Calumet the unit is characterized by scattered centimeter thick beds of arkose and by approximately 27 m of interbedded iron-poor argillite and cherty sideritic iron formation at its base (Lucente and Morey, 1983).

The transition from the lower argillaceous lithosome to the overlying upper silty and sandy lithosome is gradational. The upper unit is characterized by approximately 30% fine grained siltstone interbedded with 5% fine-grained

sandstone in 1 to 5 m thick packages separated by 6 to 30 m thick intervals of argillite. Individual beds of the siltstone and sandstone range in thickness from several mm to approximately a meter (Lucente and Morey, 1983).

Carbonate concretions occur throughout the Virginia Formation. Most lie within argillaceous intervals and are lenticular or elliptical in shape (Lucente and Morey, 1983).

Lucente and Morey (1983) considered four different depositional processes to be operative at various times:

1. The deposition of mudstone by pelagic processes involving the slow accumulation of fine-grained sediments from dilute suspension, or by hemipelagic processes involving the action of slowly flowing diffuse turbidity currents.
2. The deposition of poorly sorted sandy and silty beds, including allochemical limestone units, by the action of sediment-laden turbidity currents.
3. The deposition of well-sorted sandy beds by the action of nonturbidity currents that reworked previously deposited sediments.
4. The deposition of chert and iron-rich beds by chemical processes during periods of reduced clastic influx.

The formation's early history was characterized by the slow deposition of black mud, now argillite, in quiet water below wave base. The presence of locally abundant carbonaceous material implied deposition under anoxygenic conditions, possibly in deep water (Lucente and Morey, 1983). Periods of

reduced clastic supply resulted in the dominance of episodic chemical depositional processes.

Subsidence of the basin and uplift of the bordering craton likely resulted in the change from a chemical to a clastic depositional regime at the Biwabik-Gunflint / Rove-Virginia-Thompson contact (Lucente and Morey, 1983). The added presence of minor amounts of fine-grained pyroclastic material during the transition indicates volcanism was contemporaneous, with the source area somewhat distant from the basin. Continued subsidence exceeding fill rate produced a bottom slope, with the introduction of silt and sand by turbidity currents. Lucente and Morey (1983) considered the abundance of thin-bedded turbidites to indicate deposition from a number of partially overlapping submarine fan lobes. Minor thick-bedded turbidite occurrences are considered to have originated proximal to the edge of the basin near or within feeder channels. Hemipelagic or pelagic mud interbedded with the turbidites indicate diversion or extinction of a feeder system for a submarine fan lobe. The presence of scattered sandstone lenses 1-3 cm thick within the upper part of the lower argillaceous unit south of Calumet is attributed to the operation of bottom hugging currents in this area (Lucente and Morey, 1983).

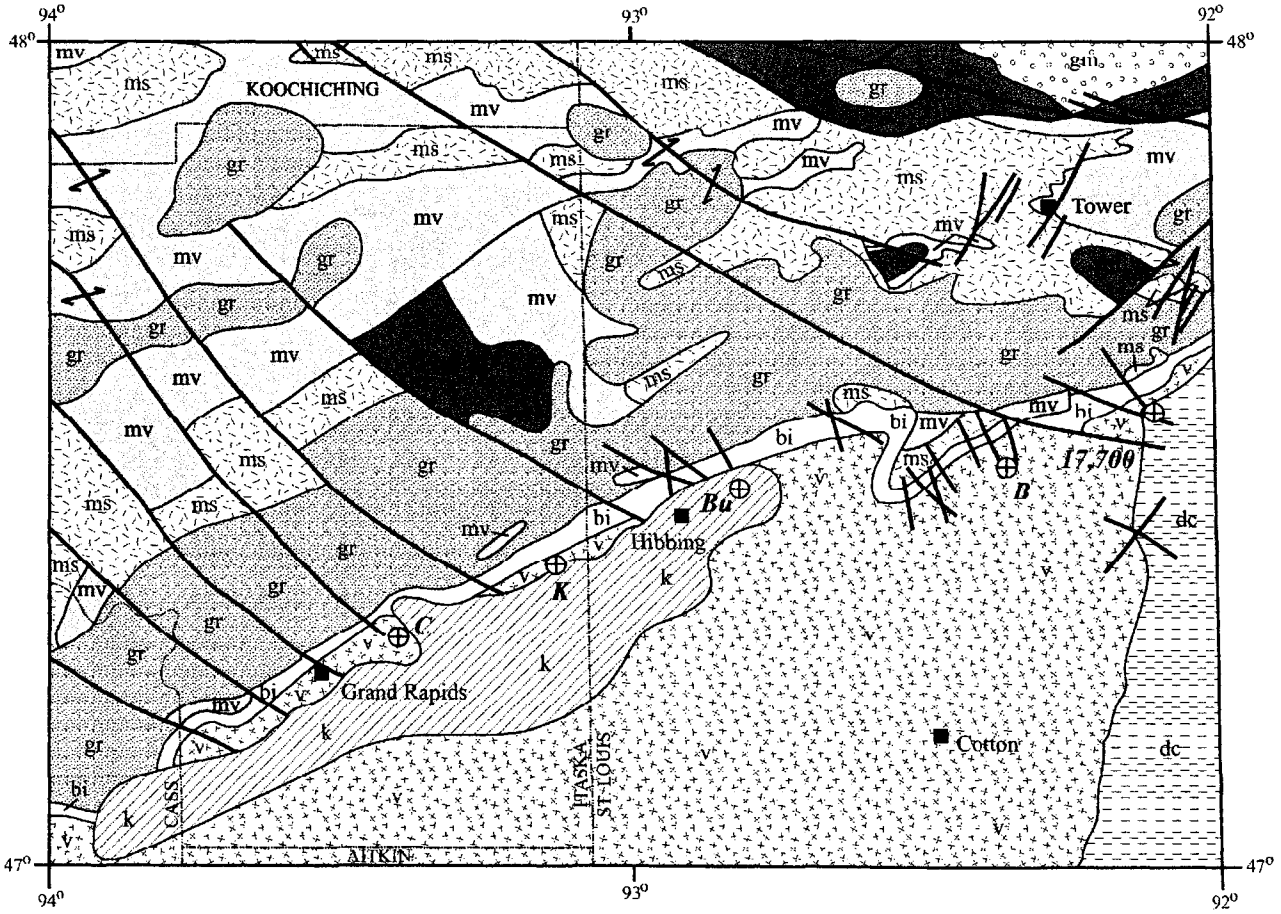

EXPLANATION

k	clastic sedimentary rocks, undivided
dc	Duluth Complex, undivided
v	Virginia Formation
bi	Biwabik Iron Formation and Pokegoma Quartzite
gr	granitic rocks including the Giants Range batholith in the central part of the sheet
ms	metamorphosed sedimentary and felsic volcanic rocks, undivided
mv	metamorphosed mafic-intermediate volcanic rocks
sm	paragneiss and schist-rich migmatite
gm	granite-rich migmatite

Fig. 5 Geologic map of the Mesabi range, Core location of MGS-8(C), MGS-7(K), MGS-6(Bu), and MGS-2(B) holes (Lucente and Morey, 1983).

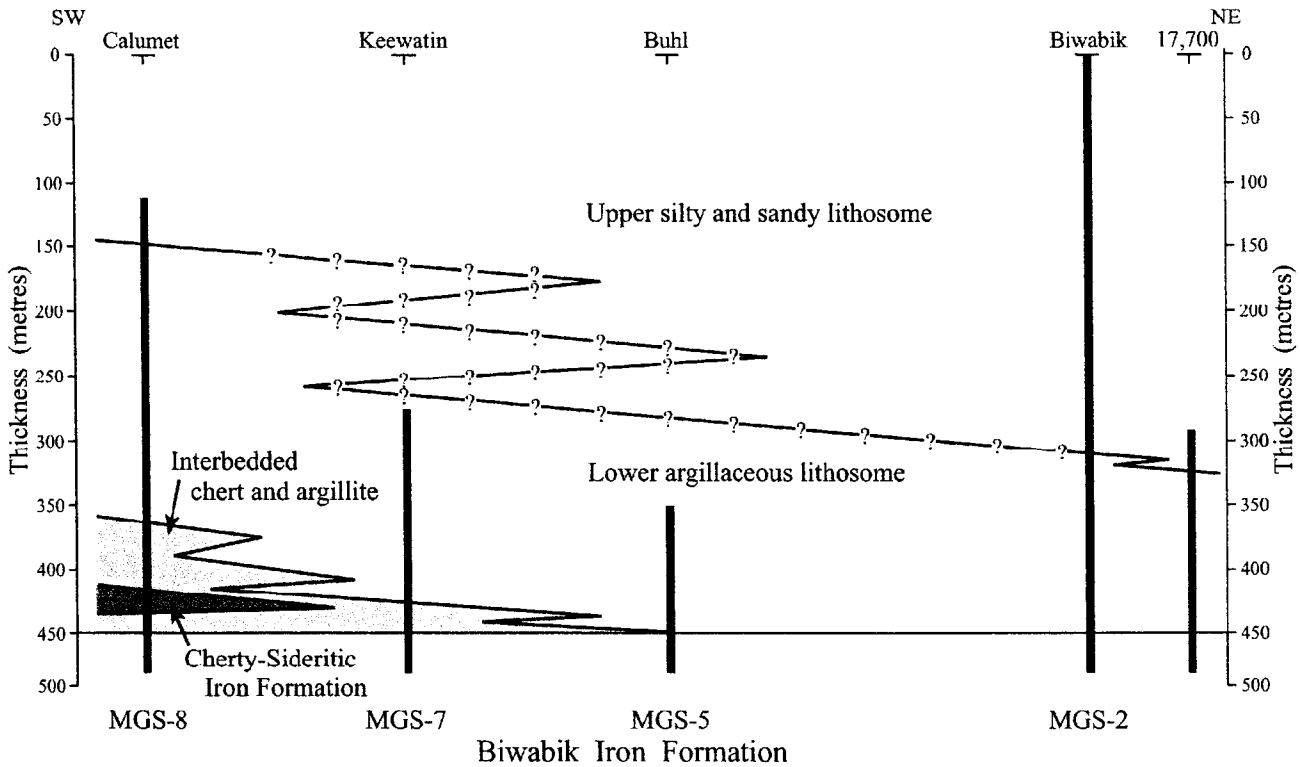

Fig. 6. Correlation of drill holes MGS-8, MGS-7, MGS-5 and MGS-2. (Lucente and Morey, 1983).

1.3.3 Thomson Formation

An investigation of the sedimentology of the Thomson Formation of east-central Minnesota by Morey and Ojakangas (1970) discovered numerous similarities with the Rove Formation. Comparison of lithology and stratigraphy indicates derivation of the sediments from a similar source terrain and deposition by similar mechanisms. The interbedded metagraywackes, metasiltstones, and slates of the Thomson Formation have similar bedforms, sedimentary structures, and carbonate concretions as the Rove. The Thomson Formation differs in containing beds of limestone, graphitic black slate and sulphide or carbonate facies iron formation in its lowermost portion.

Thickness has been estimated at greater than 6000 m but is difficult to discern accurately due to lack of continuous exposures, absence of recognizable marker beds and because neither the top nor bottom of the formation is exposed (Morey and Ojakangas, 1970). Metamorphism during the Penokean Orogeny produced greenschist facies metamorphism which increases in grade to the south.

Paleogeographic, stratigraphic mineralogical and geochronologic considerations indicate that the Thomson Formation, the Virginia Formation and the Rove Formation are probably correlative representing deposition in different parts of the basin (Morey and Ojakangas, 1970). The Virginia and Rove

Formations are located just south of the apparent north shore of the basin, while the Thomson Formation is considered to have been deposited at least 100 km farther from the shoreline. The original muds settled slowly from suspension, with the silt and sand probably deposited by turbidity currents down a southward dipping paleoslope (Morey and Ojakangas, 1970).

1.4 Purpose of the Study

Previous studies of these formations have mainly been concerned with stratigraphy and sedimentology. Many of the factors influencing sedimentary deposition such as eustacy, subsidence, sediment supply, climate and basin configuration have not previously been dealt with in depth. The intent of this study is to incorporate recent techniques such as sequence stratigraphy along with detailed logging of the core to determine stratigraphy and correlation of the facies. This will include consideration of the tectonic regime operating at the time and its effect on the sedimentary processes which produced these formations. Quantitative studies were also conducted using ICP-AES (see section, 2.2.2.1) to ascertain the geochemistry of tuffaceous zones. As well some microscopic examinations of siltstone horizons within shale were undertaken.

CHAPTER 2: LITHOFACIES DESCRIPTIONS

2.1 Logging techniques

A total of 3200 m of core from eleven continuously drilled holes (89-MC-1, PR-99-4, PR-98-1, PR-98-2, PR-98-3, MGS-2, LWD-99-1, MGS-5, MGS-7, MGS-8, 18290) and one twice drilled hole (GF-3) extending from southwest of Duluth to northeast of Thunder Bay were examined and logged in detail. Locations of core sites in Canada and the USA are given in Figures 7 and 8. Graphic logs averaging approximately 5 m in length were drawn for each of the logged holes.

Three basic sedimentary lithologies are present, (shale, siltstone, and sandstone) as well as tuffaceous units. Only sharp contacts were noted. Load structures such as flames, load-casted ripples, and ball-and-pillow structures were noted when encountered. Features such as current ripples, climbing ripples, cross-stratification, flaser, lenticular and wavy bedding were recorded. Bedding planes in the same lithofacies were noted and marked as shorter horizontal lines on the graphic logs. A typical example of a section of a graphic log derived from these data is given in Figure 9.

Shale and siltstone in some cases were difficult to log, mixing of the two occurred and the two lithologies were commonly finely interbedded. Where shale and siltstone formed thicker distinct layers they were graphed as such. A scale

of 1/100 was used, and bedding thicknesses were drawn to scale. Tuffaceous zones were marked off to the left and veins and diabase were noted. Figure 9 depicts a typical log graph of units which were clearly defined while Figure 10 represents lithologies which were finely interbedded making distinction between them more difficult. Diabase sheets were labeled but not drawn to scale.

All drill-holes were used for correlating across the basin, except core #18290, which was highly modified due to folding. Features of lithofaces, coarsening upwards trends, areas dominated by shale, diabase, and tuffaceous zones were all used systemically in correlating. The northeast section of core presented little difficulty, due to the presence of concordant diabase horizons and similarities in lithofacies.

Iron formation was present and used as a base line for correlation in all cores with the exception of PR-99-4, PR-98-2, and PR-98-3. In cores PR-99-4 and PR-98-3 diabase horizons were used in conjunction with diabase at similar stratigraphic levels in cores 89-MC-1 and PR-98-1 respectively. A diabase horizon approximately 200 m above the baseline correlates across cores 89-MC-1 and PR-99-4, and PR-98-1. Another diabase horizon at approximately 340 m correlates across cores PR-99-4, PR-98-1, and PR-98-2. Three distinctive sandstone beds at approximate elevations of 485, 520, and 530 m were used for correlation between cores PR-98-2 and PR-98-3. Correlating on the basis described above provided a starting point from which more detailed correlation sedimentary lithologies could be made.

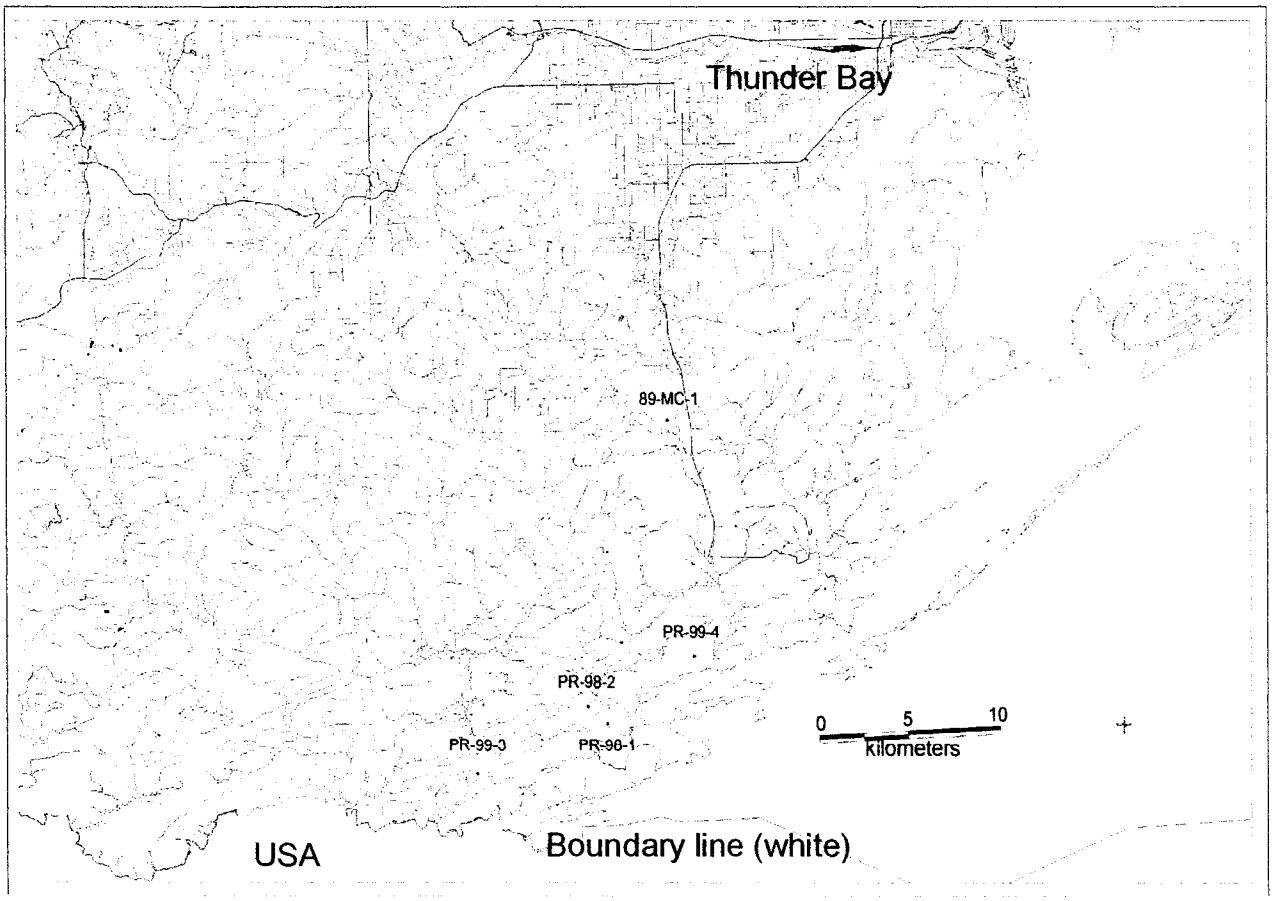

Fig. 7. Location of cores in Canada near Thunder Bay which is in the upper right corner. USA (white area) is to the south of Thunder Bay (Ministry of Northern Development and Mines).

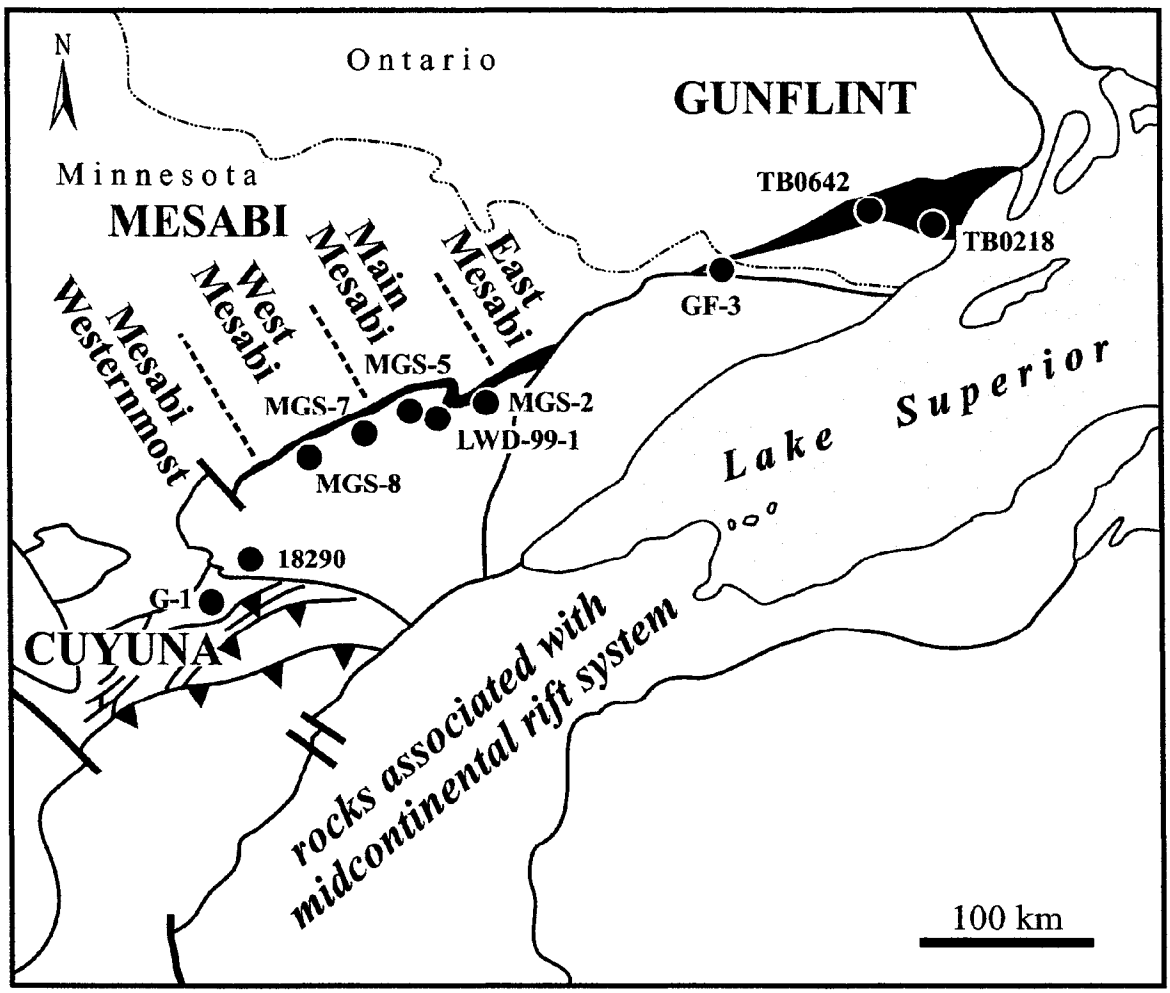

Fig. 8. Locations of cores in Minnesota area. Core TB0218 is MC-89-1 and Core TB0642 was not logged (modified from Pufahl, 1996).

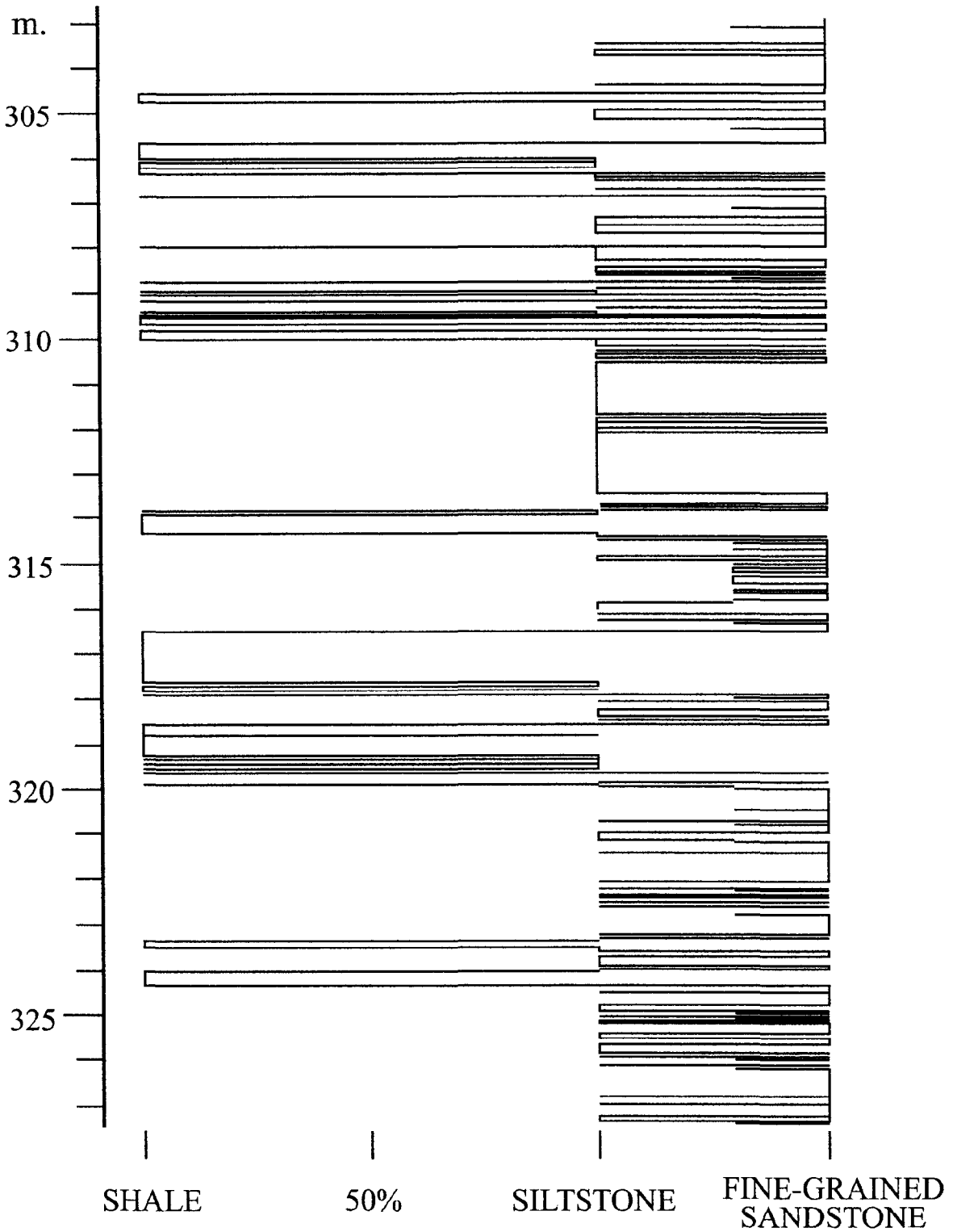

Fig. 9. An example of section of a cored drill-hole logged and drawn according to thickness and type of sediment.

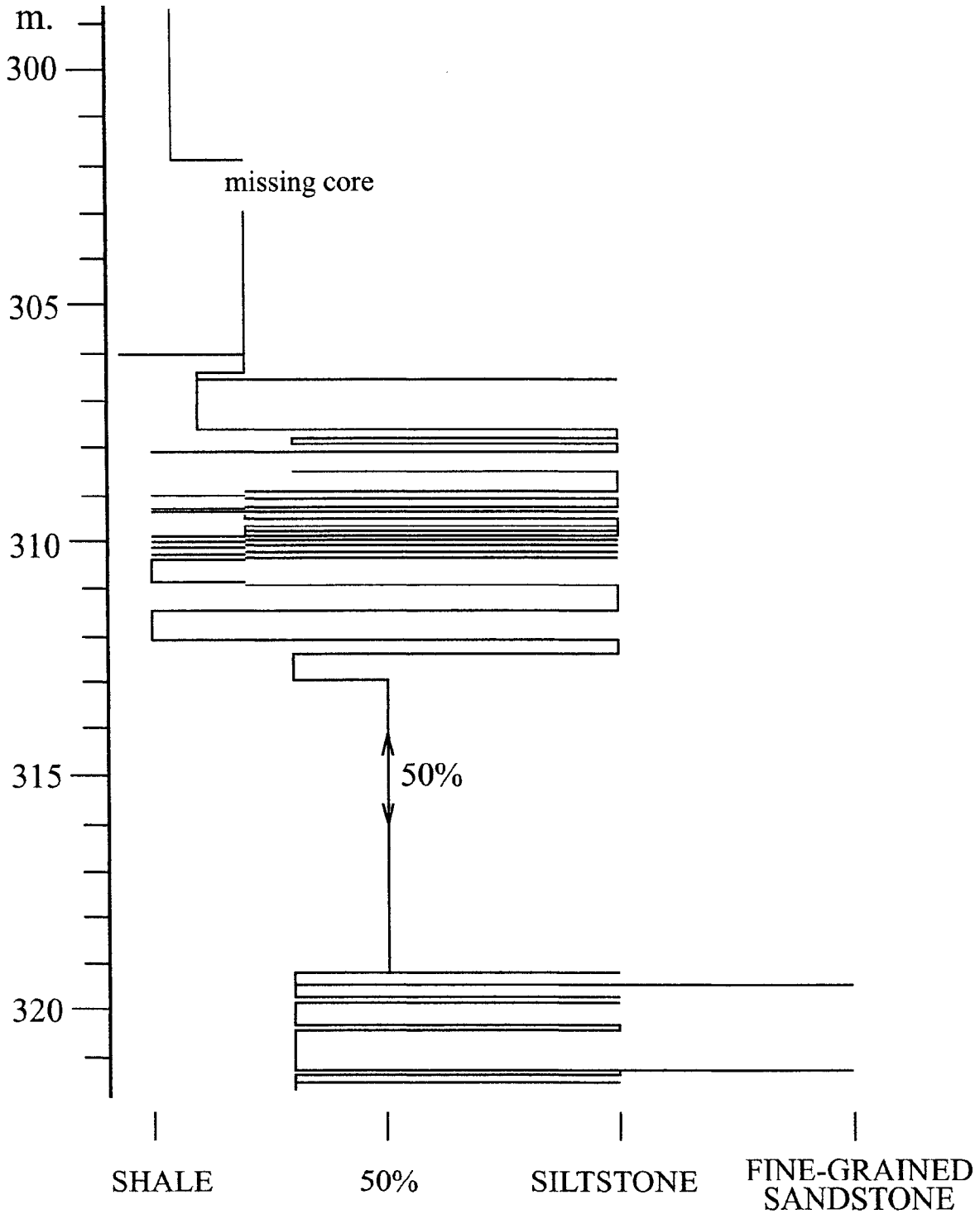

Fig. 10. Logging technique estimating percentage of shale to siltstone.

2.2 Units Present:

Seven different units were identified and correlated according to common attributes and location of tuffaceous horizons (Fig. 11). The lowest unit, the basal siltstone and shale was deposited on the subaerially weathered (Addison et al., 2005) Gunflint surface during initial flooding of the basin. Approximately 15 m in thickness, it correlates across the entire basin with the exception of core MGS-5 in which it is absent. The second unit is finer grained, carbon rich and dominated by shale. This starved succession is correlative across the basin and has two coarser grained units sandwiched within it. A siltstone and shale succession up to approximately 30 m thick is present within the lower half of the shale unit and, like the other two units outlined above is traceable across the basin. A coarser grained clastic wedge occurs within the upper half of the shale unit. It thins to the north and does not extend into the Rove Formation north of the Duluth intrusive complex. The combined thickness of this sandwich of units averages approximately 100 m. Tuffaceous layers occur in the lower units. The shale unit is succeeded by two coarsening and thickening upwards successions of graded beds which represent the first sizable influx of sand into the basin. Reaching a maximum thickness of approximately 80 m, these thin slightly toward the north and south, and are composed of shale, siltstone, and sandstone. The next unit is approximately 400 m thick. It is sand dominated and composed mostly of coarsening upwards cycles of graded beds each separated by a few tens of centimetres to metres of black shale. Sediment influx was from the north

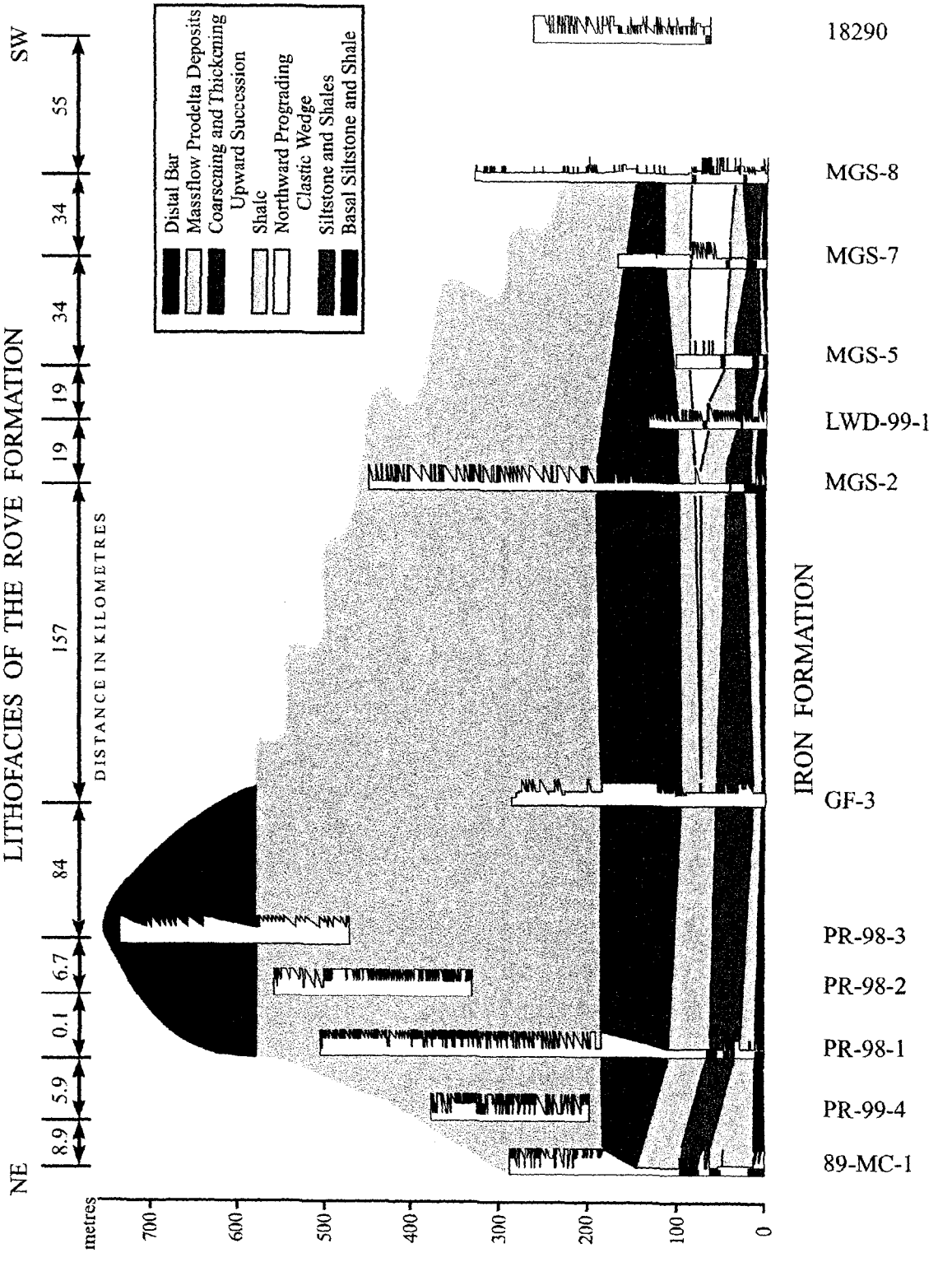

Fig. 11. Correlation of the drill holes in the Rove and Virginia Formations. Red bars on core are tuffaceous intervals

and west (Morey, 1967). The uppermost unit is present only in core PR 98-3. It is approximately 150 m thick and composed of shale, siltstone and sandstone. Sandstone with ripple laminations dominates the upper portion.

2.2.1 Basal Siltstone and Shale

The underlying iron formation is present at the base of cores, 89-MC-1, PR-99-4, GF-3, MGS-2, LWD-99-1, MGS-5, MGS-7, and MGS-8. The basal Rove/Virginia Formation is composed of a tuffaceous zone, shale, siltstone, and sandstone. The siltstone and sandstone layers fine upwards in core 89-MC-1 and coarsen upwards in cores PR-98-1, GF-3, MGS-2, LWD-99-1, and MGS-8. Several tuffaceous ash layers are interbedded in this assemblage. Finer black shale is present in cores 89-MC-1, PP-99-4 and MGS-2, and silty-shale in cores GF-3, LWD-99-1, MGS-5, MGS-7, and MGS-8. Further southwest, sandstone layers occur with less frequency than in more northeasterly cores, but are present in all cores except MGS-5.

The assemblage of shale, siltstone, and sandstone, and tuffaceous zones thins from the northeast to the southwest and is virtually absent in core MGS-5. Siltstone dominates this section.

Tuffaceous layers: Highly fissile light green layers with sharp bottom and top contacts with the less fissile siltstones are common in this assemblage. The tuff is very fine grained with only small amounts of silt-sized material (Figs. 12 and 13). Layers average 3cm thick with the thickest layer 12 cm. The thinner layers commonly are the same colour from bottom to top and very sharp sided. The

thicker layers commonly become greyer in their upper 1 to 4 cm denoting a greater presence of detrital clay and silt mixed with the volcanogenic material in this zone (Figs. 14 and 15).

The tuffaceous layers are also present in overlying units, though a trend towards an increase in the amount of intermixed siliciclastic material appears to occur upwards. This results in uncertainty as to whether some layers contain tuffaceous material. Geochemistry was used to further identify tuffaceous intervals as the geochemistry of the tuffaceous zones is quite distinct from the siliciclastic sediment.

Fig.12. Basal Siltstone and Shale unit, highly fissile tuffaceous layers between coherent siltstones with sharp top and bottom contacts. Up is to the left Core MC-89-1

Fig.13. Basal Siltstone and Shale unit, fine grained sandstone just below the tuffaceous layer. Up is to the left. Core MC-89-1

Fig.14. Basal Siltstone and Shale unit, highly fissile tuffaceous layers which vary in colour from light to darker green. Up is to the left. Core MC-89-1.

Fig.15. Basal Siltstone and Shale unit, less fissile tuffaceous layer. Up is to the left. Core MC-89-1.

2.2.2.1 Geochemistry of Tuffaceous Zones

Inductively coupled plasma-atomic emission spectrometry (ICP-AES) was used to determine elemental abundances present in some of the tuffaceous zones.

Twenty samples were selected from what appeared to be tuffaceous intervals in logged cores. In addition to the distinctly coloured, fissile tuffaceous horizons, tuffaceous material also occurs in other beds where its appearance may be masked by abundant detritus derived by erosional processes. Samples were crushed to approximately 75 microns in size using a tungsten ball mill. Dissolution of samples was carried out as follows: 0.5 grams were weighed out and placed in Teflon crucibles, then 10 ml of double distilled de-ionized water and 5ml of nitric acid was added to each sample and left at 90°C for 12 hours. Crucibles were then filled with 10 ml nitric acid and 5 ml hydrofluoric acid and left at low heat for 12 hours (this addition of nitric and hydrofluoric acid was repeated three times). On the last cycle temperature was increased to 150° C and samples evaporated to dryness. The temperature was then turned down to 90° C, 5 ml of hydrochloric acid was added and simmered for 10 minutes. Solutions were transferred to a 100 ml volumetric flask and made up to 100ml by addition of double distilled de-ionized water upon cooling. For each run three blanks were prepared and one internal standard (Tables 1 and 2).

Table 1.
Geochemistry data results, major and minor elements
Data of Rove and Virginia Formation tuff locations and depths of samples.

Sample	Core	Depth	Al2O3	CaO	MgO	Na2O	K2O	Fe2O3	MnO	TiO2	P2O5
1	PR-88-1	627.90	15.86	0.95	1.19	0.91	4.70	2.43	0.027	0.27	0.068
2	PR-98-1	621.25	8.89	0.44	0.55	3.20	3.20	1.24	0.013	0.27	0.098
3	GF-3	834.46	7.20	11.30	2.11	0.76	0.13	13.72	0.523	0.20	0.081
4	GF-3	813.35	15.48	5.83	3.95	3.37	3.12	5.50	0.350	1.01	0.23
5	MGS-2	474.22	24.34	0.35	1.60	1.03	7.59	2.75	0.015	0.70	0.089
6	MGS-2	474.95	20.09	0.18	1.30	0.39	6.65	1.56	0.011	0.40	0.38
7	MGS-2	479.60	22.13	0.44	1.53	1.22	6.75	2.89	0.016	0.90	0.15
8	MGS-2	476.45	23.75	0.25	1.55	0.46	7.85	1.81	0.014	0.57	0.024
9	MGS-2	444.25	24.27	2.20	1.44	1.04	7.40	2.18	0.036	1.21	0.13
10	MGS-2	480.15	24.17	0.33	1.66	0.60	8.14	2.21	0.010	0.57	0.055
11	MGS-5	151.50	8.35	11.47	3.39	0.62	2.40	9.38	1.55	0.27	0.071
12	MGS-5	149.01	21.98	0.80	1.74	0.40	9,04	2.55	0.40	1.23	0.15
13	MGS-5	150.01	17.70	0.25	1.63	0.38	7.72	4.12	0.037	0.56	0.12
14	MGS-5	144.40	21.34	0.67	1.53	0.35	8.27	3.13	0.037	1.36	0.34
15	MGS-7	207.01	22.06	0.45	2.87	0.53	7.38	2.68	0.057	0.60	0.16
16	MGS-7	207.25	24.66	0.55	2.05	0.61	8.42	1.62	0.036	1.50	0.19
17	MGS-7	216.01	23.06	3.42	2.09	0.53	8.00	3.20	0.56	0.53	0.10
18	MGS-7	216.55	22.48	2.93	1.96	0.43	7.80	3.01	0.49	0.50	0.092
19	MGS-7	102.90	24.43	0.48	1.63	0.80	7.62	3.02	0.024	1.36	0.16
20	MGS-8	304.50	25.80	0.08	1.60	0.37	8.87	2.14	0.021	0.62	0.036
Rove Tuff x, n=3			25.57	0.43	3.51	0.13	8.03	1.48	0.010	0.53	0.013
Rove Sandstone x, n=7			12.95	1.22	2.61	1.08	3.88	4.30	0.030	0.53	0.11

Table 2.
Geochemistry data results, trace elements
Data of Rove and Virginia Formation.

Sample	Ba	Ce	Cr	Li	Nb	Ni	Sr	V	Y	Zr
1	591	93	32	26	12	18	96	22	14	202
2	340	227	31	18	17	17	31	77	37	193
3	24	59	38	19	3	83	73	56	38	82
4	922	103	184	61	13	73	192	136	47	226
5	892	28	47	41	24	25	54	52	65	581
6	554	190	8	27	21	8	33	36	103	820
7	792	100	126	49	21	24	60	385	59	498
8	711	40	12	44	29	9	41	42	123	976
9	904	47	15	23	20	24	90	72	71	532
10	568	199	13	45	28	12	46	48	120	772
11	241	48	59	56	1	64	127	191	20	93
12	626	39	23	48	22	17	53	193	45	460
13	771	154	77	92	12	42	41	183	32	261
14	1130	103	40	25	17	30	56	146	65	440
15	489	36	30	110	10	16	45	107	32	350
16	453	140	21	62	30	8	54	160	47	785
17	557	324	24	37	30	26	59	17	92	564
18	539	270	7	36	29	18	55	16	85	523
19	856	64	18	26	24	18	73	75	77	567
20	1400	133	8	57	42	11	36	21	147	1043
Tuff	206	227	7	59	22	5	54	5	119	1150
Sandstone	472	44	90	46	5	43	64	81	13	134

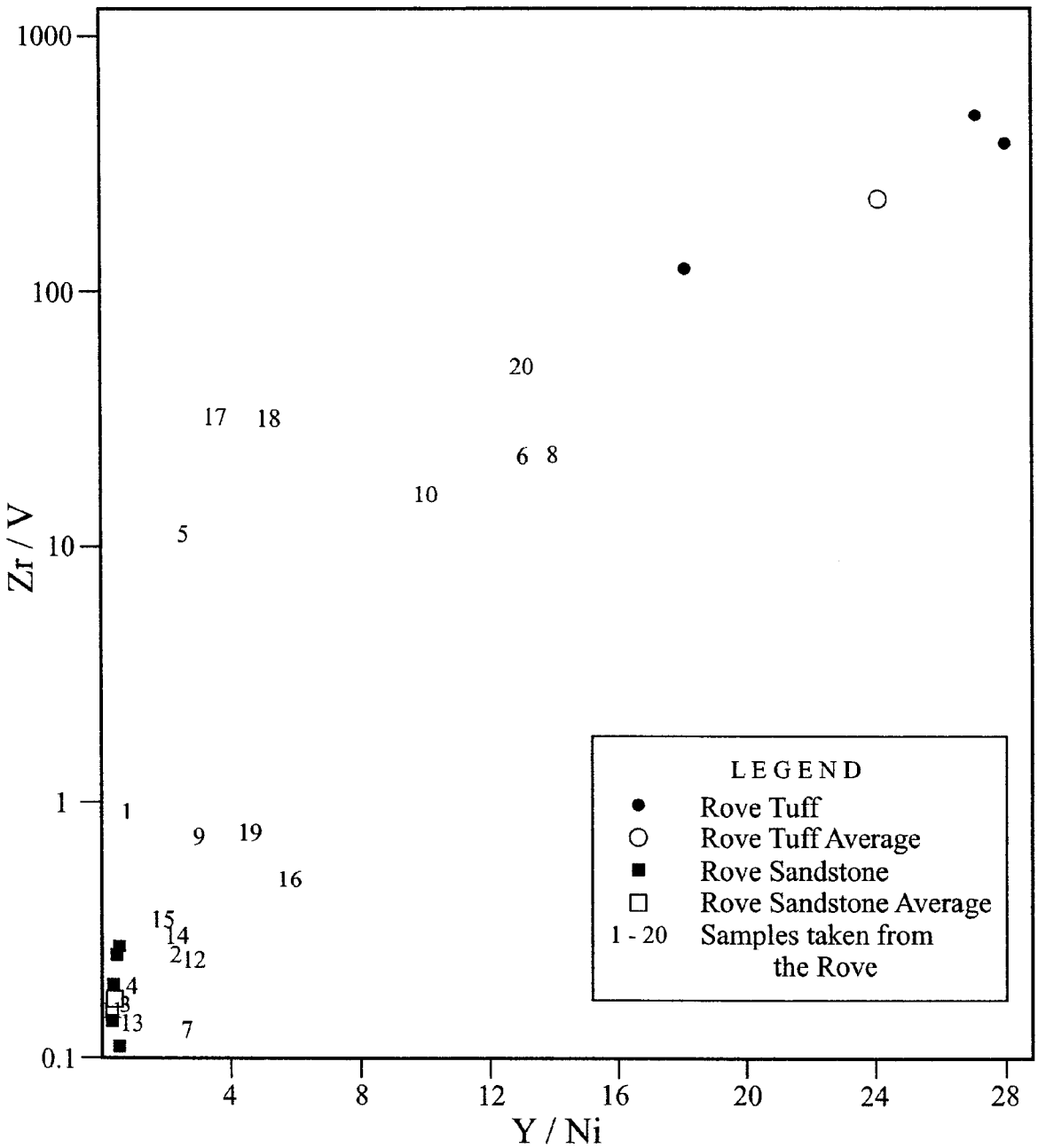

Fig.16. Graph of elemental ratios for layers possibly containing tuffaceous material. Note the mixing trend between the pure tuffaceous and pure siliciclastic end members. Sandstone samples from MC-89-1.

The extreme high field strength element (HFSE) enrichment in the felsic tuffs (Hemming et al., 1995) enable the identification of this detritus even when mixed with large quantities of low HFSE bearing erosional detritus. Tables 1 and 2, and Figure 16, clearly demonstrate that these samples contain varying mixtures of volcanogenic and clastic detritus. Samples 3 and 4 from core GF-3 and samples 11 and 13 from core MGS-5 fall on the averages of pure Rove Sandstone and therefore can be eliminated as containing tuffaceous material.

Tuffaceous zones in the drill core, delineated in Figure 11, are outlined below. All depth measurements are taken upwards from the base of the formation to the base of each tuffaceous zone, their thickness extending upward.

Core 89MC-1 contains three zones, one in each of the lower units. A 10 m thick zone occurs at the base of the formation, and two others at 50 m and 80 m with thicknesses of 8 m and 10 m, respectively. Similarly, core PR-98-1 also contains three zones, one in each of the lower units. A 5 m thick zone occurs at the base. The others at 35 m and 55 m are both 6 m thick. Core MGS-2 contains a 15 m thick zone at the base of the formation and a 2 m thick zone at 25 m within the Siltstone and Shale Unit. Two zones occur in core LWD-99-1. The first at 20 m in the Siltstone and Shale Unit has a thickness of 1 m and the second at 70 m within the Northward Prograding Clastic Wedge Section is 2 m thick. Core MGS-5 contains three zones, each 3 m thick, one at the base and the others at 8 m in the Basal Siltstone and Shale Unit, and at 50 m in the Siltstone and Shale Unit. Core MGS-7 contains three zones, an 8 m thick one 10 m above the base within the Siltstone and Shale Unit, a 1 m thick one at 100 m

within the Shale Unit, and a 1 cm thick band at the 140 m level within the Coarsening and Thickening Upward Succession. Core MGS-8 contains two zones, each 2 m thick. One occurs at 20 m near the top of the Siltstone and Shale Unit and the other at 89 m in the upper part of the Northward Prograding Clastic Wedge Section. Core 18290 contains a single 1 m thick zone at its base, depth unknown.

The northeast part of the basin contains a significantly greater number of more distinct tuffaceous layers than farther to the southwest. In the southwest part of the basin the tuffaceous zones extend into the Northward Thinning Clastic Wedge, whereas in the northeast part the upper limit of the volcanogenic sediment is the Siltstone and Shale lithofacies (see Fig. 11; red bars on drill logs).

Shales: The very finest black shales are a few millimetres to 5 cm thick. Lighter coloured (dark grey) silty shale layers are up to 25cm thick. The black shales average 0.5 cm in thickness and the dark grey silty shales average 1.0 cm. The black shales are massive with very sharp contacts. The dark grey silty shales are similar but commonly have more silt-rich layers averaging a few millimetres thick within them. Thicker silt layers split the silty shale areas into separate layers. The thin silty layers are internally parallel laminated at the millimetre-scale. The dark grey shale rarely forms the tops of thin graded layers from coarse silt to silty shale averaging about 1cm thick. Most shale-rich units sit on sharp bottom contacts. Approximately 4 m above the basal contact the black shales gradually become more dominant grading into the overlying shale unit.

Siltstones: These form the most abundant layer type dominating areas up to 35cm thick. They are parallel laminated on the millimetres to 1cm scale. The laminations are composed of coarser silt layers and more clay-rich layers. The laminations can be either sharp sided or have diffuse gradational boundaries. Graded layers are rare. Some coarse siltstones up to 5 mm thick are lenticular but do not appear to be internally ripple laminated. There are some irregular erosive scours but these are not very distinct and may be overlain by any of the lithologies.

Sandstones: The uncommon sand dominated intervals are up to 28 cm thick and clay-rich with very fine-grained sand uncommon. Lamination characteristics are similar to those described for the siltstone. Some laminations are composed of fine-grained sand. Small, sand sized mud rip-ups are commonly mixed with the sand. No graded bedding was observed. The grain size of individual, laminations within a bed do not follow any coarsening or fining upward pattern.

2.2.2 Shale

The carbon-rich shales are black to grey in colour and generally featureless. Some tuffaceous zones are present near the bottom of the Shale Dominated Succession in cores 89-MC-1 and MGS-2. The carbon-rich shales prevail in the north east part of the basin with silty-shale more common towards the south west.

Shale dominates this unit with siltstone subordinate and sandstone uncommon. Some tuffaceous layers are present.

Shale: Carbon-rich black to dark grey shale dominates this succession. These shale intervals are meters thick and separated by siltstone-dominated intervals centimetres to 1 m thick (Figs. 18, 19 and 20). The black shales have discontinuous 1 to 2 mm thick fine siltstone layers spaced an average of 1 cm apart throughout the succession (Fig. 21). The shales are characterized by consistently high carbon content throughout. Small masses of pyrite are also common.

Siltstone: The siltstone dominated areas are similar to those in the lowest unit. Some of the coarser silt laminations contain fine sand grains (Figs. 22 and 23).

Sandstone: Sandstones are very rare with commonly only one or two layers a few centimetres thick per cored interval through the unit. Core 89-MC-1, for example has one 2 cm thick, very fine-grained sandstone layer. These sands have a distinctive green colour possibly indicative of the presence of volcanogenic sediment.

Tuff: Tuffaceous layers are much less common than in the lowest unit. They are sharp-sided, occurring in layers up to 12 cm thick. Slightly darker in colour than the tuffaceous intervals lower in this succession, they appear to contain a small amount of carbonaceous mud. The zone 1 cm below the basal contact of one tuffaceous layer contained submillimeter, interlayered tuff and carbonaceous black shale. The tuffaceous layers higher in the succession are medium grey in colour rather than green, probably reflecting a further increase in erosional detritus mixed with the volcanogenic sediment.

Fig.17. Carbon-rich shale, note the fine layers of evenly distributed parallel laminae of siltstone. Up is to the left. Core MC-89-1.

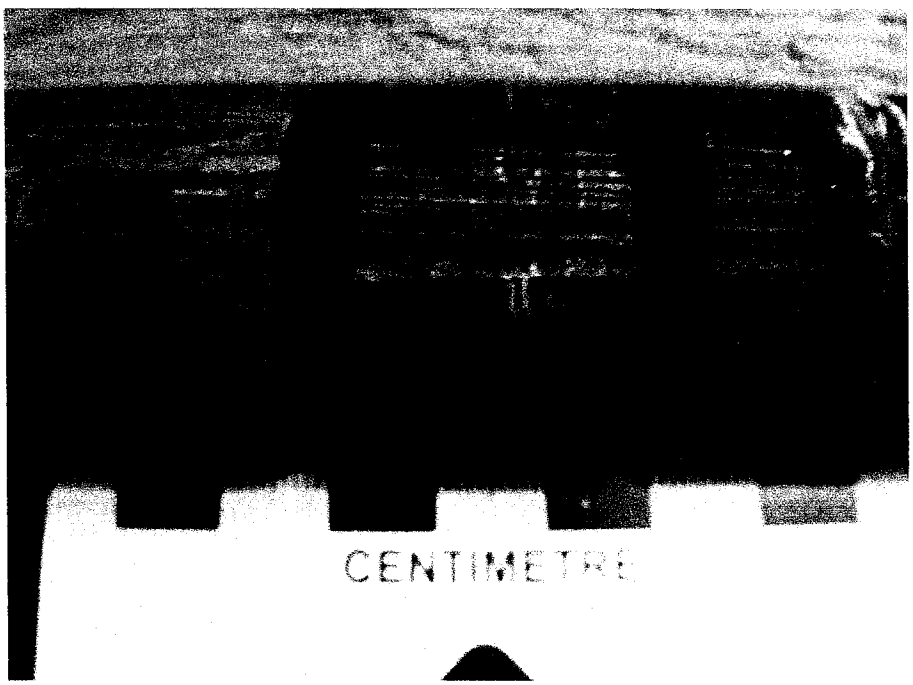

Fig.18. High carbon shale with silty-shale sections. Up is to the left. Core MC-89-1.

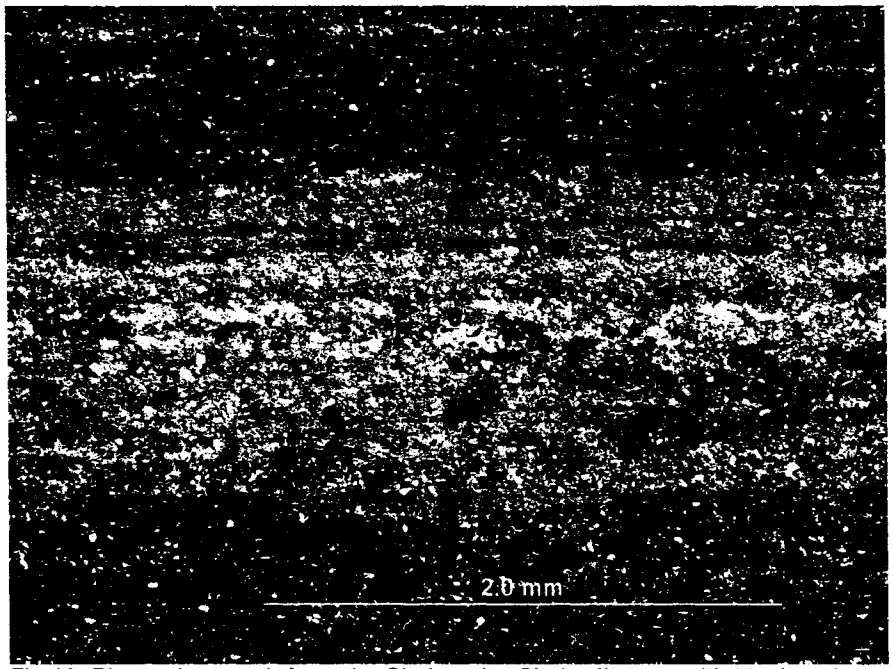

Fig.19. Photomicrograph from the Shale unit. Shaly siltstone with black carbonaceous shale above and below. Shale rip-ups in the silty mid section. Very fine grained sand to silt grains throughout the slide. Photomicrograph-plane polarized light. Core MC-89-1.

Fig.20. Silty-shale with evenly distributed parallel beds of siltstone. Up is to the left. Core MC-89-1.

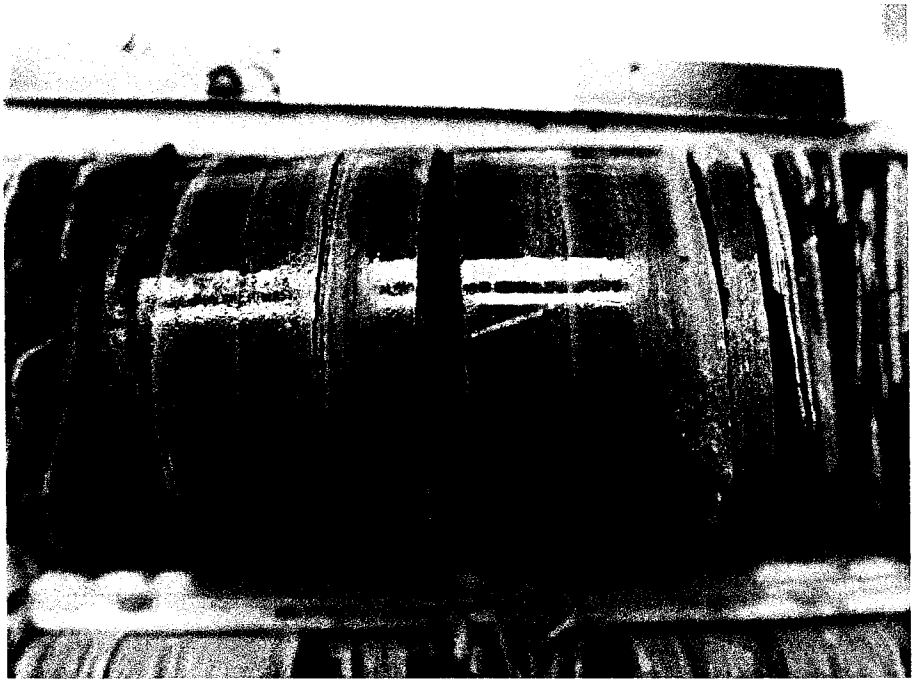

Fig.21. Fining up silty-shale, inter-bedded units of various thicknesss, note rip-ups in the siltstone. Up is to the left. Core MC-89-1.

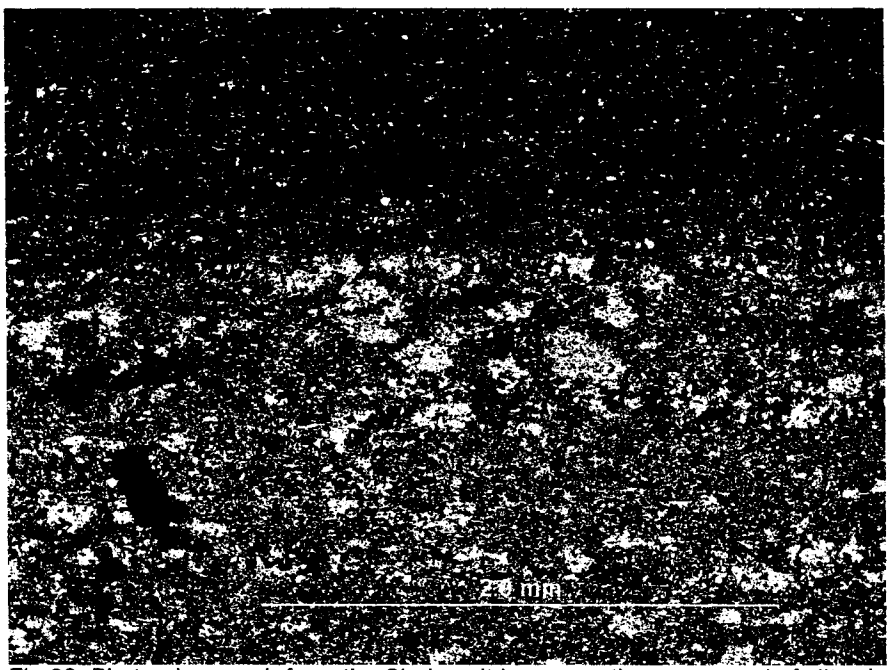

Fig.22. Photomicrograph from the Shale unit Lower section composed of silty shale with black carbonaceous shale and rip-ups. The top section is mainly black carbonaceous shale with very fine-grained sand to silt grains throughout the slide. Photomicrograph-plane polarized light. Core MC-89-1.

2.2.3 Siltstone and Shale

Sandstone dominates the lower portion of this section. The basal sandstone-rich assemblage fines up to siltstone and shale. The unit extends across the basin in cores 89-MC-1, PR-98-4, CF-3, MGS-2, LWD-99-1, MGS-5, MGS-7, and MGS-8. Tuffaceous zones are present, with the exception of core GF-3. Carbon-rich shale with distinct silt and sand layers dominates the northeast of the basin with silty-shale more common in the southwest. Thickness of the unit is fairly constant throughout most of the basin, with some variation occurring in the southwest.

Shale: This is the typical back shale which dominates through this section. It is composed of 1 mm thick black shale layers alternating with 1 mm thick or less silty shale layers. These parallel laminations are sharp-sided with no evidence of erosive scouring or grading. The black shale dominated areas average 10cm thick and are separated by siltstone layers (Figs. 24, 25 and 26).

Siltstone: These are sharp-sided coarse siltstone layers. They are either massive or parallel laminated, and generally ungraded. No ripples or lenticular shaped layers are present. The layers are up to 5 cm thick averaging 1cm in thickness. Siltstone is more common in this unit than in the shaley units above and below (Figs. 27, 28, 29 and 30).

Sandstone: The tuffaceous layers are a greenish grey colour, intermediate in colour between the greener layers below this interval and the greyer layers above it. They are up to 6 cm thick, averaging 1 cm in thickness (Fig. 31).

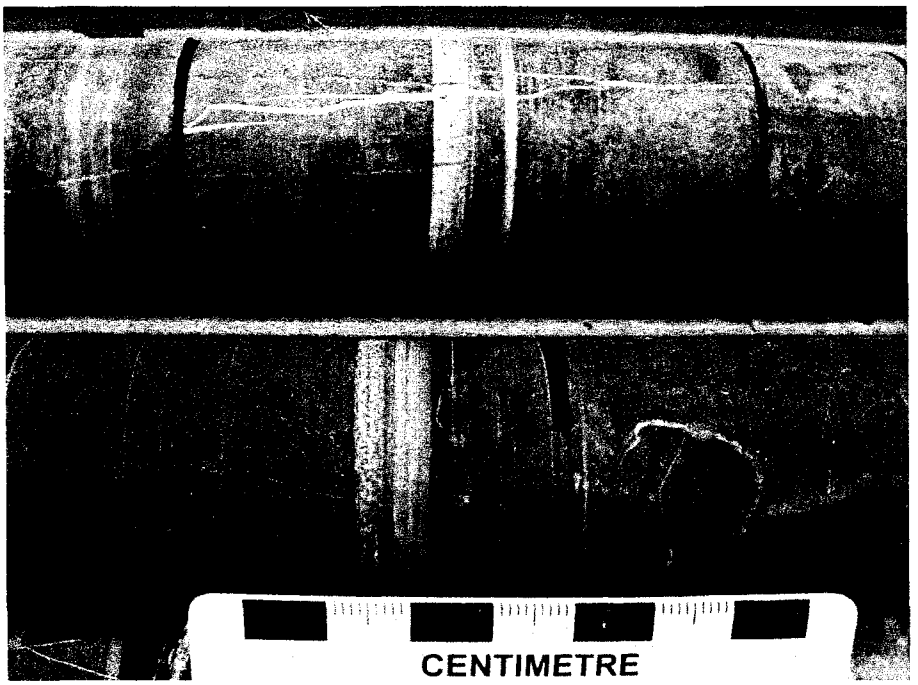

Fig.23. Siltstone and Shale units. Bands of silty-shale, with small rip-ups. Up is to the left. Core MC-89-1.

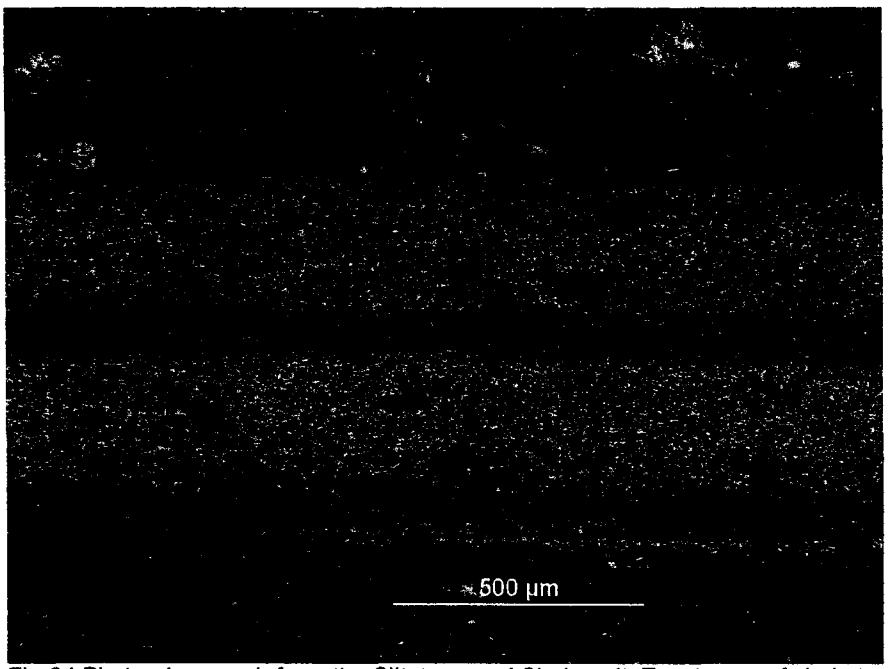

Fig.24 Photomicrograph from the Siltstone and Shale unit. Two layers of shale to siltstone coarsening up, note sand grains sprinkled throughout. Rip-ups of carbon-rich shale in the silty section as well as silty rip-ups in the carbon-rich layers. Photomicrograph-plane polarized light. Core MC-89-1.

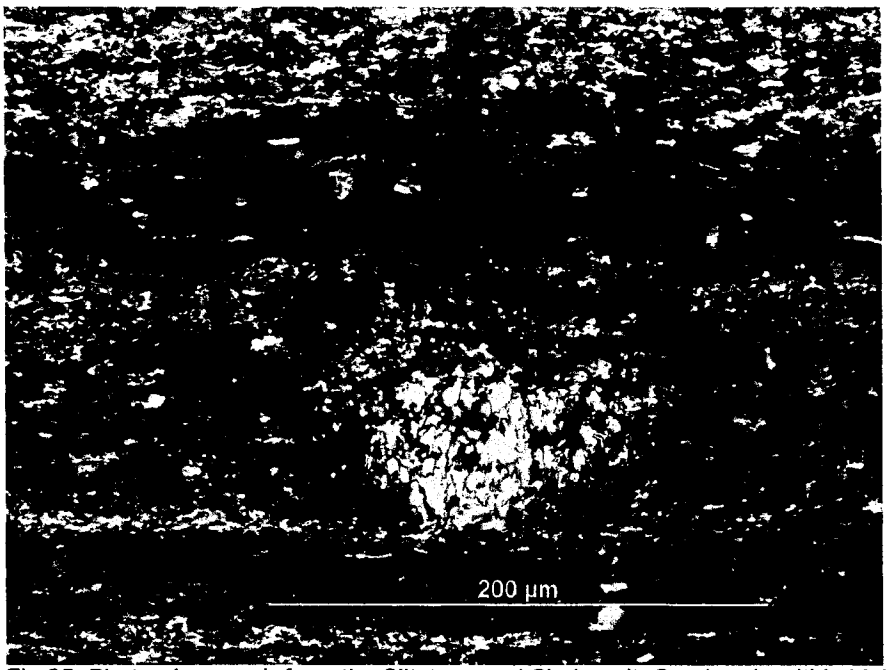

Fig.25. Photomicrograph from the Siltstone and Shale unit. Sand grain within highly carbonaceous shale. Angular very-fine sand to coarse silt grains are randomly oriented throughout. Photomicrograph-plane polarized light. Core MC-89-1.

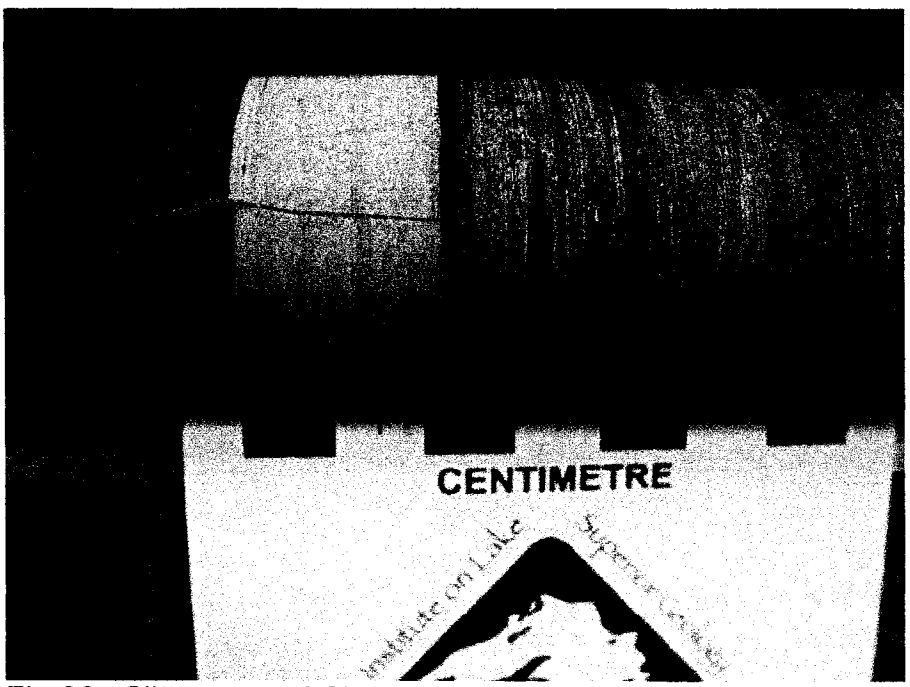

Fig.26. Siltstone and Shale unit. Very fine grained sandstone very slightly fining upwards. Up is to the left. Core MC-89-1.

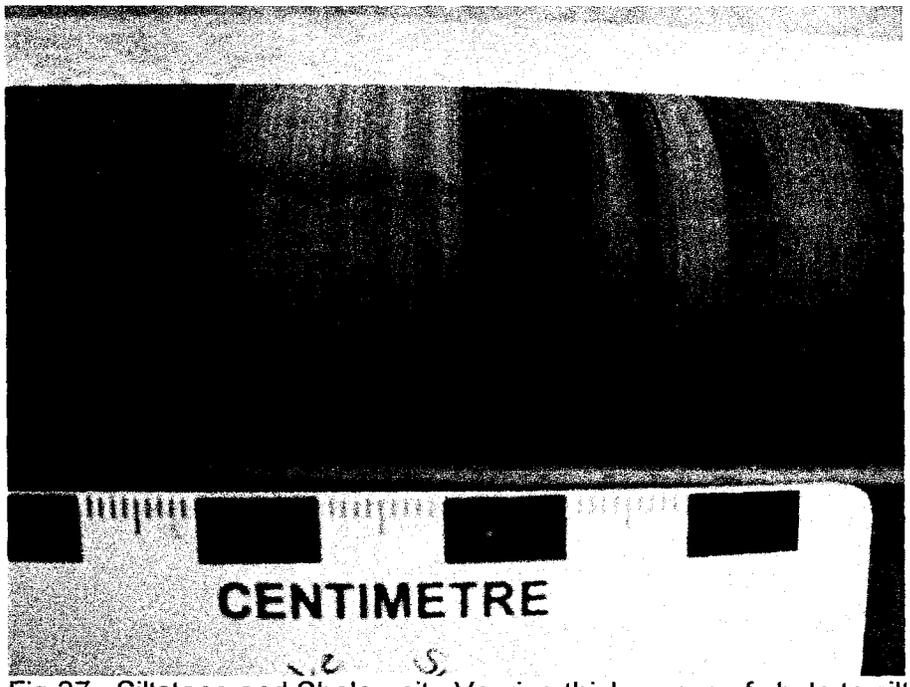

Fig.27. Siltstone and Shale unit. Varying thicknesses of shale to silty-shale with very fine-grained sandstone layers composed of parallel laminae of clay-rich and clay-poor sand. Up is to the left. Core MC-89-1

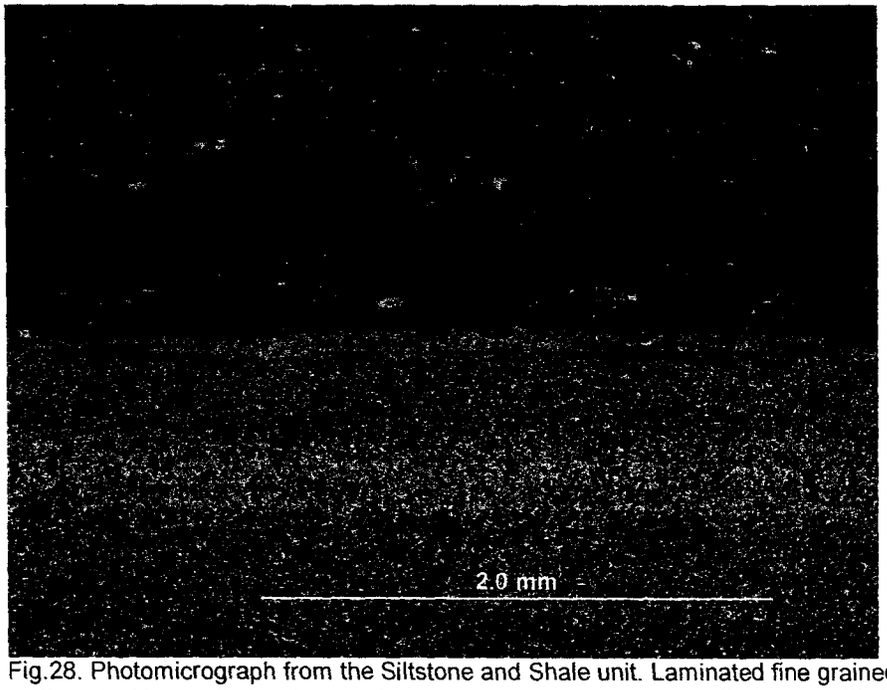

Fig.28. Photomicrograph from the Siltstone and Shale unit. Laminated fine grained sediment with two distinct layers. Lower section is composed of siltstones with black carbonaceous shale grains. It is comprised of several laminae. Top section is mainly black carbonaceous shale with sand and silt grains sprinkled throughout. It contains a very carbonaceous shale-rich layer. Photomicrograph- plane polarized light. Core MC-89-1.

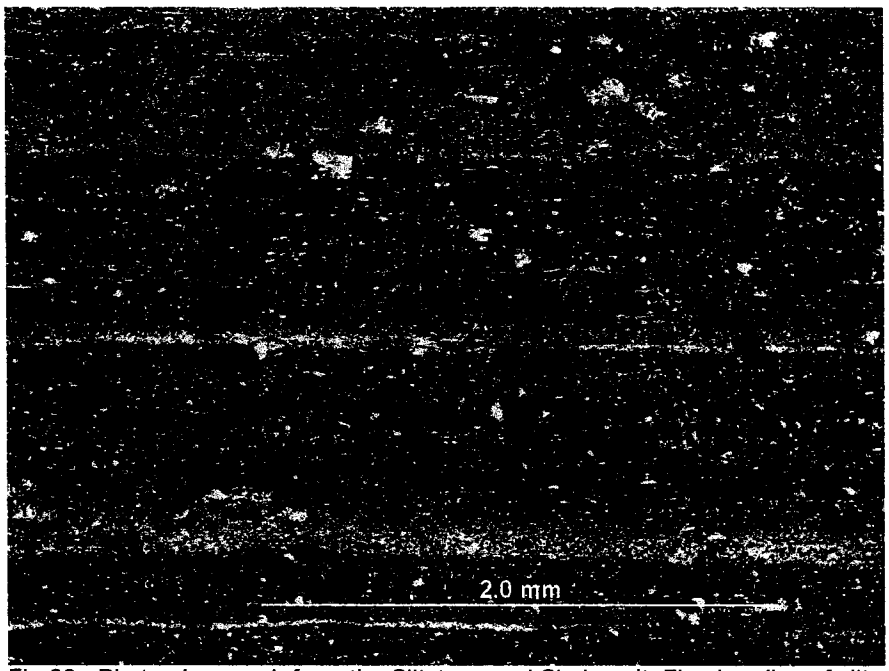

Fig.29. Photomicrograph from the Siltstone and Shale unit. Fine banding of silty-shale and highly carbonaceous shale, with sand grains throughout the four fining up laminae. Photomicrograph-plane polarized light. Core MC-89-1.

Fig.30. Siltstone and Shale unit. Highly fissile light green tuffaceous layers with sharp bottom and top contacts with sandstone, siltstone, and shale. Up is to the left. Core MC-89-1

2.2.4 Northward Prograding Clastic Wedge

Sandstone, siltstone, shale, and silty-shale, bounded by tuffaceous zones, are present in this unit. Sandstone with silty-shales dominates the southwest part of the basin and thins out to the northeast, petering out in core GF-3. The unit coarsens upwards from silty-shale to sandstone and silty-sandstone. Cores MGS-8, MGS-7, MGS-5, LWD-99-1, MGS-2, and CF-3 all display this trend. The unit thins from approximately 55 m in the southwest to 300 km to the northeast.

Shales: Generally a mixture of black shales a few millimetres to 20 cm thick with alternating silty shales. Lighter coloured silty shales are generally thicker ranging up to 30 cm. Rip-ups and ripple marks are present in the lighter silty shale (Fig. 32).

Siltstone: The siltstone beds range from millimetres to metres in thickness and are graded with sharp contacts (Fig. 33).

Sandstone: The very fine-grained sandstone beds are graded. Contacts are sharp and distinct. Some features present are cross bedding, load-casted ripples, and slump structures. Beds occur in thicknesses from 0.5 cm to a few centimetres. They alternate with shale and siltstones in coarsening upwards sequences (Figs. 34 and 35).

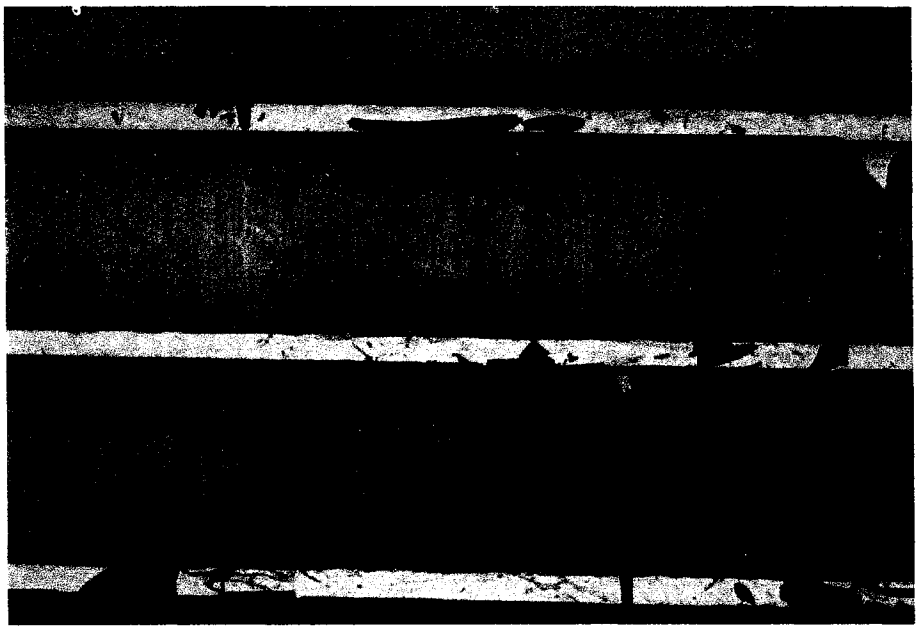

Fig.31. Northward Prograding Clastic wedge. Fining upwards sandstone beds. Up is to the left. Core MGS-7.

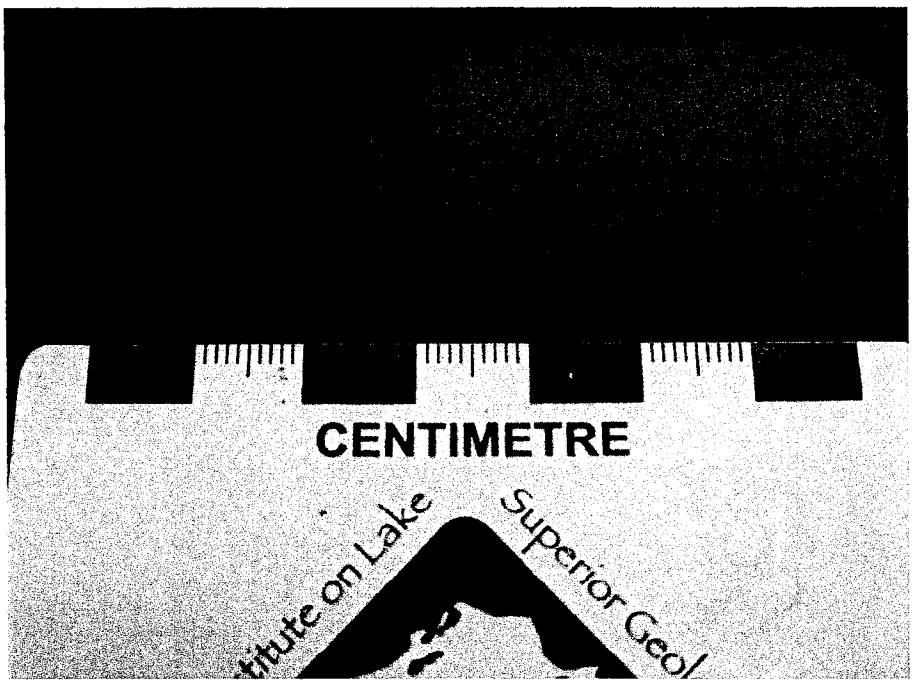

Fig.32. Northward Prograding Clastic wedge. A typical upward fining sandstone to siltstone bed. Up is to the left. Core MGS-7.

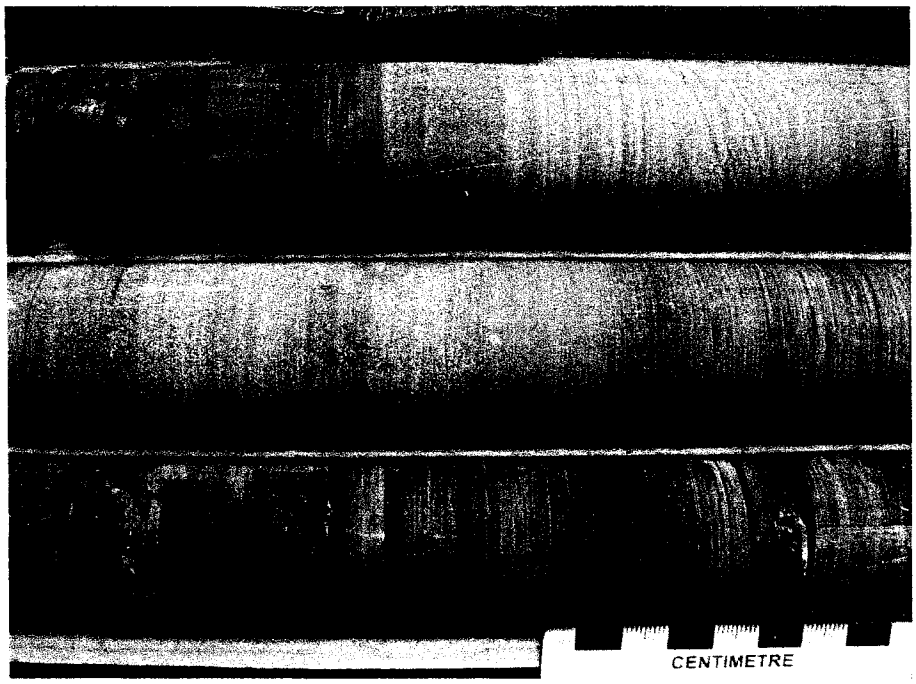

Fig.33 Northward Prograding Clastic Wedge. Graded sandstone beds with some partial Bouma sequences. Note abundant parallel laminated and cross laminated (ripples) sands (in the top right corner). Up is to the left. Core MGS-7.

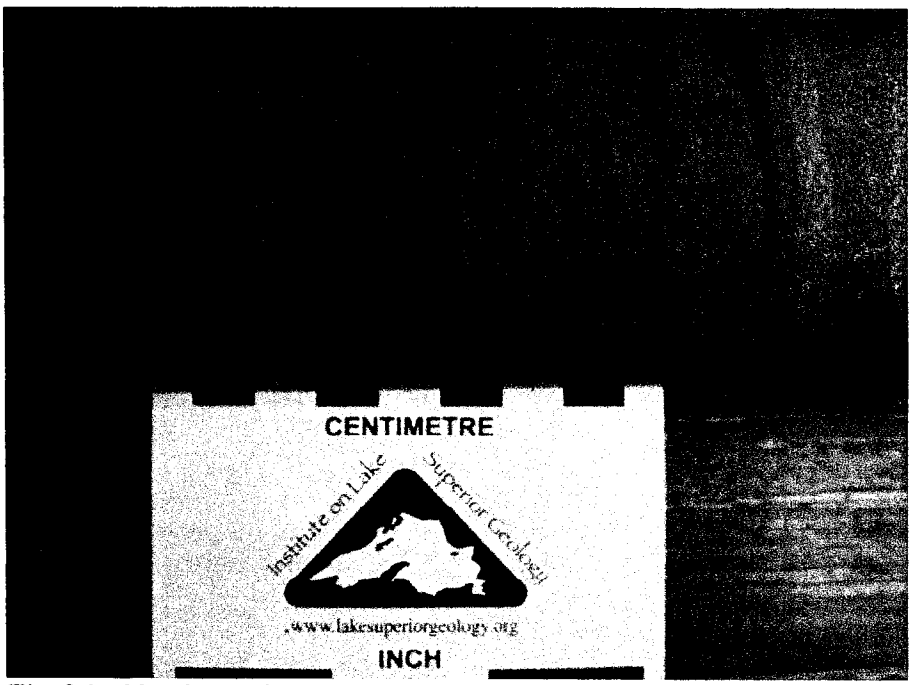

Fig.34. Northward Prograding Clastic wedge. A typical parallel laminated and graded sandstone bed. Up is to the left. Core MGS-7

2.2.5 Coarsening and Thickening Upward Succession

Alternating sandstone, shale, and siltstone dominate this section. Sharp-sided, thin (average 5 mm) siltstone layers increase upward through the black shale, inter-layering with sandstones which begin to appear approximately 10 m above the beginning of this transition. The frequency of sandstone layers increases upward and the sandstones also coarsen upwards in cores 89-MC-1 and PR-98-1. Sandstone thins out farther into the basin towards the southwest, grading to siltstone in core MGS-7 with thin strands of siltstone appearing in core MGS-8. The facies represents graded beds which increase in frequency and in thickness upwards. In the northeast, distinct coarsening upwards units of siltstone to sandstone occur, thinning to the southwest and alternating with silty-shale units.

Black Shale: These are similar to the black shale in the shale-rich zone but with more medium grey siltstone layers. The shales become slightly lighter in colour and more silt-rich upward through the lower 10 m of the coarsening upward succession (Figs. 36, 37 and 38).

Siltstone: Siltstones are very abundant in this unit. They are medium grey, and up to 5 cm thick averaging 5 mm thick. This average does not take into account copious laminae that are less than 1 mm thick. Layers over a few millimetres thick are internally parallel laminated with the silt size and clay content varying from one laminae to another (Fig. 39). The layers and laminae are both mostly sharp-sided. Some layers less than a centimetre thick have diffuse bottom contacts and very sharp top contacts. Some layers which appear

to be graded may just be alternations of layers with varying clay content. One anomalously thick graded siltstone bed 25 cm thick contains abundant feather-like dewatering structures where underlying clay has injected into it. The other siltstone layers are surprisingly free of dewatering or load structures (Fig. 40).

Sandstone: Medium-grained and fine-grained sandstones begin to appear in the lower portion of this unit and become more common upwards. They average about 5 cm in thickness and are up to 20 cm thick in the lower portion of the coarsening upwards succession. The thicker ones are composed of multistory, stacked sandstone layers with sand sizes and clay contents varying between different layers in the stacked assemblage. Grading is common though not all layers are graded. Some graded layers coarsen again at their tops (this appears to represent reworking of the tops of graded layers). Most are parallel laminated with laminations less than 1- 3 mm thick. Less commonly graded layers are cross- stratified throughout. Load structures are common along the bottoms of some sandstone layers overlying black shale, and ball-and-pillow structures of sand also occur in the shales. As well ball-and-pillow structures of clay-poor sand occur in clay-rich sand. Non-graded, medium grained, sharp-sided cross-stratified sand layers also exist. Approximately 35 m above the point where the coarsening upward trend begins thicker, graded sandstone begin to appear. The graded sandstones average 20 cm in thickness with a typical 23 cm thick sandstone composed of a graded medium-grained sand lower section, about 2 cm thick when present, parallel laminated medium sand averaging 6 cm thick, cross-stratified medium to fine sand averaging 3 cm thick when present, and 12

cm of parallel laminated fine sand grading to silt (the upper 2 cm of this is parallel laminated silt and clay with laminae less than 1 mm to 2 mm thick). This is overlain by variable thicknesses (up to 30 cm) of black shale. The base of these layers is commonly sharp and non-loaded, with the exception of some of the thinner layers which do load at their bases (Fig. 41).

Fig.35. Coarsening and Thickening Upward Succession. A carbon-rich shale and siltstone interval (upper two rows). Up is to the left. Core MC-89-1.

Fig.36. Photomicrograph from the Coarsening and Thickening Upward Succession. Carbonaceous black shale with platy rip-ups, Note the erosive truncation of the underlying layer, left center portion of the photomicrograph. Photomicrograph-plane light. Core MC-89-1.

Fig.37. Photomicrograph from the Coarsening and Thickening Upward Succession. Carbonaceous black shale containing abundant rip-ups of silty gains. Photomicrograph-plane light. Core 89-1.

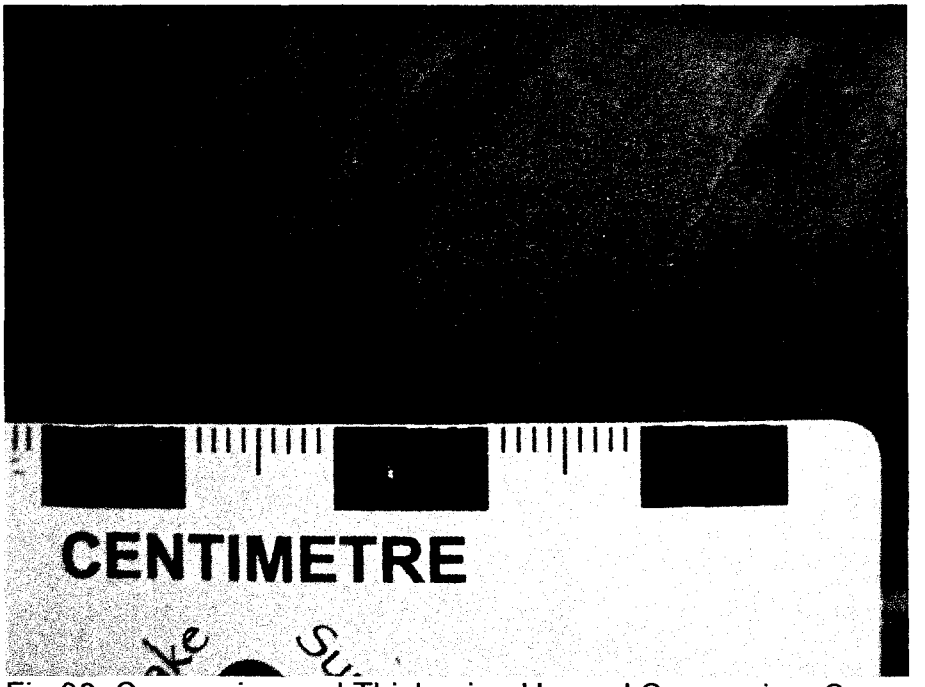

Fig.38. Coarsening and Thickening Upward Succession. Seven stacked, thin graded beds. Up is to the left. Core MC-89-1.

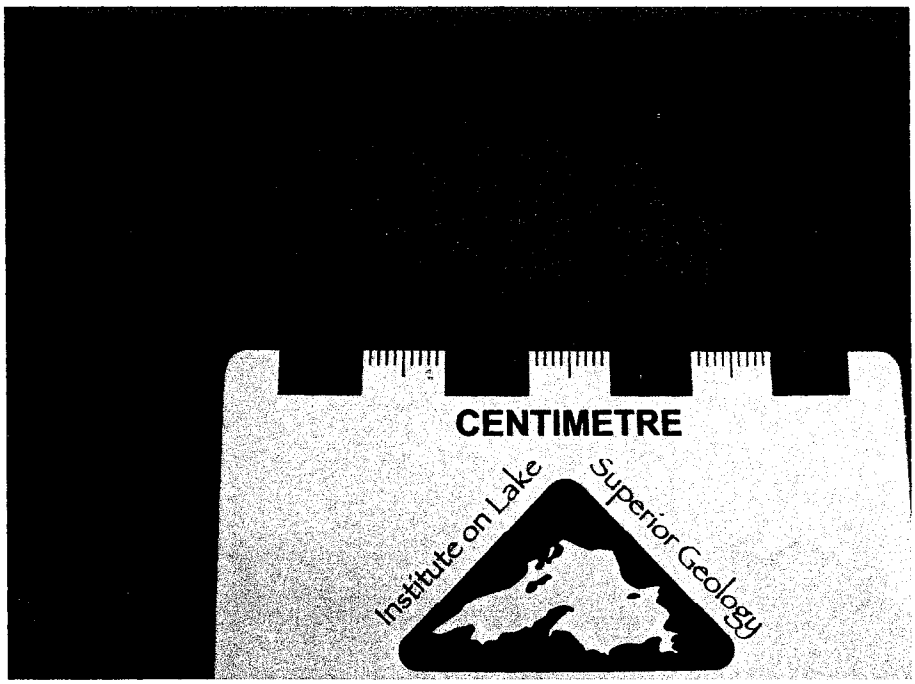

Fig.39. Coarsening and Thickening Upward Succession. A graded bed with Bouma A, B and D divisions. Up is to the left. Core MC-89-1

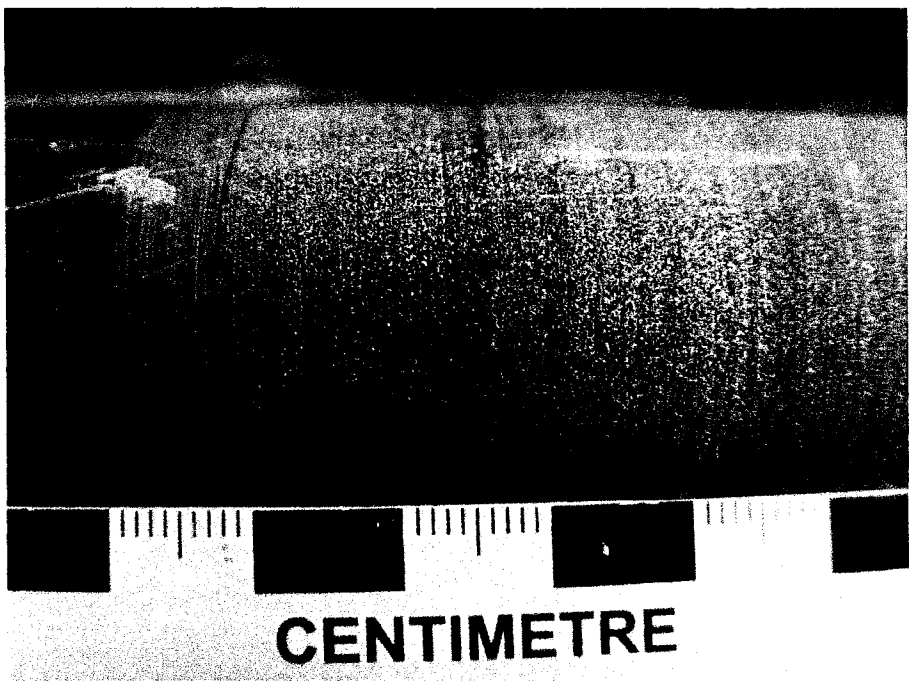

Fig.40. Coarsening and Thickening Upward Succession. Very-fine grained sandstone fining up. Up is to the left. Core MC-89-1.

2.2.6 Massflow Prodelta Deposits

Sandstone and siltstone dominate this area in cores 89-MC-1, PR-99-4, PR-98-1, PR-98-2, and PR-98-3. Shale, silty-shale, siltstone, and sandstone are present in cores GF-3, and MGS-2. Core MGS-2 contains shale, silty-shale, and siltstone. All cores display a coarsening upward trend to primarily sandstone near the top of the unit. Graded bedding and cross-stratification features are present throughout the core. Sandstone increases upwards and dominates this section. Shale separates sandstone successions, with siltstone less common. Distinct coarsening upwards units of shale to siltstone to sandstone occur in the northeast, thinning out to the southwest in core MGS-8. Thickness varies from approximately 380 m in the NE to approximately 100 m in core MGS-8.

Shale: Thin shale layers (a few millimetres to several centimetres thick) commonly separate the sandstone layers except where the sandstone layers cut down into one another. These shales are black to dark grey, the colour varying depending on silt content. The graded silty shales of underlying graded beds grade up into the purer shales capping the beds. These are the E division (Fig. 42) rainout clays which separate the graded beds. Thicker shale dominated areas (average 1.5 m thick) separate the sandstones into separate packages. These black shales have golden brown zones, very organic-rich in appearance, averaging 2 cm thick and up to 8 cm thick. Both the black shales and golden brown shales are parallel laminated with 1mm thick silty shale layers. These successions contain one or two graded sand layers averaging 5 cm thick per 1.5 m shaley succession (Figs. 42).

Siltstones: Siltstones are uncommon except in the upper portions of some graded beds. Some siltstone beds averaging 5 cm in thickness are present in the shale intervals. Their upper and lower contacts are somewhat diffuse rather than sharp and flat.

Sandstones Graded, fine-grained sandstones dominate most of this section. The lowest portions of some of these layers consist of medium-grained graded sand (Figs. 43, 44 and 45). Most of these layers are dominated by parallel lamination, with laminae of 1 to 10 mm thickness. Massive areas are also common. Ripples and cross-stratification are uncommon though they increase in abundance upward through the succession (Fig. 43). A few graded sand layers have cross-stratified fine sand at their base but these are rare. The graded sand layers which commonly occur stacked one on top of another are similar to those in the transition zone which constitute regularly isolated occurrences in the shaley succession. Ripples and cross-stratification are uncommon in the graded layers in the lower portion of this unit. The bases of some of these layers are extensively loaded whereas others are sharp and flat. Small clastic dykes, which may represent water escape structures, are also present, intruding upward from sandy areas into the fine-grained upper portions of graded layers.

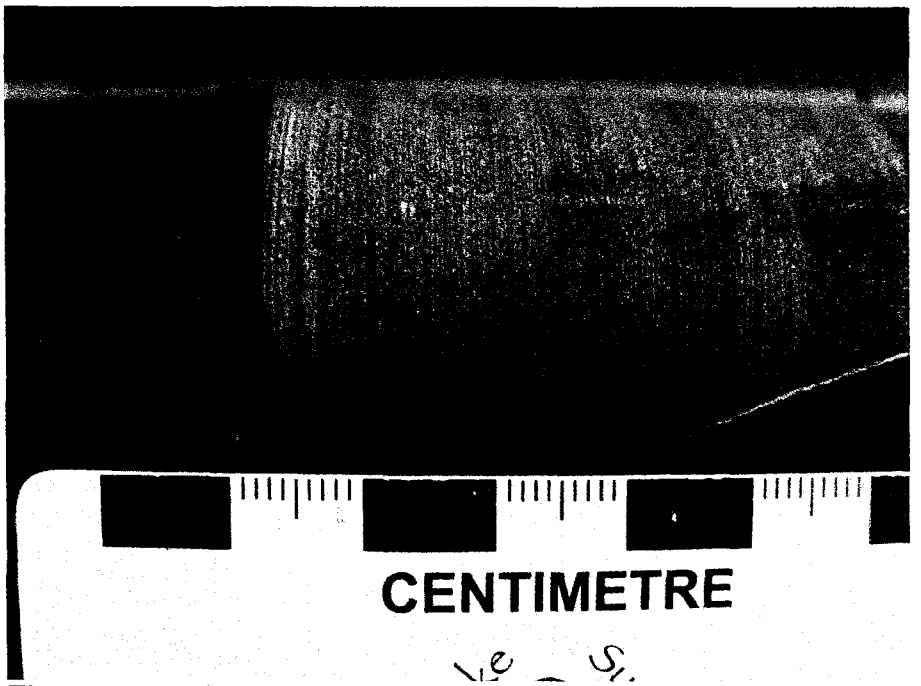

Fig.41. Massflow Prodelta Deposits. Very fine grained sandstone with sharp contact with carbon-rich shale. Up is to the left. Core PR-98-1.

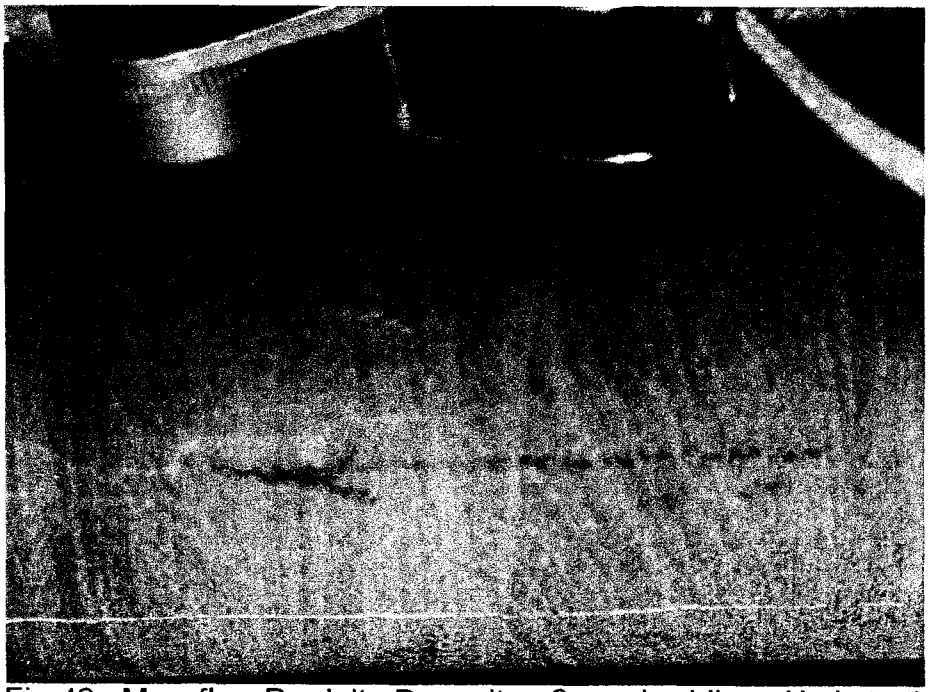

Fig.42. Massflow Prodelta Deposits. Cross bedding. Up is to the left. Core PR-98-1

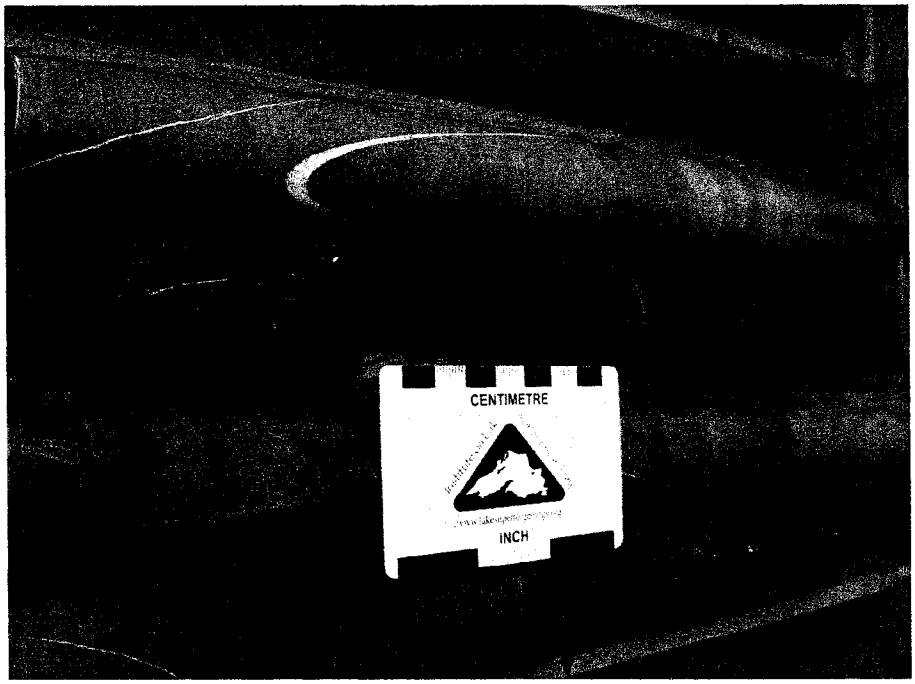

Fig. 43. Massflow Prodelta Deposits. Sandstone thickening upwards with silty-shale and shale separating the sandstone packages. Up is to the left. Core PR-98-1.

Fig.44. Massflow Prodelta Deposits. Sandstone thickening upwards with carbon-rich shale separating the sandstone-rich areas. Up is to the left. Core PR-98-1.

2.2.7 Distal Bar

Alternating layers of shale, siltstone and sandstone occur throughout core PR-98-3. Varying thicknesses of sandstone dominate the top part. Features present include flaser, lenticular and wavy bedding with both current and wave ripples.

Shale: The shales form layers of alternating black shales to grey silty shales with laminae less than a millimeter to a few millimeters in thickness. Contacts are sharp between beds which are interlayered with ripple marks (Figs. 46 and 47).

Siltstone: The siltstone generally alternates with the shale and is also associated with thin sandstone beds.

Sandstone: Alternating from discontinuous to even parallel bedding up to 15 cm in thickness. Grain size is very fine, sedimentary structures present include cross-bedding, piled load-casted ripples, slump structures, flaser, lenticular, and wavy bedding. The rippled sandstones are commonly 8 cm or less in thickness. The massive sandstones are generally 8 to 15 cm in thickness (Figs. 48, 49, 50 and 51). Draped foresets and bundled up-building were used to identify wave ripples, which are common.

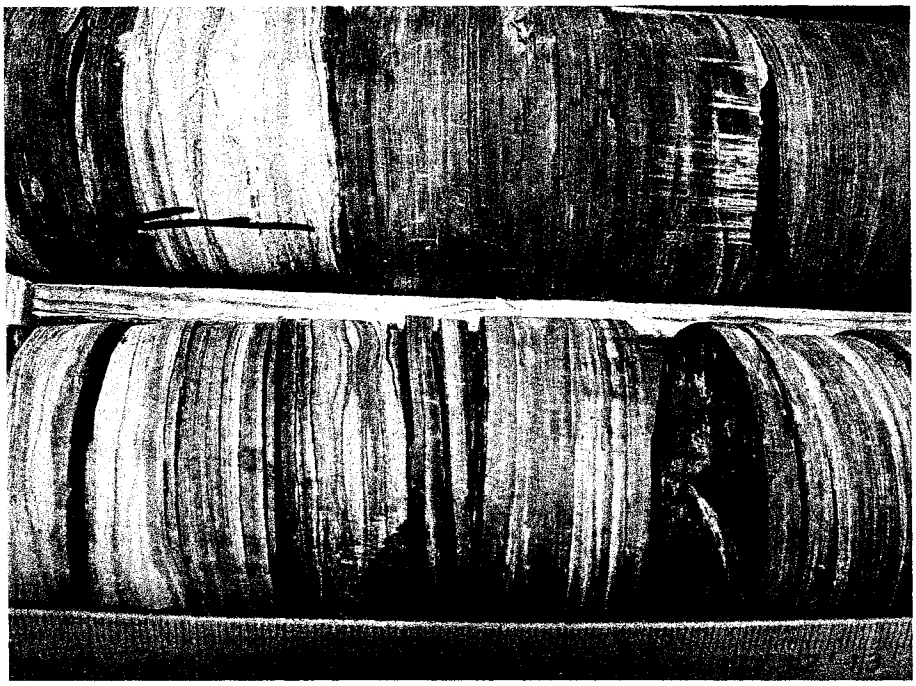

Fig.45. Distal Bar. Flaser wavy and small scale lenticular bedding are all present in this interlayered sandstone. Shale assemblage typical of this unit. Up is to the left. Core PR-98-3

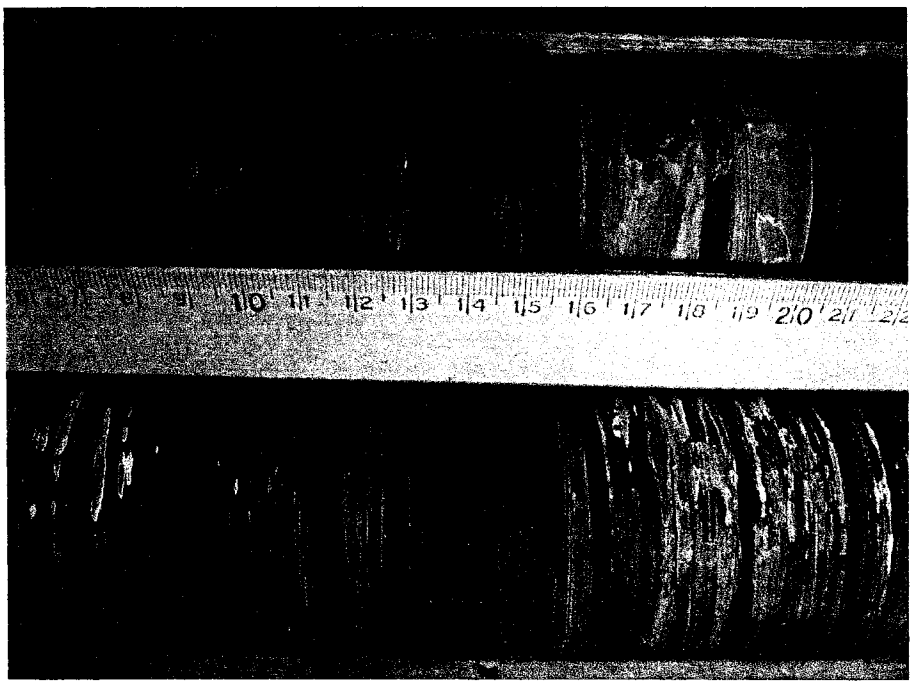

Fig.46. Distal Bar. Sandstone laminae varying in thickness alternating with black shale throughout the unit. Up is to the left. Core PR-98-3.

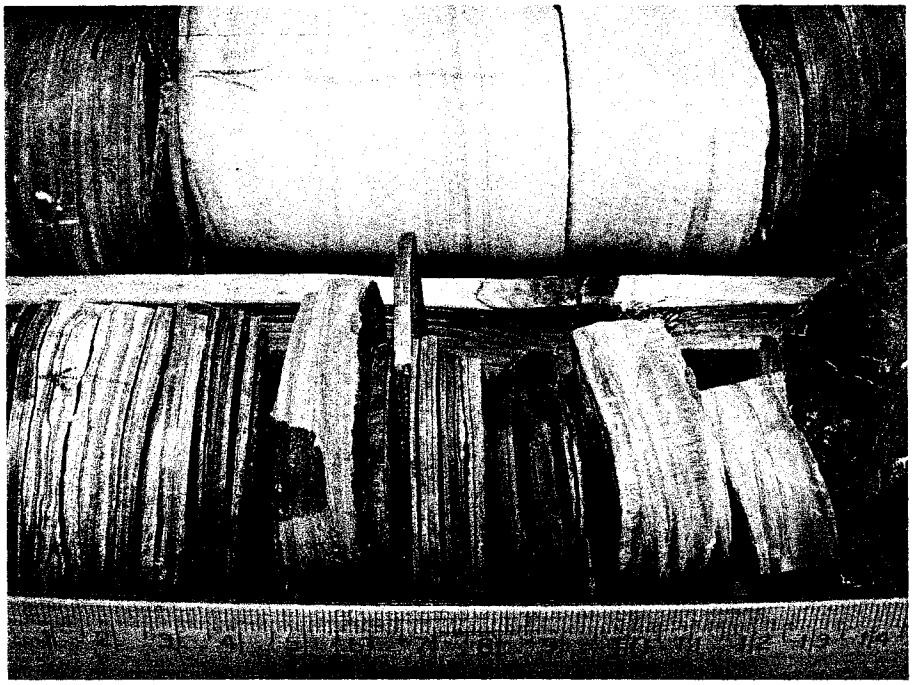

Fig.47. Distal Bar. Sandstone layers, including a thicker (15cm) parallel laminated bed. Up is to the left. Core PR-98-3.

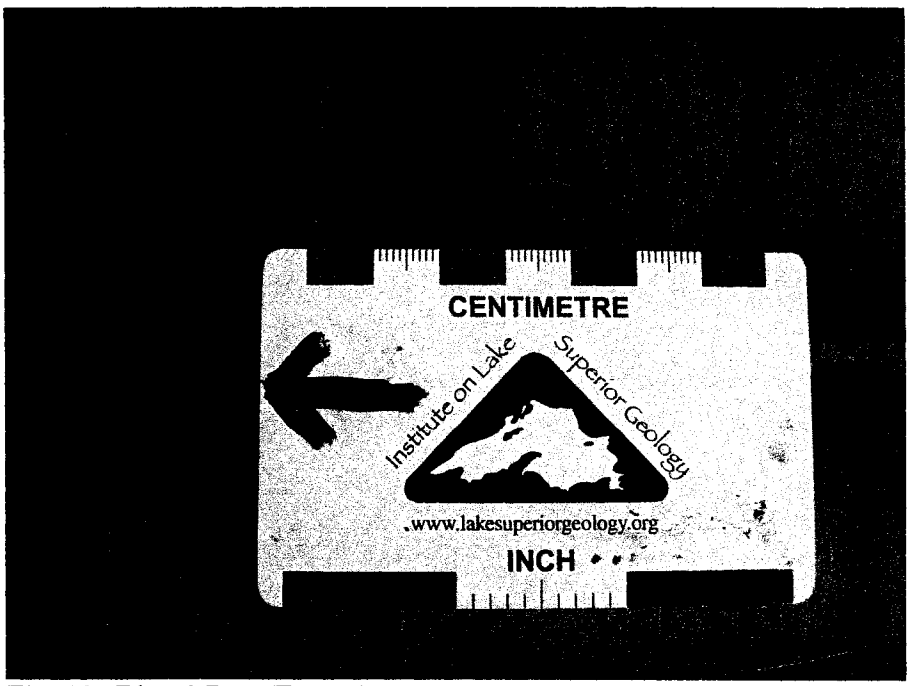

Fig.48. Distal Bar. Trough cross stratification, (top right). Up is to the left. Core PR-98-3.

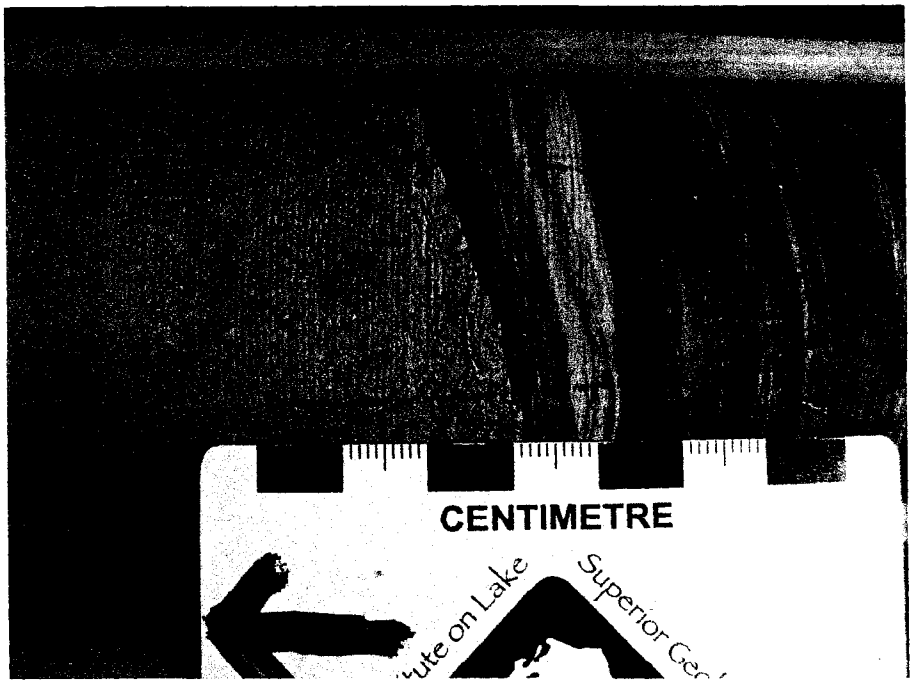

Fig.49 Distal Bar. Dewatering feature. Clay injections in the base of a sandstone layer probably formed during dewatering of the underlying flaser bedded sandstone to shale. Ripple laminated unit. Up is to the left. Core PR-98-3.

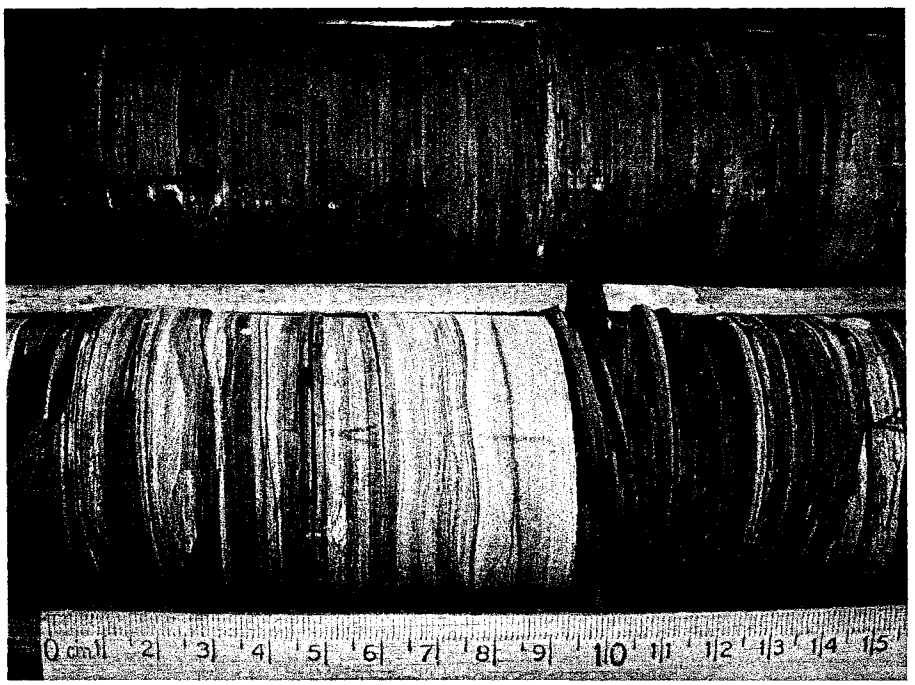

Fig.50. Distal Bar. Lenticular wavy and flaser bedded wave ripples. Up is to the left. Core PR-98-3.

CHAPTER 3: DEPOSITIONAL ENVIRONMENT

The basal Rove/Virginia siltstone and shale succession was deposited during the initial flooding of the basin. It correlates across the entire basin with the exception of core MGS-5 in which it is absent (Fig. 11). No coarser shoreline deposits are associated with this fairly fine-grained facies. Deposition was probably initiated in the south, nearest the open ocean, and migrated northward with progressive flooding as inferred from thinning of sediments northward. Felsic volcanism, occurring at 1835 Ma during the waning stages of the Penokean Orogeny to the immediate south (Sims et al., 1989), contributed volcanogenic ash layers. Some errosive scouring and abundant mud rip-ups in the siltstone indicate reworking by current activity. With increasing water depth this unit grades upward into the shale dominated succession. This facies formed in a quiet basinal environment by deposition of fine-grained sediment from suspension. Limited siliciclastic supply allowed proliferation of organic material, producing a condensed succession in an anoxic environment as attested to by the very fine grain size and abundant carbon. An 1835 Ma U-Pb age from tuffaceous layers at the base of this unit and a 1780 Ma youngest zircon age from detrital zircons in a sandstone overlying this unit indicates this condensed succession required at least 55 My to be deposited. Ash layers are less common in this carbon-rich shale unit. Some scattered oversized fine sand grains observed in thin sections may indicate aeolian delivery. Paleoflow directions are inferred from Morey's (1965, 1967) data for the Rove Formation as well as from

sedimentation types and patterns across the basin, e.g. thickening and coarsening upwards trends, fining and thinning basinward of the clastic wedge.

Deposition of a coarser siltstone-rich unit traceable across the basin and sandwiched within the lower half of the shale succession may indicate a temporary inflection in water level, or increase in sediment supply. No evidence of emergence is present in any of the drill holes. The siltstone layers are ungraded, parallel laminated, and sharp-sided with no evidence of erosive scouring. Tuffaceous layers are also present.

The fine-grained Northward Prograding Clastic Wedge (Fig. 11), within the upper half of the shale unit, thickens to the south. Coarser sediment in the most southerly drill hole (18290) indicates some sediment was being supplied from the Penokean Orogen, which is located approximately 80 km south of this hole and was active from approximately 1860 Ma to 1830 Ma (Sims et al., 1989).

The coarsening and thickening upwards successions consist of shale with siltstone content increasing upward. Graded sandstones, with reworking of some of the tops of layers, also become more abundant and thicker upwards. Internal structures and textures in the sandstone layers are typical of deposition by turbidity currents (Lucente and Morey, 1983). The sandstone beds increase in frequency and thickness upwards and the succession thins to the south probably representing a submarine fan (or ramp) complex prograding from the north (Lucente and Morey, 1983).

The Massflow Prodelta Deposit unit (Fig. 11), a thick sandstone-dominated succession, commonly exhibits massive or parallel laminated sand

beds that are graded, with ripples and cross stratification appearing at higher levels in the succession. Some bases are loaded while others are sharp and flat. Sedimentary structures are more prevalent in the north, becoming more diffuse to the south. The sandstones are separated by shales, mainly in thin layers, some of which are parallel laminated with silt. The shales also contain organic-appearing golden brown zones. A coarsening upward trend is apparent throughout the 400 meters of section containing this assemblage with sandstone dominating the top of the unit. Deposition of sandstones was by turbidity currents whereas the shales represent periods when rainout of fines dominated. The progradation represented by the general coarsening upward trend is a continuation of the trend established in the underlying unit though not as marked. Internally the general coarsening upward trend is composed of approximately 75 coarsening and thickening upward asymmetric cycles, each averaging 5 m thick. The cycles are separated by thicker black shales representing intervals of sediment starvation. The approximately 400 m thick unit is dominated by paleocurrents showing detritus was derived from the north (Morey, 1967) most likely indicating a massive influx of sediment from the Trans-Hudson Orogen occurring to the north and west.

The Distal Bar unit consisting of alternating shales, siltstones, and sandstones displays flaser, lenticular, and wavy bedding with current and wave ripples indicative of a shallower water depth. A coarsening upwards trend is also evident. These features are characteristic of distal bar portions of distributary mouth bar deposits. While tidal flats can contain similar features, ripples in tidal

flats commonly display bi-directional flow patterns which are not evident within these deposits.

The successions of the Rove/Virginia Formations represent subaqueous facies in which the fine-grained sediment starved basin deposits are succeeded by turbidites forming submarine fan or ramp deposits. These grade vertically and to the north (landward) into the overlying rippled unit which may represent the distal bar deposits of an advancing delta front.

In the classic deltaic sedimentation model based on the Mississippi, low density turbid fresh river water enters denser saline water of a basin (see Bates, 1953; Wright and Coleman, 1974). This water may contain only a small percentage of sand with high concentrations of silt and clay. As an effluent plume leaves its river mouth and expands, velocity decelerates and hence the coarser sediments, the sands, settle rapidly from suspension, and almost all of the sand is deposited near the vicinity of the river mouth in distributary mouth bar assemblages (Morgan, 1970; Wright, 1977; Coleman and Prior, 1980). Variations in turbulence and flow rates can cause deposition of silts and clays in this environment also, which tend to be reworked, cleaned and sorted by marine wave processes leaving clean, well-sorted sands (Wright, 1977).

Constantly waning velocity seaward, with expansion of the effluent plume, widely distributes the remaining fine-grained sediment load, with the rate of clastic deposition gradually decreasing seaward. Deposition of rippled very fine-grained sands to coarse silts and some of the clays results in creation of a month bar. The finest grained silts and clays are carried beyond, eventually settling

from suspension to form prodelta facies. Prodelta deposits represent the basal portion of an actively prograding delta. Deposition occurs entirely from suspension, commonly creating parallel laminae of alternations of fine graded silt layers within anotherwise fine-grained clay. The shallower water portions of the prodelta deposits tend to show laminae that are thicker and grain size that is normally coarser (Coleman and Prior, 1980), with parallel and lenticular silt laminae more common. Clays predominate in more distal portions. During the most dynamic flood events, silt laminations may form thin graded beds. With dip angles usually averaging < 0.2° - 0.3°, prodelta deposits can attain considerable thicknesses and lateral extents. In the Mississippi delta they range from 20 to 100 m thick with a lateral spread of 200 to 250 km (Coleman and Prior, 1980). The fine-grained pro-delta sediments can move seaward great distances, and it is not uncommon to find clays beyond the shelf edge, deposited from suspension in the upper slope environment (Coleman and Prior, 1980). Sands found in the outer shelf and upper slope result from mass-movement processes by which large parts of the river mouth bar deposits are moved en masse seaward and incorporated into the shelf-edge and upper slope deposits (Coleman and Prior, 1980).

These mechanisms are considered responsible for deposition of the Rove/Virginia turbidite deposits forming a prodelta facies which appears to conform to a delta-fed submarine ramp model, as described by Heller and Dickinson (1985). Submarine ramps occur at basinal depths where sandy deltas prograde to the shelf-slope break or beyond and deliver coarse sediment directly

down the basin slope from multiple points along the delta front. These turbidite flows form relatively monotonous and laterally continuous sheets of sandstone of random thicknesses which thin downramp with decreasing sandstone/shale ratios. They are characterized by overall thickening, coarsening upward progradational successions and by a reduction in thickness of slope-shale facies between the ramp sandstones and overlying delta-front sandstones. Typical submarine fans, which form by deposition from point sources of sediment such as from submarine canyons, display distinct facies segregation into channel and overbank or interchannel deposits. A submarine ramp, however, builds out into a basin along a broad front, displaying little or no differentiation of the facies typical of most submarine fan deposits. Turbidites can be commonly generated off frontal slopes of deltas that have built out into deep water. The two main ramp subfacies are better termed as distal and proximal ramp facies, which are respectively sand-poor and sand-rich with a gradual transition zone. Distal ramp deposits form by lower energy, lower density turbidite sheet flows which merge with the basin plain. Overlying proximal ramp deposits form by higher density turbidite sheet flows that spread out onto the ramp surface and bank up against the prograding delta slope. The prodelta slope lacks a dominant feeder channel or canyon and is traversed by multiple shallow gullies or delta slope troughs. The overlying delta platform consists of a subaerial delta plain and narrow marine shelf along the submerged delta front. Heller and Dickinson (1985) infer this type of sediment delivery to be enhanced on narrow shelves where deltaic progradation is rapid, and the system contains coarse sediment. In the

Rove/Virginia depositional units, the coarsening upwards successions probably represent distal ramp deposits, with the overlying sand-dominated unit analogous to proximal ramp deposits, the two combined units forming a deltaic prodelta ramp facies.

Turbidite flows can be generated off a delta front by a number of mechanisms, including storm events, river flooding, high rates of sedimentation or seismic activity (Pattison, 2005). They may also occur simply due to instability of a saturated sediment pile on a gentle slope. The sediments form a broad apron of stacked successions at the base of the delta front, eventually becoming overlain by distal bar and shallower water facies with delta progradation. Modification by wave and/or tidal effects can occur, producing variations in bed type, ripples and cross stratification. Wave modified turbidites commonly display criteria such as well graded beds, Bouma beds, flute marks, thick packages of climbing ripples, assymmetrical folds in abundant convolute bedding, hummocky cross stratification and rare small two-dimensional ripples (Myrow et al., 2002). Tides produce cycles of erosion and deposition and fluctuations in tidal range can enhance either process. Tidal effects may be more commonly observed in shallower water facies, producing interbedded sands and muds on the seabed, which are influenced by both fluvial and tidal activity (Jaeger and Nittrouer, 1995). Energy of the system and amount of sediment supply will influence bedding types and sedimentary structures formed. Periods of large tidal range produce thick sand interbeds sand and thin mud interbeds while periods of small tidal range produce thin sand interbeds sand and thick mud interbeds (Jaeger

and Nittrouer, 1995). Flaser bedding, with mud filling the troughs and draping partially over the crests of rippled sand beds, or lenticular bedding consisting of sand lenses preserved within muddy beds can be produced by higher or lower energy tidal ranges respectively. Tidal deposits commonly display bi-directional paleocurrent indicators in close stratigraphic proximity such as herringbone cross lamination and superposition of ripples with opposite facing directions (Darymple et al., 2003). These types of structures were not observed in the Rove/Virginia Formation.

Overlying the prodelta facies, distal bar deposits (Wright, 1985), also known as the distal delta front or platform (Allen, 1970) are a basinward continuation of distributary mouth bars and are characterized by a decrease in both sedimentation rates and coarseness as compared to the proximal distributary mouth bar. Deposited along the seaward-sloping margin, dip angles are slightly higher, rarely exceeding 0.5° and assemblages have lower lateral continuity than the prodelta clays. Lithologically these deposits can be characterized as parallel laminated clays with rippled silts and silty sands (Coleman and Prior, 1980). Most dynamic flood events can produce a variety of sedimentary structures including small-scale cross-laminae, current ripples, and scour-and-fill structures as well as erosional truncations (Coleman and Prior, 1980). Successions of graded beds that coarsen upwards are a common feature (Coleman and Prior, 1980). The uppermost unit of the Rove/Virginia successions displays features indicative of shallower water depth, including flaser, lenticular and wavy bedding, wave ripples and discontinuity of some of the beds. These

attributes are characteristic of distal bar deposits. Tidal flats may also display the same features, however ripples will display bi-directional current patterns which are not evident in the deposits studied.

Deltas are sensitive to subsidence trends, sea-level fluctuations and basin tectonics (Elliot, 1986). Delta-front regimes are used to define delta types, and may be dominated by fluvial or wave or tidal processes or combinations of each. Distal deltaic deposits among the different types are generally quite similar in character. Prodelta shales and siltstones grade upward into coarser distal bar deposits, which consist of alternating sandstone, siltstone and shale. The delta type represented by the Rove/Virginia successions is indeterminate due to the erosional removal of the shallowest water and subaerial facies, however the presence of wave ripples indicates the probable influence of wave activity. Consideration of the basin's earlier history, which displayed influences of tidal activity (Ojakangas, 1983), indicates the possible involvement of tidal influences, though apparent evidence wasn't observed.

Many similar sedimentary successions have been recognized in other ancient deltaic systems in comparable tectonic settings and include the following examples.

The Eocene-Oligocene Annot sandstones in Southeast France display a similar depositional trend as the Rove/Virginia Formations. They accumulated within 2 sub-basins as delta-fed submarine ramps in an Alpine foreland basin. Both sub-basins derived sediment from the uplifted Alpine mountain belt to the east. The southern sub-basin was fed additionally from the southern Provençale

and Corsican/Sardinian massifs. Sedimentation in the northern sub-basin developed as at least two sand-rich delta-fed submarine ramps/aprons, with turbidite filled channels cut into the prodelta foresets (Sinclair, 2000). The successions consist of 300 m of alternating sandstone and mudstone overlain by 480 m of cross-bedded and planar laminated fine sandstone (Sinclair, 2000). Channel fill conglomerates are locally present interbedded with planar-laminated sandstones. The successions are interpreted as the accumulation of sheeted sand bodies associated with numerous shallow, broad channels deposited off a delta front by low and high concentration turbidity currents in a basin floor to base of slope setting (Sinclair, 2000). Sedimentation in the southern sub-basin developed similarly, initially with a steeper and coarser delta front characterized by more mass flows (Sinclair, 2000). As the smaller, confined southern sub-basin filled, sediment was funneled to the northern sub-basin via the Coyer Trough linking them.

Similar successions occur in the Upper Cretaceous Book Cliffs in eastern Utah and western Colorado. The Cretaceous Western Interior Seaway, which covered the eastern half of Utah, accumulated siliciclastic sediment shed from the Sevier Highlands to the west as a series of marine shale-encased isolated sandstone bodies (Pattison, 2005). One of the westernmost units, the Hatch Mesa succession has been interpreted as a storm-influenced, prodelta turbidite complex deposited on the shallow inner shelf between fair weather and storm wave base (Pattison, 2005). Thin bedded siltstones and mudstones are combined with sandstones to form a stack of three or four coarsening-upwards

cycles each 3 to 8 m thick (Pattison, 2005). The sediments display similar structures and bed types to the Rove/Virginia successions. Turbidity currents generated by delta front instabilities and storm waves are considered responsible for transporting and depositing sand in the prodelta region (Pattison, 2005). Modification by wave activity is apparent. The depositional model includes a delta front and prodelta turbidite complex linked by a subaqueous channel network.

The Cambrian Starshot Formation within the Ross Orogen in the central Transantarctic Mountains is dominated by wave modified turbidites deposited in a shoreline to shelf-slope setting. Sedimentation was initiated by uplift associated with active tectonism. The succession grades upward from shale to thin to medium bedded shale and sandstone to proximal sandstone and conglomerate facies.

In northern England, the Namurian Kinderscout Grit delta system grades upwards from basinal muds into a distal turbidite apron and submarine fan complex, (Reading, 1964). The overlying delta front slope consists of a 100 m thick coarsening upwards succession dominated by mudstones and siltstones that are cut by turbidity channels and slump scars. Topped by the delta plain facies, the entire system is 700 m thick (Reading, 1964). Within the same basin, the Roaches Grit delta differs in that the delta front is dominated by ripple, laminated turbidites rather than mudstones and siltstones. The turbidity currents are attributed to synsedimentary faulting in the upper delta front (Jones, 1980). Deposition was dominated by sand-rich turbidity currents.

A similar, ancient system, the Eocene Tyee Formation of Oregon (Chan and Dott, 1983; Heller and Dickinson, 1985), consists primarily of deltaic sediments and turbidites deposited northward into the southern part of the Oregon Coast Range Basin from the region of the Klamath Mountains (Chan and Dott, 1983; Heller and Dickinson, 1985).

The Paleogene Matilija Formation in the Western Transverse Ranges of southern California formed by similar processes (Link and Welton, 1982). Deposition of Eocene turbidites is attributed to the progradation of a major delta front (Link and Welton, 1982).

Similar systems also occur in volcanic terrains. The Archean Beardmore-Geraldton Basin contains a series of fans that were fed from a shelf by multiple canyons, the sediment transported across braidplains from an active volcanic terrain (Barrett and Fralick, 1989).

Later systems formed by similar processes include the Claymore-Galley systems of the North Sea (Boote and Gustav, 1987; O'Driscoll, Hindle, and Long, 1990) and the Campos Basin of Brazil (Guardado, Gamboa, and Lucchesi, 1989).

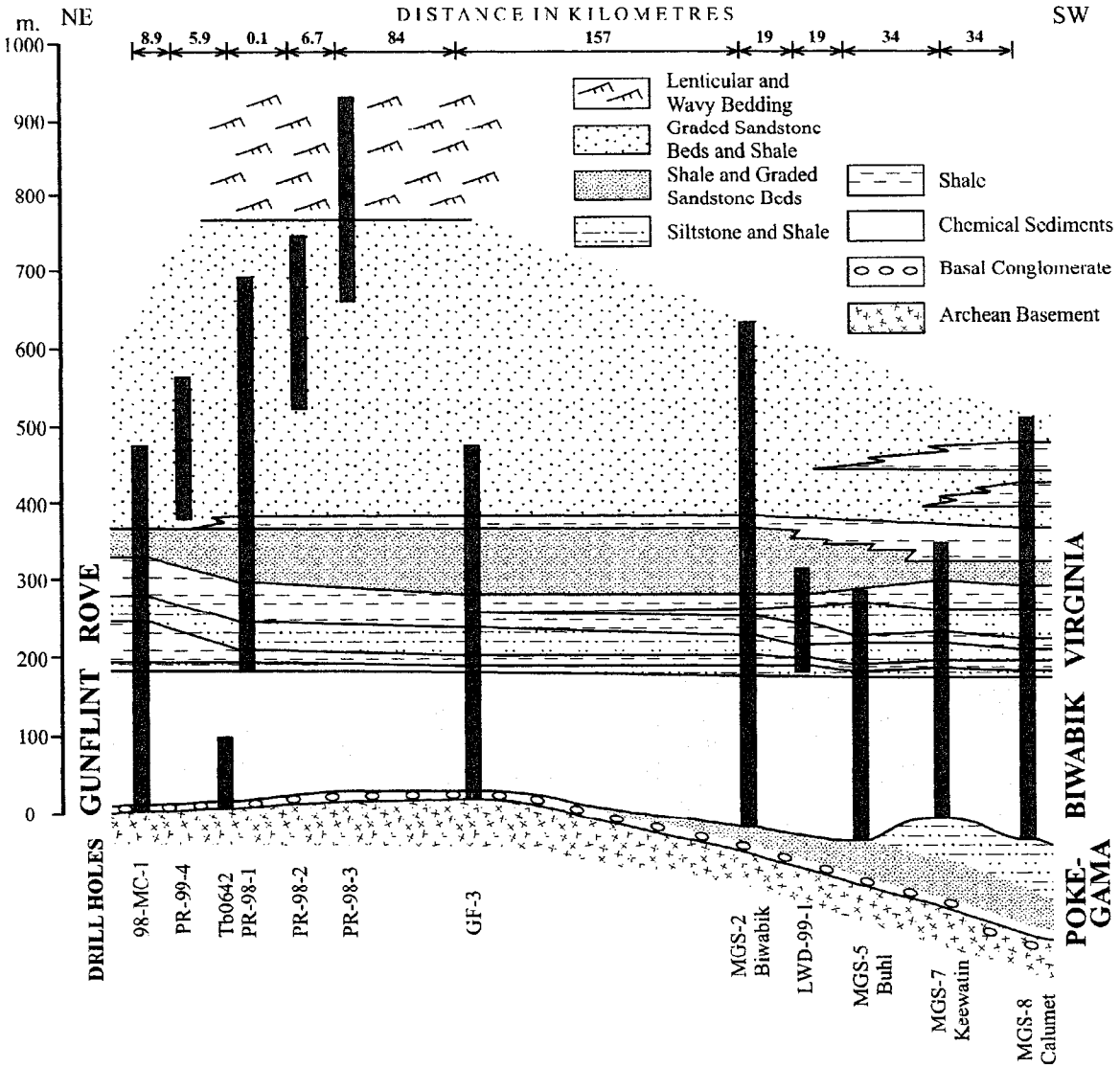

Fig. 51. Correlation of Rove and Virginia Formations and the Gunflint and Biwabik Formations. The Gunflint and Biwabik iron formation represent a stable shelf phase. They are capped by a 40 My hiatus spanning the Penokean Orogeny to the immediate south. The lower black shale dominated portions of the Rove and Virginia Formations represent the sediment starved initial foredeep development of the foreland basin with limited clastic influx from the Penokean Orogenic zone to the south. The overlying coarsening upwards turbidite to delta front assemblage represents progradation of sediment derived from the Trans-Hudson Orogeny which underwent final closure at a slightly younger age than the Penokean Orogeny.

CHAPTER 4: SEQUENCE STRATIGRAPHY

Sequence stratigraphy, a relatively recent concept employed in interpretation of sedimentary systems, considers individual packages of strata deposited during cycles of relative sea-level change and/or changing sediment supply (Vail et al., 1977). The stratigraphic packages are bounded by chronostratigraphical surfaces which include unconformities formed during relative sea-level fall and flooding surfaces formed during relative sea-level rise (Vail et al., 1977; Parkinson and Summerhayes, 1985; Coe and Church, 2003). This information provides insight into environmental changes through time as well as allowing correlation of a range of depositional environments at various locations.

Sedimentary systems strive to achieve and preserve an equilibrium (or depositional) profile where available accommodation space for sediment deposition is balanced by the amount of sediment supplied (Coe and Church, 2003). Disruption of the equilibrium by alteration of the rate of sediment supply or rate of change of accommodation space will cause regression (seaward shift of the shoreline) or transgression (landward shift of the shoreline), and changes to areas of erosion and deposition on land. In alluvial systems, the level along the equilibrium profile below which sediment will be deposited and above which sediment will be eroded is referred to as base level. Shallow marine environments incorporate several base levels, including fair weather and storm wave-bases. Sea-level position is particularly important in affecting deposition

and erosion along both non-marine and marine equilibrium profiles (Coe and Church, 2003).

In siliciclastic environments much of the sediment which is eroded and transported from non-marine systems is deposited in shallow marine environments. Sediment erosion, transport, and deposition is affected by several factors. Climate largely controls rates of erosion and transportation. Tectonics affect sediment supply and accommodation space by altering the positions of the sea bed and land surface. Both factors are important in affecting relative sea-level change. Compaction of sediments provides increased accommodation space independent of sea-level and sediment supply rates.

Packages of sediment which represent small-scale successions of relatively conformable beds or bed sets bounded by flooding surfaces are termed parasequences (Coe and Church, 2003). Each parasequence is deposited during a short time interval reflecting relatively constant conditions, though on the larger scale sea-level, accommodation space and sediment supply vary through time. Their thickness can vary from less than a meter to a few tens of meters and their lateral extent from tens to thousands of square km (Coe and Church, 2003). Sequence stratigraphy considers how these parasequences stack together to form sequences due to changes in accommodation space and/or sediment supply over longer periods of time (Coe and Church, 2003). While most parasequences coarsen upwards, a few fine upwards, such as in estuarine or muddy tidal flats to subtidal environments. A shallowing upwards trend is commonly represented regardless. As the smallest bed-scale cycle observed,

parasequences are the smallest unit usually considered in sequence stratigraphy. Successions of parasequences which form distinctive stacking patterns are termed parasequence sets (Coe and Church, 2003) which may be progradational, retrogradational or aggradational.

A retrogradational pattern occurs with a landward shift of the shoreline causing the parasequences to backstep or retrograde. This reflects an increase in accommodation space which exceeds the rate of sediment supply.

Aggradation occurs when the increase in accommodation space keeps pace with the rate of sediment supply, the shoreline remaining in the same position. The parasequence sets stack vertically on top of each other.

With progradation the constant rate of sediment supply exceeds the increase in accommodation space with a basinward shift of the shoreline and of successive parasequence sets. Exposure may cause subaerial erosion of more proximal areas. A relative sea-level fall resulting in reduced accommodation space also results in progradation. This is termed a forced regression and is independent of fluctuations in sediment supply. A normal or depositional regression occurs when the rate of sediment supply exceeds the rate of increase in accommodation space through either a relative sea-level rise or a stillstand (Coe and Church, 2003).

A succession of parasequence sets comprises a depositional sequence. These can vary in thickness from a few meters to tens or hundreds of meters. A sequence represents one cycle of change in the balance between accommodation space and sediment supply (Coe and Church, 2003). Specific

sections of this cycle within each sequence may be represented by up to four "systems tracts", with each tract made up of at least one parasequence set. Not all systems tracts may develop or be preserved depending on conditions.

Absolute highs and lows in relative sea-level are considered along with rates of relative sea-level change. Fluctuations in the rate of change of accommodation space are controlled by the rate of sea-level change. Maximum rates of sea-level rise and fall generally occur approximately midway through each rise-and-fall cycle with corresponding changes in accommodation space (Coe and Church, 2003).

Systems tracts which can occur within sequences include the highstand systems tract (HST), the falling stage systems tract (FSST), the lowstand systems tract (LST), and the transgressive systems tract (TST). Successive sequences are terminated by maximum flooding surfaces (MFS) and separated by sequence boundaries (SB).

Accommodation space is created most rapidly during the period of maximum rate of sea-level rise. Sediments deposited during the time interval between the maximum rate of sea-level rise and maximum sea-level from the Highstand Systems Tract (HST), and consist of aggradational to progradational parasequence sets (Coe and Church, 2003).

With a fall in sea-level, rivers will incise and erode the exposed sediment creating an unconformity. Sediments will be transported further into the basin with a corresponding shift of the shoreline basinward. The unconformity formed during this sea-level fall is termed the Sequence Boundary (SB). Farther

offshore this erosional unconformity is transitional to a non-erosional surface of correlative conformity which is overlain by sediments deposited during the interval of falling sea-level. Representative of the time at which sea-level began to fall, correlative conformities can be difficult to identify as they often exhibit no distinct change in facies.

Sediment deposited during falling sea-level between maximum and minimum relative sea-levels forms the Falling Stage Systems Tract (FSST). A FSST occurs only with forced regression resulting in progressive downstepping of parasequences as the shoreline moves basinward. Preservation of the FSST can be variable to nil depending on sediment supply and rate of sea-level fall with consequent erosion.

Sediment deposited between the minimum relative sea-level and a more pronounced increase in sea-level and accommodation space forms the Lowstand Systems Tract (LST) (Coe and Church, 2003). This consists of progradational to aggradational parasequence sets as the shoreline begins a landward migration.

A progressive rise in sea-level will produce a transgression when accommodation space exceeds sediment supply. The Transgressive Surface (TS) which occurs forms the base of a set of retrogradational parasequence sets termed the Transgressive Systems Tract (TST). These are deposited during the interval when rate of increase of accommodation space exceeds the rate of sediment supply until maximum sea level is reached. Low sediment supply will produce a thin or non-existent TST.

Sediment starvation in distal parts of the depositional profile can occur with increasing sea-level rise. This starvation reaches its most landward position between the maximum rate of relative sea-level rise and the maximum sea-level (Coe and Church, 2003). This results in the formation of a condensed bed, the top of which is termed the Maximum Flooding Surface (MFS), and is associated with the most landward position of the shoreline. Condensed beds may be highly fossiliferous due to lack of siliciclastic sediments. Marine sediments are often deposited in proximal areas which were previously entirely non-marine. With the achievement of a balance between the rate of increase of accommodation space and sediment supply, deposition of the next HST will occur between the maximum rate of relative sea-level rise and maximum relative sea-level. Repetition of the cycle will produce another depositional sequence.

The development of system tracts is usually ascribed to changes in relative sea-level. However, a supply of coarser sediment is also necessary or relative sea-level change will have no effect on sediment accumulating in the offshore. Commonly, systems tracts are described over small lateral distances of less than 100 km where lateral transport of coarse sediment is only rarely incapable of producing traceable sequence tracts. In this study the 425 km of lateral distance separating the northernmost and southernmost sections leads to the complication that sediment delivery to one side of the basin may lead to the recording of sequence tracts there, but in the distal areas all the tracts are represented by the accumulation of organic-rich muds. In the basin studied this general problem is further complicated by sediment first being delivered from the

south and later from the north. Thus, the systems tracts are discussed in two sections; the first dealing with those developed during northern sediment delivery and the second on southern sediment delivery systems tracts.

Systems Tracts dominated by sediment input from the northeast beginning from core 89-MC-1:

Core PR-98-1 is used to graphically demonstrate the vertical sequence and stratigraphic framework of the units studied (Fig. 52). Lateral variation across the basin is outlined in Figure 53. Four system tracts are present, FSST, LST, TST, and HST, as well as three boundaries, SB, TS, and MFS (Figs. 56 and 57).

The SB marks the beginning of relative sea level fall. During this event deposition does not occur in the proximal part of the depositional profile (alluvial, coastal plain and near shore). Instead, erosion occurs with continual sea level drop, producing an unconformity. Sediment is transported further into the basin producing a depositional systems tract consisting of a coarsening upward trend. The SB is placed at the base of the Coarsening and Thickening Upward Succession where a definite coarsening upward trend is initially noted (Fig. 53). The shale unit below the SB represents a quiet offshore environment and is observed from core 89-MC-1 in the northeast along the basin to the southwest in cores PR-98-1, GF-3 and MGS-2 (Fig. 53). No correlative conformity is apparent, considering the location of the SB within the basin.

Continual sea level fall and consequent erosion of previously deposited sediment produces a supply of reworked siliciclastics which are deposited in

progradational parasequence sets. Variations in rate of sea-level fall and sediment supply may produce different types of depositional profiles. Stranded or detached parasequences are separated from each other, while attached and stepped down parasequences form a lateral succession.

A set of progradational parasequence sets comprise the FSST which extends upward from the SB ending with the beginning of sea level rise. The FSST is 20 m thick in core 89-MC-1, increasing to 64 m thick in PR-98-1. It thins to 25m and 30 m respectively in cores GF-3 and MGS-2, possibly due to the slope gradient and/or greater distance from the sediment input source. The FSST in all of the above cores initially develops as detached parasequences, ending with stepped-down parasequences. The siltstone/sandstone layers vary in thickness from 1 cm near the base up to 30 cm near the top of the FSST. Frequency of siltstone/sandstone packages increases upwards and shaley intervals between them thin from 1-2 m thick to 1-2 cm thick near the top of the FSST. The FSST in core PR-98-1 consists of 31 coarsening up parasequences of shale, siltstone and sandstone and 6 similar parasequences in core 89-MC-1. In core GF-3 the FSST is represented by 5 siltstone-shale parasequences and 3 of shaley-siltstone. Two parasequences of shale, siltstone, and sandstone occur in core MGS-2 with stringers of sandstone between shale units. Eight shaley-siltstone parasequences comprise the FSST in core LWD-99-1. The FSST is not apparent in cores MGS-5 and 7 however the boundaries were extended through them to core MGS-8 where the FSST, while indistinct, is arbitrarily placed where sand stringers occur in the shale.

The FSST is followed by the LST as sea level falls to a minimum and begins to rise. Accommodation space begins to increase and the shoreline begins a landward migration. Progradational to aggradational parasequence sets are produced. Progradational parasequences occur in cores 89-MC-1, PR-98-1, GF-3, and MGS-2 which all exhibit a coarsening upward trend. The thickness of the LST varies from 14 m in 89-MC-1 and PR-98-1 to 70 m in GF-3 and MGS-2. LST parasequences are composed of shale, siltstone, and sandstone. Toward the southwest the packages become less distinct, as increasing distance from the sediment source leads to a reduction in grain size. The LST and FSST form a portion of the shelf-slope ramp deposits. In core 89-MC-1, the LST consists of a set of 6 shale-siltstone-sandstone parasequences. In core GF-3, 1 parasequence of silty sandstone interlayered with sandstone forms the LST up to the shale unit. In core MGS-2, 3 parasequences of shale-siltstone-sandstone occur, as well as shale horizons with stringers of sand. The LST is not apparent in cores LWD-99-1 or MGS-7. In MGS-8 the LST is represented by sand stringers in shale. Frequency of individual parasequences decreases with increasing distance from the sediment source.

With transgression a significant sea level rise occurs and creation of accommodation space exceeds the rate of sediment supply. Retrogradational parasequence sets are produced, the base of which forms the TS. In coastal environments of the shoreface and foreshore, a minor unconformity is produced during sea-level rise by erosion and reworking of sediments by increased wave, tide and storm activity. In proximal areas in modern environments the TS may

have marine sediments overlying non-marine sediments. In cores 89-MC-1, PR-98-1, GF-3 and MGS-2, the TS is sharply defined at 185 m above the Iron Formation. In cores MGS-7 and 8 the TS is placed at the top of the sand units which appear to be the best fit correlative with core MGS-2

The TST occurs when sediment supply does not keep pace with the rate of sea-level rise resulting in retrogradational parasequences. A low sediment supply will produce a thin or absent TST. Maximum rate of relative sea level rise marks the end of the TST. In core 89-MC-1, the TST is represented by a retrogradational parasequence which thins upward. It forms a thin shaley interval in cores PR-98-1 and MGS-2. A 50 m thick retrogradational succession culminating in shale forms the TST in GF-3.

The MFS occurs with maximum sea level rise and distal parts of the depositional profile may be completely sediment starved. Absence of siliciclastic sediments and proliferation of marine organsims will produce a submarine unconformity with a fossiliferous condensed bed assemblage. TST's and MFS's developed in Precambrian strata will have similar grain size responses to their Phanerozoic analogs. However, due to the lack of carbonate, phosphate and silica secreting organisms the sediment supply to Precambrian condensed intervals will be reduced even over their Phanerozoic relatives. Ample evidence of the delivery of organic remains to the bottom does occur in the shaley condensed sequence examined. But, instead of fossil material, abundant disseminated carbon and carbonaceous layers in the black shales bear witness to the organic-rich nature of the sediment. The MFS is located in cores 89-MC-1,

PR-98-1, GF-3 and MGS-8 in black shales below the beginning of the sandstone successions (Fig.53). Coarsening upward sequences in sandstones are representative of proximal coastal environments, which are evident in cores 89-MC-1 and PR-98-1.

The HST occurs where the rate of increase of accommodation space is balanced or exceeded by the rate of sediment supply producing aggradational or progradational parasequences, respectively. The HST begins at the base of the sandstone, and above this an extended coarsening upward trend is apparent in all cores. The HST in core 89-MC-1 is composed of approximately 5 shale-siltstone-sandstone parasequences and approximately 7 siltstone-sandstone parasequences as well as individual units of siltstone and sandstone, with shale units less common. In core PR-99-4, parasequences present include 15 shale-siltstone-sandstone, 4 shale-siltstone, 8 siltstone-sandstone, and individual units of sandstone. In core PR-98-1, the HST comprises 25 shale-siltstone-sandstone, 2 shale-siltstone, and 50 siltstone-sandstone parasequences. Sandstone-rich intervals in cores 89-MC-1 and PR-98-1 vary from a few meters to 5 m in thickness, the variability possibly due to differing stepped changes in water level. HST parasequences in core PR-98-2 include units of sandstone ranging in thickness from 1 to 5 m and 35 siltstone-sandstone packages and 3 of shale-siltstone-sandstone. Three parasequences of shale-siltstone-sandstone near the top of the core appear to represent an event which resulted in the development of several systems tracts (Fig. 53), above which the HST is continual to the top of core PR-98-3. This core is composed of siltstone-sandstone parasequences of

varying thicknesses. The thickest, at 60 m marks the beginning of the distal bar deposits. In core GF-3, the HST is composed of 8 silty shale-sandstone parasequences and individual units of silty shale located between two coarsening up sequences. In core MGS-2, the HST is represented by 25 shale-siltstone-sandstone parasequences. The coarsening upwards sequences of shale, siltstone and sandstone thin from the northeast to the southwest further indicating that sediment input is from the northeast.

Systems tracts dominated by sediment input from the southwest :

The bulk of the sediment input occurred from the northeast. The generally quiet basinal environment dominated by shale to the southwest was intermixed with coarser sediment from a lesser input source to the southwest. Systems tracts may still be distinguished and minimally modified from those defined in the northeast.

The SB was placed at the top of sandstone units in cores MGS-7, MGS-5, LWD-99-1, MGS-2 and GF-3 and traced across the basin using the tuffaceous layers as a guide where possible. The FSST and LST are most evident in core MGS-8. Both tracts are progradational and extend up the core approximately 25 m in each core. Both system tracts thin toward the northeast. Coarsening up parasequences constituting the FSST and LST are apparent in both MGS-8 and 7. Individual parasequences are not clearly apparent in cores MGS-5, which contains sand stringers within shale, and LWD-99-1 in which shaley-siltstone dominates. A coarsening upward shale-siltstone parasequence in core LWD-99-1 thins in core MGS-2, pinching out in core GF-3.

Sequence and System Tracts

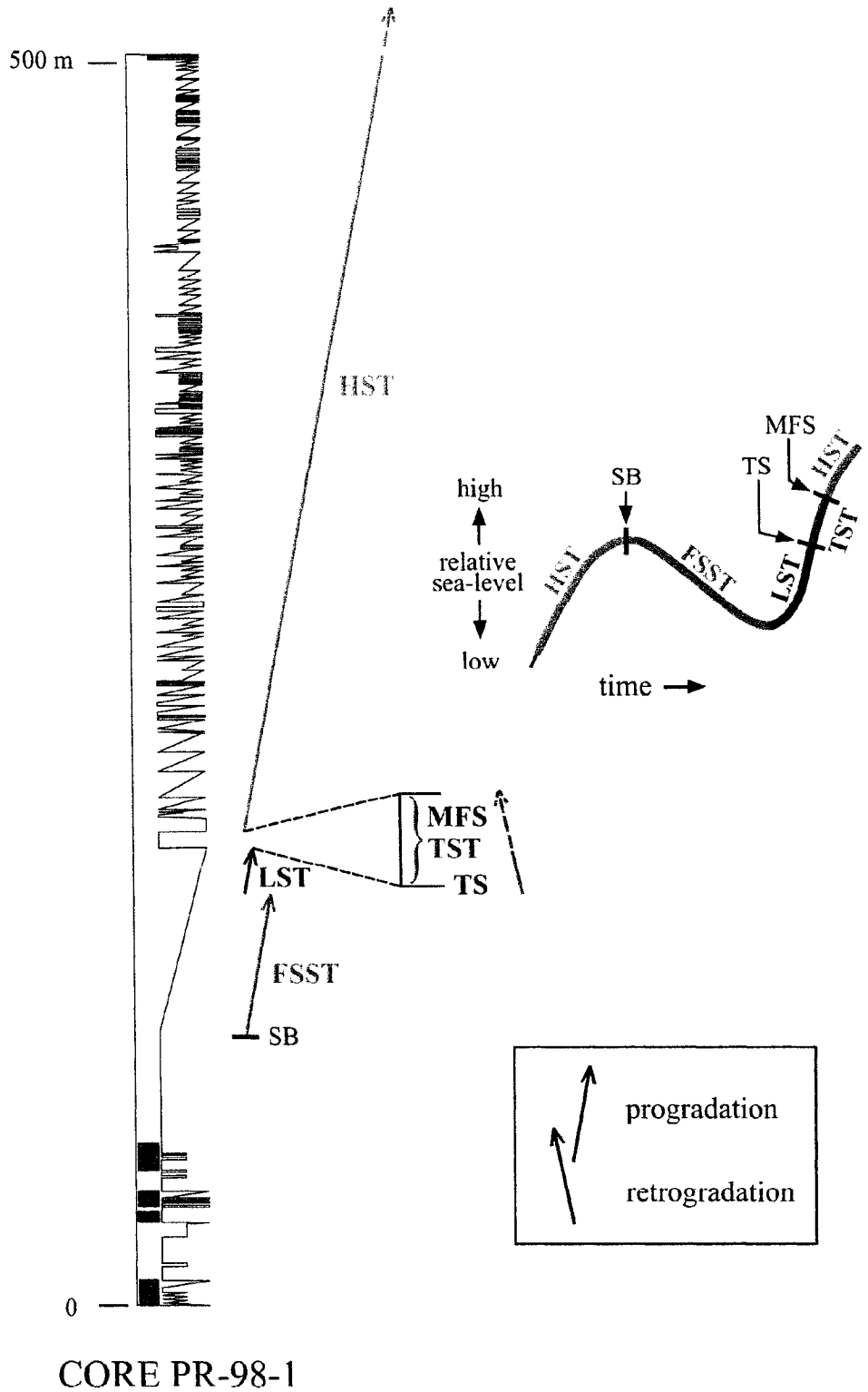

Fig. 52. System Tracts, applied from the Coarsening and Thickening Upward Successions to the top of the drill hole. Red bars are tuffaceous intervals.

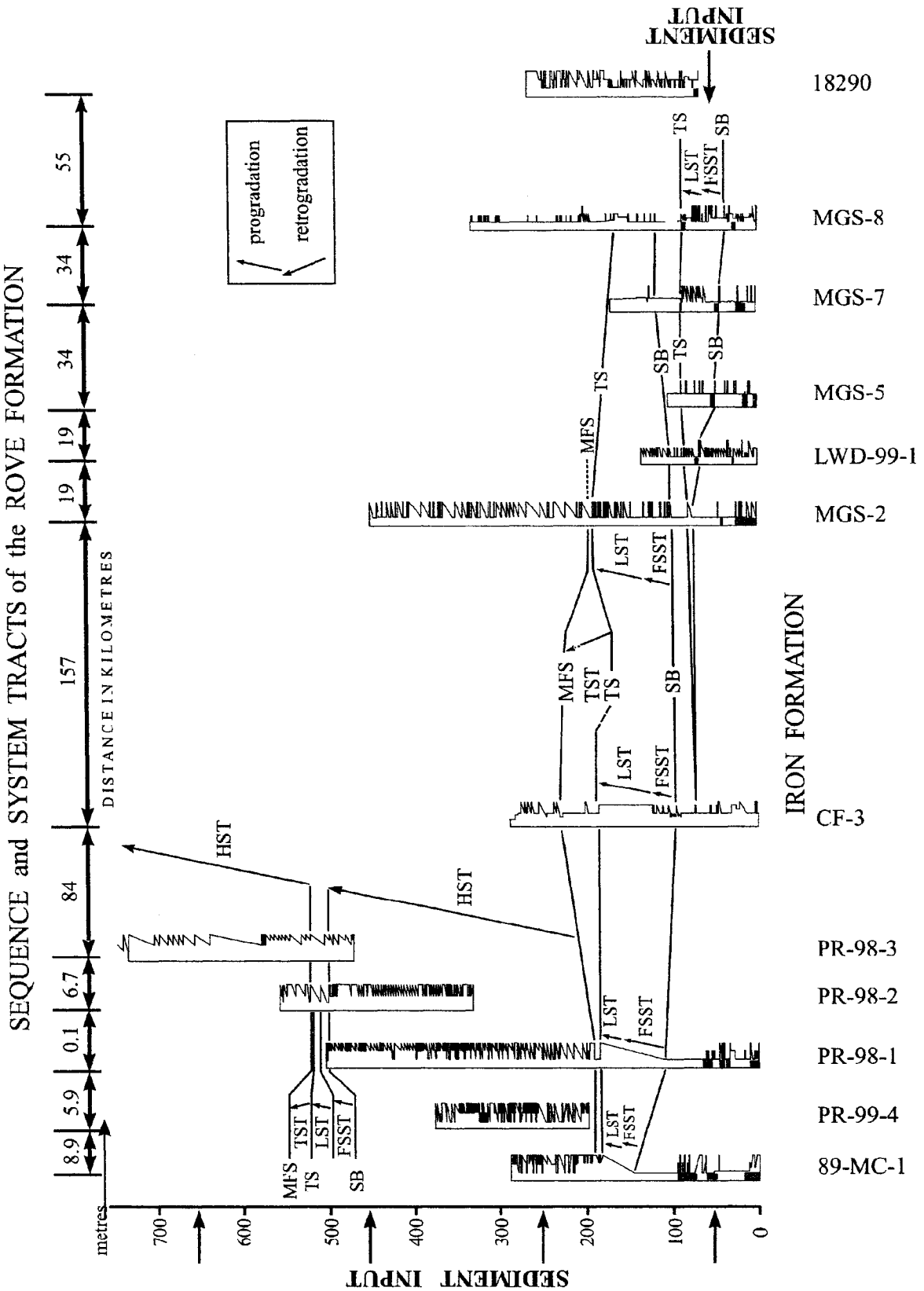

Fig. 53. Correlation of system tracts of the Rove Formation. Red bars on core are tuffaceous intervals.

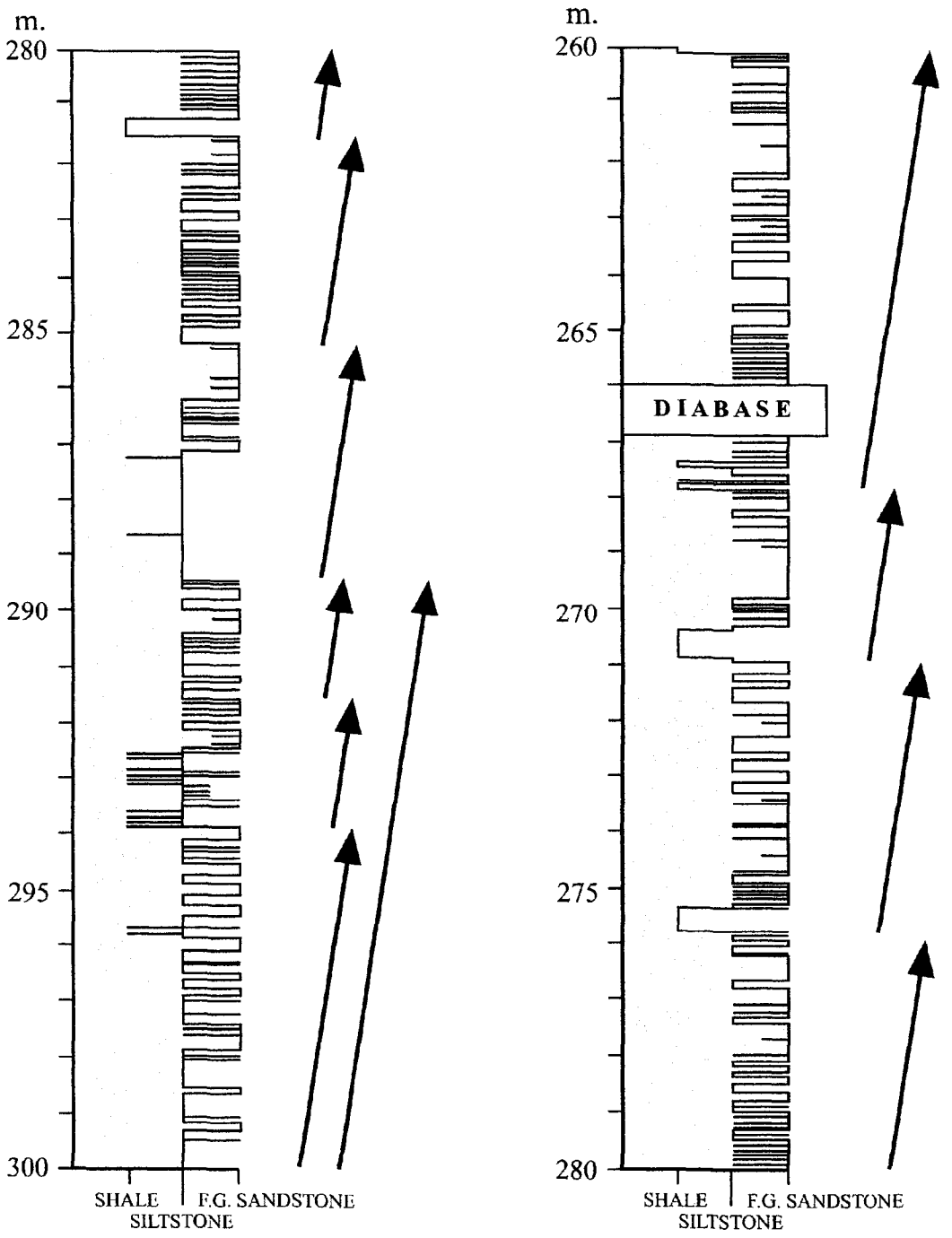

Fig. 54. Typical portion of a graphic log showing coarsening upward parasequences in the Massflow Prodelta Deposits. The parasequences in places are grouped together into parasequence sets. The entire Graded Sandstone and Shale Succession represents progradation of HST deposits.

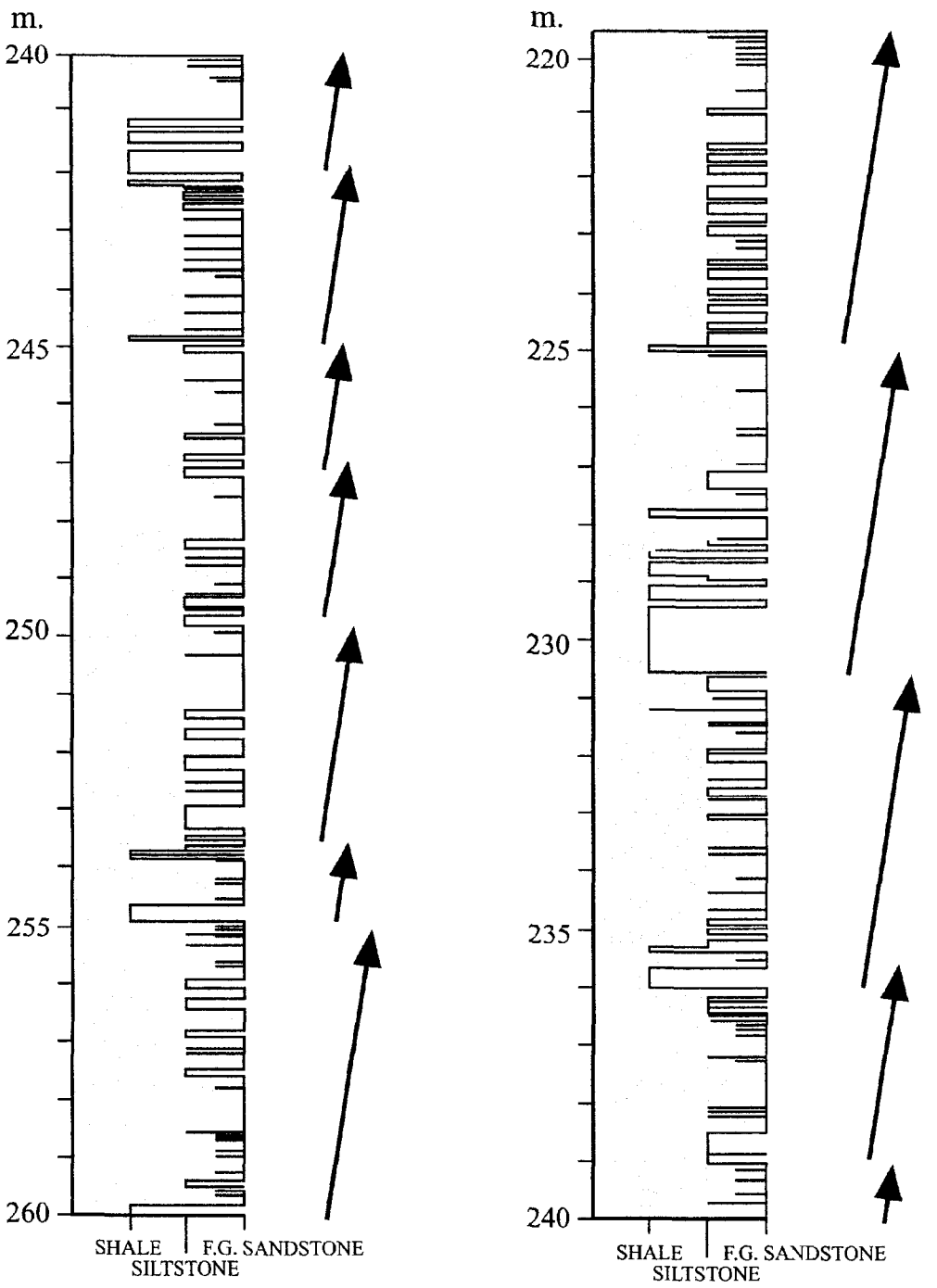

Fig. 55. The continuation of Fig. 54. Massflow Prodelta Deposits. Note, well defined parasequences at 236 m to 230.5 m, 230.5 m to 225 m, and 225 m to 19.5 m, representing aggradation of HST

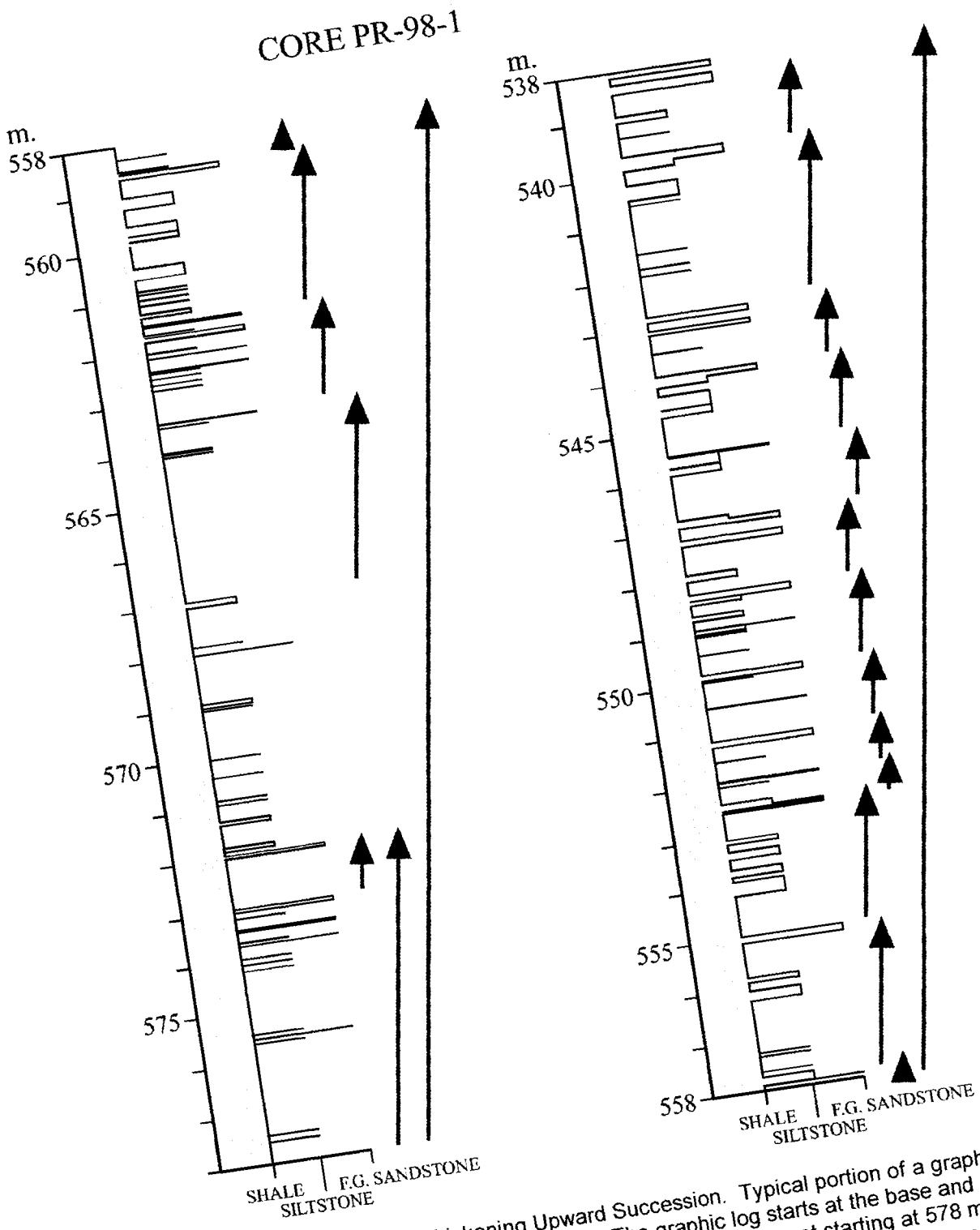

Fig. 56. Coarsening and Thickening Upward Succession. Typical portion of a graphic log showing coarsening upward parasequences. The graphic log starts at the base and continues to its top in Figure 11. Note the parasequence and parasequence set starting at 578 m depth and extending to 514 m depth. This represents the FSST. Section continued in Figure 11.

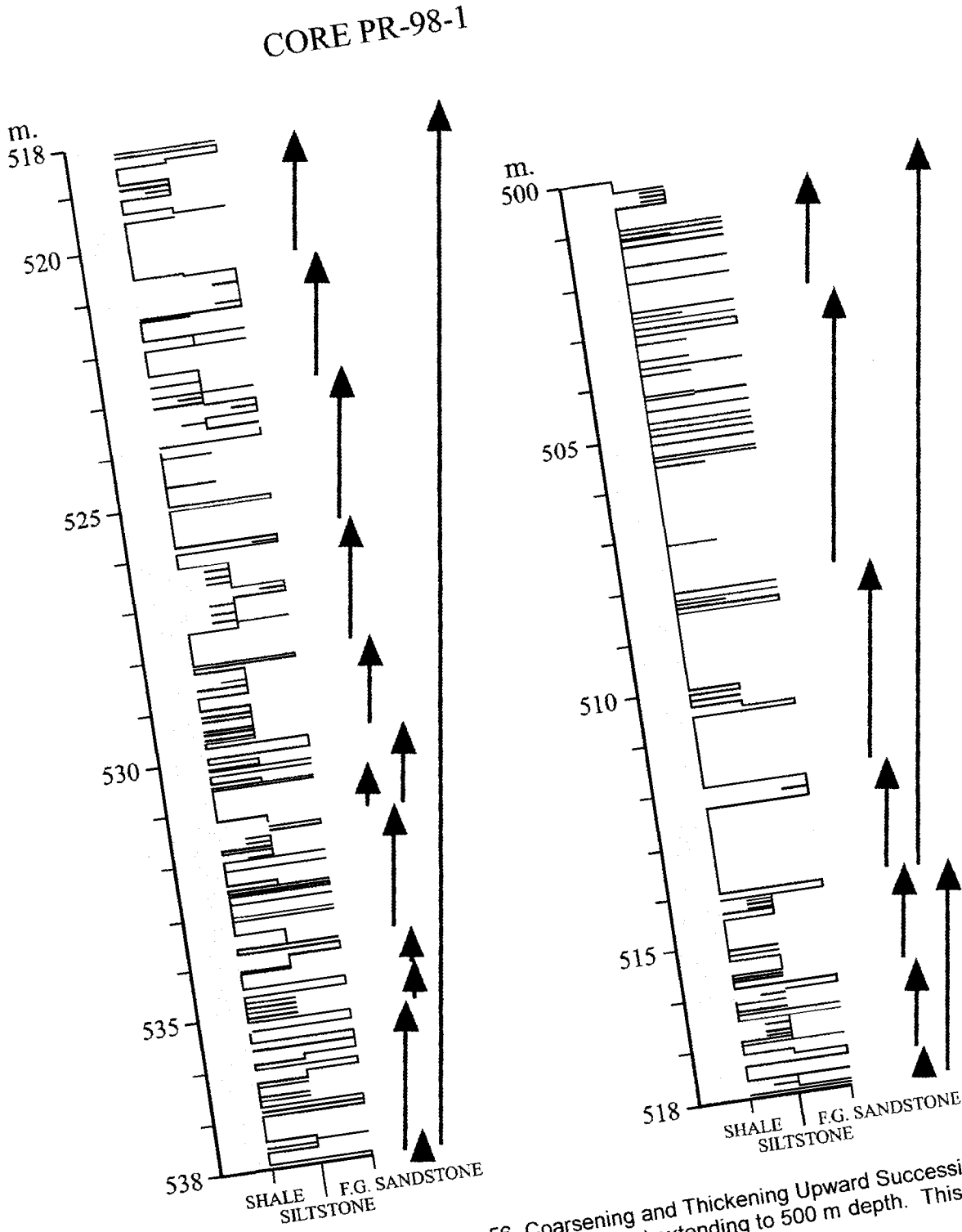

Fig. 57. Continued from Figure 56. Coarsening and Thickening Upward Succession. Note the parasequence set starting at 514 m depth to and extending to 500 m depth. This represents the LST.

CHAPTER 5: Summary and Conclusions

The Animikie basin initially developed as a back-arc rift related basin (Hemming, 1994; Kissin and Fralick, 1994; Hemming et al., 1995; Pufahl and Fralick, 1995; Pufahl, 1996). A succession of basal clastic sediments was followed by deposition of iron formation in the north represented by the Biwabik and Gunflint Formations. Uplift and subaerial exposure occurred during the Penokean Orogeny at ~ 1.870 - 1.835 Ga (Sims et al., 1989). Increased loading during the orogeny with resulting isostatic readjustment caused resubmergence of the basin, with initiation of a clastic depositional regime represented in the northern portion of the basin by the Virginia and Rove Formations. As flooding progressed from the south, a basal succession of shale and siltstone was deposited. Increased subsidence and greater water depths produced a condensed shale-dominated unit within a quiet, anoxic, sediment starved environment probably with high organic loading in the bottom sediments leading to abundant carbon in the shales. Tuffaceous layers are present in both of these lower units and were probably contributed by Penokean related volcanism to the south where 1.83 Ga felsic volcanism has been recorded (Sims et al., 1989). Two coarser units are sandwiched within the shale. A siltstone-shale unit present in the lower half of the shale is traceable across the basin and may be attributed to a fluctuation in water depth or increase in sediment supply. It thickens toward both the northern and southern basin margins with a greater frequency of coarser beds in general occurring in the southern third of the basin. A northward prograding clastic wedge present within the upper half of the shale unit may be

the product of sediment shed from the Penokean Orogen. The coarsening, thickening upwards successions overlying the shale extend across the basin, thinning towards the north and south. Paleocurrents (Morey, 1967) and grain size trends (Figs. 52 and 53) indicate that the thick sandstone dominated unit is the product of a massive influx of sediment supplied by the Trans-Hudson Orogeny which had just previously occurred to the north and west. The succession fines to the south. The uppermost unit of alternating shale, siltstone, and sandstone displays attributes of current activity and shallower water depth.

Morey (1965, 1967) identified two major lithosomes in the Rove Formation, a lower argillaceous unit and an upper silty and sandy unit (Fig. 6). Lucente and Morey (1983) identified the same two major lithosomes within the Virginia Formation. They also identified a gradational boundary between the two units which correlates loosely with the location of the boundary between the Shale Unit and the Coarsening and Thickening Upward Unit defined in this study. Detailed logging and correlative efforts identified additional units which clarified the interpretation of the depositional environment and tectonics involved.

Morey (1965, 1967), and Lucente and Morey (1983) attributed the Rove and Virginia Formations to deposition by turbidites occurring on lower and mid-fan portions of a submarine fan complex. Pelagic and hemipelagic muds deposited on a basin plain grade upwards to thin-bedded turbidite deposits which increase in frequency from the lower fan to the outer part of the mid-fan area (Morey, 1965, 1967; Lucente and Morey, 1983). The thickening and coarsening

Table 3.

General correlation between units of the Rove/Virginia Formation

Morey (67-83)	Maric
-Lower argillite	-Basal Siltstone and Shale -Shale -Siltstone and Shale -Northward Prograding Clastic Wedge
-Transition zone	-Coarsening and Thickening Upward Succession
-Upper unit of greywacke and argillaceous siltstone	-Massflow Prodelta Deposits -Distal Bar

upwards successions present are characteristic of submarine fan complexes, however they are not exclusive to this type of depositional regime.

Observations made during this study indicate that the turbiditic deposits represented by the coarsening and thickening upwards unit and sand-dominated units, grade upward into progressively shallower water facies. The turbiditic units together are considered to represent prodelta facies deposited in a slope-ramp setting by sheet flows originating off a delta front. The silt-rich coarsening and thickening upwards unit forms the distal ramp portion deposited by lower energy, gradually waning turbiditic sheet flows. The overlying sand-dominated unit deposited by higher density turbidity currents forms the proximal ramp portion. The lateral continuity of individual beds and absence of major flow channels favors this setting rather than that of a submarine fan complex. The uppermost

unit which displays features indicative of shallower water depth including wave ripples, and flaser, lenticular, and wavy bedding, is thought to constitute the distal bar section of a prograding delta. This progradation drives the overall coarsening upwards trend.

Deltas are significant sediment depositories and commonly play an important role in the filling of subsiding basins (Frazier, 1967), preserving the underlying facies as they advance. The facies relationships observed in this study of the Rove and Virginia Formations present convincing evidence that the thick assemblages overlying the lower shale-dominated unit form a delta-fed turbiditic submarine ramp system overlain by delta-front deposits represented by distal bar facies.

References

Addison, W.D., Brumpton, G.R., Vallini, D.A., McNaughton, N.J., Davis, D.W., Kissin, S.A., Fralick, P.W., and Hammond, A.L., 2005, Discovery of distal ejecta from the 1850 Ma Sudbury impact event: Geology: March 2005; v. 33; no. 3; p. 193-196.

Allen, J.R., 1970, Sediments of the modern Niger Delta: a summary and review. *In*, eds. J.R. Morgan and R.H. Shaver, Deltaic Sedimentation. Society of Economic Paleontologists and Mineralogists, Special Publication 15, Tulsa, Oklahoma, p. 138-151.

Bates, C.C., 1953. Rational theory of delta formation. American Association of Petroleum Geologists Bulletin, v. 37, p. 2119-2161.

Boote, D.R.D., and Gustav, S.H., 1987,Evolving depositional systems within an active rift, Witch Ground Graben, North Sea. *In* Petroleum Geology of North West Europe, eds., J. Brooks and K.W. Glennie, p. 819-833, Graham and Trotham, London.

Chan, M.A., and Dott, R.H. Jr., 1983, Shelf and deep-sea sedimentation in Eocence forearc basin, western Oregon – fan or non-fan? American Association of Petroleum Geologists Bulletin, v. 67, p. 2100-2116.

Cloud, P., 1973, Paleoecological significance of the banded iron-formation: Economic Geology, v. 68, p. 1135-1143.

Coe, A.L., and Church, K.D., 2003, Sequence stratigraphy, *in* Coe, A.L., ed., The Sedimentary Record of Sea-Level Change: Cambridge University Press, p. 57-95.

Coleman, J.M., and Prior, D.B., 1980, Deltaic sand bodies, A 1980 short course, Education note series #15, Louisiana State University.

Dalrymple, R.W., Baker, E.K., Harris, P.T., and Hughes, M.G., 2003, Sedimentology and stratigraphy of a tide-dominated foreland-basin delta (Fly River, Papua New Guinea), Tropical Deltas of Southeast Asia – Sedimentology, Stratigraphy, and Petroleum Geology, SEPM Special Publication No. 76, P. 147-173.

Drever, J. I., 1974, Geochemical model for the origins of Precambrian banded iron formations; Geological Society of America Bulletin, v. 85, p. 1099-1106.

Elliot, T., 1986, Deltas, in Reading, H.G., ed., Sedimentary Environments and Facies: Oxford University Press, Don Mills, Ontario, P. 113-154.

Fralick, P.W., 1988, Microbial bioherms, Lower Proterozoic Gunflint Formation, Thunder Bay, Ontario, *in* Geldsetzer, H.H.J., James, N.P., and Tebbutt, G.R., eds., Reefs. Canada and Adjacent Areas: Memoirs of the Canadian Society of Petroleum Geologists, Calgary, 13, p. 24-29.

Kissin, S.A, and Fralick, P.W. 1994, Early Proterozoic volcanics of the Animikie Group, Ontario and Michigan, and their tectonic significance (abstract). Inst. Lake Superior Geol. Abstract, 40, 18-19.

Fralick, P.W., and Barrett, T.J., 1995, Depositional controls on iron formation associations in Canada; Special Publications of the International Association of Sedimentologists, v. 22, p. 137-156.

Fralick, P.W., Kissin, S.A., and Davis, D.W., 1998, The age and provenance of the Gunflint Lapilli Tuff. Institute of Lake Superior Geology, Program and Abstracts, 44th Annual Meeting, p. 66-68.

Fralick, P.W., Davis, D.W., and Kissin, S.A., 2002, The age of the Gunflint formation, Ontario, Canada: single zircon U-Pb age determinations from reworked volcanic ash: Can. J. Earth Sci. 39, p 1085-1091.

Frazier, D.E., 1967, Recent Deltaic Deposits of the Mississippi River: Their Development and Chronology: Transactions – Gulf Coast Association of Geological Societies, v. XVII, p. 287 -315.

Goodwin, A.M., 1956, Facies relations in the Gunflint Iron Formation: Economic Geology, v. 51, p. 565-595.

Goodwin, A.M., 1969, Gunflint Iron Formation of the Whitefish Lake area: Ontario Department of Mines, v. 69, p. 41-63.

Guardado, L.R., Gamboa, L.A.P., and Lucchesi, C.F., 1989, Petroleum Geology of the Campos Basin, Brazil, a model for a producing Atlantic type basin *in* Divergent/Passive Margin Basins, eds. J.D. Edwards and P.A. Santogrossi, American Association of Petroleum Geologists Memoir 48, p. 3-79.

Hassler, S.W., and Simonson, B.M., 1989, Deposition and alteration of volcaniclastic strata in two large, Early Proterozoic iron formations in Canada; Canadian Journal of Earth Sciences, v. 26, p. 1574-1585.

Heller, P.L., and Dickinson, W.R., 1985, Submarine Ramp Facies Model for Delta-Fed, Sand-Rich Turbidite Systems, American Association of Petroleum Geologists Bulletin, v. 69, p. 960-976.

Hemming, S.R., 1994, Pb isotope studies of sedimentary rocks and detrital components for provenance analysis, Unpublished PhD thesis, State University of New York, Stoney Brook, pp.212.

Hemming, S.R., McLennan, S.M., and Hanson, G.N., 1995, Geochemical and Nd/Pb isotopic evidence for the provenance of the Early Proterozoic Virginia Formation, Minnesota. Implications for tectonic setting of the Animikie Basin: Journal of Geology, v. 103, p. 147-168.

Hill, M.L., and Smyk, M.C., 2005, Penokean Fold-and-Thrust Deformation of the Paleoproterozoic Gunflint Formation near Thunder Bay, Ontario. Institute of Lake Superior Geology, program and Abstracts, 51st Annual Meeting, p. 26.

Jaeger, J.M., and Nittrouer, C.A., 1995, Tidal controls on the formation of fine-scale sedimentary strata near the Amazon river mouth, Marine Geology, v. 125, p. 259-281.

Link, M.H., and Welton, J.E., 1982, Sedimentology and reservoir potential of Matilija Sandstone: an Eocene deep-sea fan and shallow marine complex, California, American Association of Petroleum Geologists Bulletin, v. 66, p. 1514-1534.

Lucente, M.E., and Morey, G.B., 1983, Stratigraphy and sedimentology of the lower Proterozoic Virginia formation, northern Minnesota: Minnesota Geological Survey Report of Investigations 28, 28 p.

Morey, G.B., 1965, The Sedimentology of the Precambrian Rove Formation in northeastern Minnesota: PhD thesis, University of Minnesota, 292 p.

Morey, G.B., 1967, Stratigraphy and sedimentology of the middle Precambrian Rove formation in northeastern Minnesota: Journal of Sedimentary Petrology, v. 37, p 1154-1162.

Morey, G.B., 1972, Gunflint Range, *in* Sims, P.K., and Morey, G.B., eds., Geology of Minnesota: A Centennial Volume: Minnesota Geological Survey, p. 218-225.

Morey, G.B., 1973, Stratigraphic framework of middle Precambrian rocks in Minnesota *in* Young, G.M., ed., Huronian stratigraphy and sedimentation, The Geological Association of Canada Special Paper Number 12, p. 211-249.

Morey, G.B., 1983, Animikie Basin, Lake Superior region, U.S.A., *in* Trendall, A.F. and Morris, R.C., eds., Iron-Formation Facts and Problems: Elsevier, Amsterdam, p. 13-67.

Morey, G.B., and Ojakangas, R.W., 1970, Sedimentology of the middle Precambrian Thomson formation, east-central Minnesota: Minnesota Geological Survey, Report of Investigations 13, 32p.

Morgan, J.P., 1979. Deltas, a resume. Journal of Geological Education, v. 18, p 107-117.

Myrow, P.M., Fischer, W., and Goodge, J.W., 2002, Wave-modified turbidites: combined-flow shoreline and shelf deposits, Cambrian, Antarctica, Journal of Sedimentary Research. V. 72, p. 641-656.

O'Driscoll, D., Hindle, A.D., and Long, D.C., 1990, The structural controls on Upper Jurassic and Lower Cretaceous reservoir sandstones in the Witch Ground Graben, UK North Sea *in* Tectonic Events Responsible for Britain's Oil and Gas Reserves, eds., R.F.P. Hardman and J. Brooks, Special Publication of the Geological Society of London, v. 55, p. 299-323.

Ojakangas, R.W., 1983, Tidal deposits in the Early Proterozoic basin of the Lake Superior region – The Palms and Pokegama Formations: Evidence for subtidal-shelf deposition of Superior-type banded iron-formation, *in* Medaris, L.G., ed., Early Proterozoic Geology of the Great Lakes Region: Geological Society of America Memoir 160, p. 49-66.

Ojakangas, R.W., and Morey, G.B., 1982, Keweenawan pre-volcanic quartz sandstones and related rocks of the Lake Superior region, *in* Wold, R.J., and Hinz, W.J., eds, Geological Society of America Inc. Memoir 156.

Parkinson, N. and Summerhayes, C., 1985. Synchronous global sequence boundaries. American Association of Petroleum Geologists, v. 69, p. 685-687.

Pattison, S.A.J., 2005, Storm-influenced prodelta turbidite complex in the lower Kenilworth member at Hatch Mesa, Book Cliffs, Utah, U.S.A.: Implications for shallow marine facies models, Journal of Sedimentary Research, v. 75, no. 3, p. 420-439.

Poulton, S.W., Fralick, P.W., Canfield, D.E., 2004, The transition to a sulphidic ocean ~ 1.84 billion years ago: Nature, V.431, p. 173-177.

Pufahl, P.K., 1996, Stratigraphic architecture of a Paleoproterozoic iron formation depositional system: the Gunflint, Mesabi and Cuyuna iron ranges. Unpub. M. Sc. Thesis, Lakehead University, 167.

Pufahl, P.K., and Fralick, P.W., 1995, Paleogeographic reconstruction of the Gunflint-Mesabi-Cuyuna depositional system: a basin analysis approach: Proceedings of the Institute on Lake Superior Geology, v. 41, p. 59-60.

Pufahl, P. and Fralick, P., 2000, Depositional environments of the Paleoproterozoic Gunflint formation *in* Institute on Lake Superior Geology field trip guide book, v. 46, Minnesota Geological Survey.

Pufahl, P.K., and Fralick, P.W., 2004. Depositional controls on Paleoproterozoic iron formation accumulation, Gogebic Range, Lake Superior region, U.S.A. Sedimentology, vol, 51, p.791-808.

Reading, H.G., 1964, A review of the factors affecting the sedimentation of the Millstone Grit (Namurian) in the Central Pennines. In: *Deltaic and Shallow Marine Deposits,* ed. By L.M.J.U. Van Straaten, p. 340-346.

Sims, P.K., and Peterman, Z. E., 1983, Evolution of Penokean foldbelt, Lake Superior region, and its tectonic environment *in* Early Proterozoic Geology of the Great Lakes Region, Geological Society of America Memoir #160, p. 3-14.

Sims, P.K., Van Schmus, W. R., Schulz, K.J., and Peterman, Z.E., 1989, Tectonostratigraphic evolution of the Early Proterozoic Wisconsin Magmatic terranes of the Penokean orogen: Canadian Journal of Earth Sciences, v. 26, p. 2145-2158.

Sinclair, H.D., 2000, Delta-fed turbidites infilling topographically complex basins: A new depositional model for the Annot Sandstones, SE France, Journal of Sedimentary Research, Vol. 70, No. 3, p. 504-519.

Southwick, D.L, Morey, G.B., and Swiggen, P., 1988, Geological map (scale 1:250 000) of the Penokean Orogen, central and east-central Minnesota, and accompanying text: Minnesota Geological Survey, Report of Investigations RI-37.

Vail, P.R., Mitchum, R.M., Todd, R.G., Widmier, J.M., Thompson,S., Sangree, J.B., and Bubb, J.M., 1977. Seismic stratigraphy and global changes in sealevel *in* ed. C.E. Payton, Seismic Stratigraphy – applications to Hydrocarbon Exploration. American Association of Petroleum Geologists Memoir 26, p. 49-212.

Van Wyck, N. and Johnson, C.M., 1997, Common lead, Sm-Nd, and U-Pb constraints on petrogenesis, crustal architecture and the tectonic setting of the Penokean Orogen (Paleoproterozoic), in Wisconsin, U.S.A.: Geological Society of America Bulletin, v. 109, p. 799-808.

Wright, L.D., 1977. Sediment transport and deposition at river mouths: a synthesis. Geological Society of America Bulletin, v. 88, p. 857-868.

Wright, L.D., 1985. River deltas *in* ed. R.A. Davis, Coastal Sedimentary Environments, Springer- Verlag, New York, p. 1-76.

Wright, L.D., and Coleman, J.N., 1974. Mississippi river mouth processes: effluent dynamics and morphological development, Journal of Geology, v. 82, p. 751-778.